

## ABSTRACT

Commercial Zinc-Aluminum (Zn-Al) alloys commonly manufactured through traditional process of melting and casting. However, the problems with the casting process in producing mass production parts are associated with segregation, machining and maintaining final tolerance. Therefore, this research aims to produce commercial Zn-Al alloys from powder elements, study its sintering behavior through hybrid microwave sintering method and compared with the performance of conventional sintering. The comparative analyses are based on density, porosity, micro hardness, grain size, microstructure and XRD analysis of the sintered samples.

In this research, three different compositions of Zn-Al alloys; Zn-8wt.%Al-1wt.%Cu-0.02wt.%Mg (ZA8), Zn-11wt.%Al-1wt.%Cu-0.025wt.%Mg (ZA12) and Zn-27wt.%Al-2wt.%Cu-0.015wt.%Mg (ZA27) are mixed in a planetary ball mill at 100 rpm for 4 hours. Samples are prepared by hydraulic pressing at three compaction loads; 6, 8 and 10 tons. In conventional sintering, the green samples are sintered to sintering temperature; 360°C, the heating and cooling rates were set to 5°C/min and holding time; 30 minutes. A modification of 2.45 GHz domestic microwave oven is implemented into hybrid system by adding insulation box, susceptor and crucibles to sinter the samples at sintering temperature; 360°C and holding time; 10 minutes.

Hybrid microwave sintering technique is employed to overcome the problems in pure microwave metal sintering which requires a long warming-up before the compact will start to couple with the microwave. This will increase the risk of plasma formation in the cavity and lead to damage of microwave generator-magnetron.

The results shown that hybrid microwave sintering of Zn-Al alloys took considerably shorter processing time, higher density, higher hardness, lower porosity and uniform microstructure compared with conventional sintering. The best

compaction load for processing ZA8 and ZA12 alloys were 8 tons meanwhile for ZA27 alloy was 10 tons. ZA8 alloy obtained the highest density compared to ZA12 and ZA27 alloys because of weight percentage of zinc in the compositions. Coefficient of thermal expansion (CTE) is decreased by increasing Al fraction in the all ZA8, ZA12 and ZA27 alloys.

## ABSTRAK

Komersial aloi Zink Aluminium (Zn-Al) biasanya dihasilkan melalui proses tradisional pencairan dan penuangan. Walau bagaimanapun, masalah yang dihadapi oleh proses penuangan dalam menghasilkan bahagian secara pengeluaran besar-besaran adalah berkaitan dengan pengasingan, pemesinan dan pengekal toleransi akhir. Oleh itu, penyelidikan ini bertujuan untuk menghasilkan komersial aloi Zn-Al daripada elemen serbuk, mengkaji kelakuan pensinteran melalui kaedah pensinteran gelombang mikro hibrid dan prestasi pensinteran dibandingkan dengan pensinteran konvensional. Analisis perbandingan adalah berdasarkan ketumpatan, keliangan mikro kekerasan, saiz butiran, mikrostruktur dan analisis XRD sampel yang disinter.

Dalam kajian ini, tiga komposisi berbeza aloi Zn-Al ; Zn-8wt% Al-1wt% Cu-0.02wt% Mg (ZA8), Zn-11wt% Al-1wt% Cu-0.025wt% Mg (ZA12) dan Zn-27wt.% Al-2wt% Cu-0.015wt.%Mg (ZA27) telah dicampur di dalam pengisar bola planet pada 100 rpm selama 4 jam. Sampel disediakan dengan menggunakan penekan hidrolik pada 3 beban pemadatan; 6, 8 dan 10 tan. Dalam pensinteran konvensional, sampel hijau disinter pada suhu pensinteran; 360°C, kadar pemanasan dan penyejukan ditetapkan kepada 5°C/min dan 30 minit masa menahan. Pengubahsuaian 2.45 GHz ketuhar gelombang mikro domestik dilaksanakan ke dalam sistem hibrid dengan menambah kotak penebat, *susceptor*, dan pijar untuk pensinteran sampel pada suhu pensinteran; 360°C dan 10 minit masa menahan.

Teknik pensinteran gelombang mikro hibrid telah digunakan untuk mengatasi masalah dalam pensinteran gelombang mikro logam tulen yang memerlukan pemanasan yang lama sebelum pemadatan mula berhubungan dengan gelombang mikro. Ini akan meningkatkan risiko pembentukan plasma dalam rongga dan membawa kepada kerosakan gelombang mikro penjana-magnetron.

Hasil penyelidikan menunjukkan bahawa pensinteran menggunakan gelombang mikro hibrid aloi Zn-Al mengambil masa pemprosesan yang lebih pendek, ketumpatan dan kekerasan yang lebih tinggi, keliangan lebih rendah dan mikrostruktur seragam berbanding dengan pensinteran konvensional. Beban pemadatan yang terbaik untuk pemprosesan aloi ZA8 dan ZA12 adalah 8 tan, manakala bagi aloi ZA27 adalah 10 tan. Alois ZA8 memperoleh kepadatan paling tinggi berbanding aloi ZA12 dan ZA27 kerana peratusan berat Zink dalam komposisi tersebut. Pekali pengembangan termal (CTE) telah menurun dengan meningkatkan pecahan Al di semua aloi ZA8, ZA12 dan ZA27.

## **ACKNOWLEDGEMENTS**

Assalamualaikum w.b.t. Alhamdulillah, I am very grateful to Allah all the mighty, with His blessing that this project is successfully completed.

Firstly, my deepest gratitude to my family especially my parents, Mr. Lutfi Mhd Idris and Mrs. Zanaliah Puji and for their encouragement and prayers for my success here. I would also like to take this opportunity to express my sincere thanks and appreciation to my supervisor, Professor Dr. Mohd Hamdi Abd Shukor for his guidance and constructive comments throughout the completion of this work. I would also like to thank Dr. Reza Rahbari for sharing his views and opinions with me in achieving the goal of this research.

My special thanks go to all my AMMP Centre colleagues; Dr. Farazila, Mr. Fadzil and others for their supports and motivations. Not to forget, my appreciation also goes to technical staffs; Miss Nursiyadah (Powder Metallurgy Lab), Mrs. Hartini (Surface Lab), and others for their willingness to guide and help me to run my experiments using all available facilities.

Lastly, my heartfelt thanks also go to my lovely husband, Muhammad Firdaus Ahmad Mansor for his love, continuous moral and emotional support in order to complete this research. Thank you so much.

# TABLE OF CONTENTS

<b>Abstract</b>	i
<b>Abstrak</b>	iii
<b>Acknowledgements</b>	v
<b>Table of Contents</b>	vi
<b>List of Figures</b>	ix
<b>List of Tables</b>	xii
<b>List of Symbols and Abbreviation</b>	xiii
<b>Chapter 1: Introduction</b>	
1.1 Overview of the study	1
1.2 Importance of the study	4
1.3 Objectives of the study	4
1.4 Scope of the study	5
1.5 Report structure	6
<b>Chapter 2: Literature Review</b>	
2.1 Powder Metallurgy	8
2.2 Sintering	9
2.3 Electromagnetic radiation of microwave	10
2.4 Microwave-Materials Interaction	12
2.5 Hybrid Microwave Sintering (HMS)	13
2.6 Microwave Sintering of Metals	15
<b>Chapter 3: Experimental Procedure</b>	
3.1 Specimen Preparation	25
3.1.1 Powder Selection	25
3.1.2 Powder Weighing	25
3.1.3 Powder Mixing	26
3.1.4 Powder Compaction	27
3.2 Sintering process	28
3.2.1 Conventional Sintering	29
3.2.2 Hybrid Microwave Sintering	30

	3.2.2.1 Crucible	31
	3.2.2.2 Susceptor	31
	3.2.2.3 Ceramic Insulation Box	33
3.3	Measurement Techniques and Calculations	34
3.3.1	Temperature Measurement	34
3.3.2	Dimensional Changes	34
3.3.3	Density	35
3.3.4	Porosity	36
3.3.5	Microhardness	37
3.4	Metallographic Examination	38
3.4.1	Specimen Preparation	38
3.4.2	Microstructural Examination	41
3.5	Thermo Mechanical Analyzer (TMA)	42
 <b>Chapter 4: Results</b>		
4.1	Thermal Mechanical during Mixing Process	43
4.1.1	Introduction	43
4.1.2	Macroscopic features	44
4.1.3	Microstructure analysis	44
4.2	Evaluation of Hybrid Microwave Sintering of Zinc Aluminum Alloys	48
4.2.1	Introduction	48
4.2.2	Temperature profile and performance	48
4.2.3	Dimensional changes	51
4.2.4	Density	52
4.2.5	Porosity	54
4.2.6	Microhardness	56
4.2.7	Thermal mechanical analysis	58
4.2.8	Microstructure analysis	59

<b>Chapter 5:</b>	<b>Discussions and Analysis</b>	
5.1	Effect of mixing speeds during mixing process in a planetary ball mill	74
5.2	Conventional sintering versus hybrid microwave sintering	77
5.3	Effect of compaction load on hybrid microwave sintering	79
5.4	Influence of different masses of Zn, Al, Cu and Mg element on mechanical properties of hybrid microwave sintering	81
<b>Chapter 6:</b>	<b>Conclusions and Further Works</b>	
6.1	Conclusions	83
6.2	Further Works	84
	<b>List of publications</b>	85
	<b>References</b>	86



## LIST OF FIGURES

Figure 1.1	: History of microwave heating	2
Figure 2.1	: The steps involved in powder metallurgy process	8
Figure 2.2	: Stage of sintering on microscopic scale	10
Figure 2.3	: Electromagnetic wave	11
Figure 2.4	: Electromagnetic spectrum	11
Figure 2.5	: Categories of microwave-materials interaction	12
Figure 2.6	: Schematic diagrams of two directional sintering concepts	14
Figure 2.7	: Densification and hardness of MSP 1.5 Mo tensile bars	17
Figure 2.8	: Thermal profile of conventional and microwave sintered Cu-12Sn alloy	20
Figure 2.9	: Photographs of the premixed Cu-12Sn compacts, conventionally and microwave sintered at (a) 775°C and (b) 830°C for 30 min compacted at 150 MPa	20
Figure 3.1	: The flowchart of experiment	24
Figure 3.2	: (a) Zn-150 $\mu\text{m}$ , (b) Al-60 $\mu\text{m}$ , (c) Mg-250 $\mu\text{m}$ , (d) Cu-10 $\mu\text{m}$	25
Figure 3.3	: Retsch Planetary ball mill (PM400), (b) Ball mill's jar were clamp inside the planetary ball mill, (c) Powders and zirconia balls inside the jar	26
Figure 3.4	: (a) Green compact (b) Die and punch (c) Hydraulic Press Machine	28
Figure 3.5	: Elite Chamber Furnace	30
Figure 3.6	: Schematic diagram of hybrid microwave sintering system	30
Figure 3.7	: Alumina crucible	31
Figure 3.8	: 100g of SiC powder with (a) 75 $\mu\text{m}$ (b) 50-60 nm	32
Figure 3.9	: The steps of preparing a set of an insulation box	33
Figure 3.10	: Thermocouple Thermometer	34
Figure 3.11	: Electronic digital vernier caliper	35
Figure 3.12	: Electronic balance	36
Figure 3.13	: Magnetic Hot Plate	37
Figure 3.14	: Micro hardness tester	38
Figure 3.15	: (a) Low diamond speed saw machine (b) Specimen sectioning	39
Figure 3.16	: Basic steps of cold mounting process	39

Figure 3.17	: Grinder and polisher machine	40
Figure 3.18	: Thermo Mechanical Analyzer	42
Figure 4.1	: Zn-Al-Cu-Mg powders (a) before milling, (b) after milling 100 rpm and (c) after milling 200 rpm	44
Figure 4.2	: XRD pattern of scratched thorns grown on the zirconia balls	45
Figure 4.3	: Distribution of Zn, Al, Cu, and Mg in the interface between Zirconia ball and grown layer after etching	45
Figure 4.4	: Elemental SEM mapping has detected Zn, Al, Cu and Zr in the region	46
Figure 4.5	: EDX characterization of elements in the region	46
Figure 4.6	: EDX on the thin layer covered the surface of the ball	47
Figure 4.7	: (a) Multistage process of thorn growth, (b) Shapeless of powder inside the jar	47
Figure 4.8	: Temperature profile of conventional sintering	49
Figure 4.9	: Temperature profile of hybrid microwave sintering with different particle size of SiC powder	50
Figure 4.10	: Zinc alloy sample started melt after 10 minutes sintered in microwave with 50 nm SiC particle size as susceptor	50
Figure 4.11	: Alumina crucible cracked due to the thermal shock	51
Figure 4.12	: The density of sintered (a) ZA8, (b) ZA12 and (c) ZA27 alloys	53
Figure 4.13	: The porosity of sintered (a) ZA8, (b) ZA12 and (c) ZA27 alloys	55
Figure 4.14	: The micro hardness (HV) of sintered (a) ZA8, (b) ZA12 and (c) ZA27 alloys	57
Figure 4.15	: Micrographs of CS and HMS samples of ZA8 alloy (6 tons)	60
Figure 4.16	: Micrographs of CS and HMS samples of ZA8 alloy (8 tons)	61
Figure 4.17	: Micrographs of CS and HMS samples of ZA8 alloy (10 tons)	62
Figure 4.18	: Micrographs of CS and HMS samples of ZA12 alloy (6 tons)	63
Figure 4.19	: Micrographs of CS and HMS samples of ZA12 alloy (8 tons)	64
Figure 4.20	: Micrographs of CS and HMS samples of ZA12 alloy (10 tons)	65
Figure 4.21	: Micrographs of CS and HMS samples of ZA27 alloy (6 tons)	66
Figure 4.22	: Micrographs of CS and HMS samples of ZA27 alloy (8 tons)	67
Figure 4.23	: Micrographs of CS and HMS samples of ZA27 alloy (10 tons)	68
Figure 4.24	: EDX of ZA8 sintered alloy (8 tons)	69
Figure 4.25	: EDX of ZA12 sintered alloy (8 tons)	69

Figure 4.26	: EDX of ZA27 sintered alloy (10 tons)	70
Figure 4.27	: XRD results of (a) ZA8, (b) ZA12 and (c) ZA27 after hybrid microwave sintering	71
Figure 4.28	: The grain size of sintered (a) ZA8, (b) ZA12 and (c) ZA27 alloys	72

## LIST OF TABLES

Table 2.1	: Physical and mechanical properties of microwave sintered FC-0208 (Fe-2Cu-0.8C) and FN-0208 (Fe-2Ni-0.8C) iron steel samples	16
Table 2.2	: Effect of heating mode on the densification and mechanical properties of 316L and 434L stainless steel sintered at 1400 °C	18
Table 2.3	: Comparison of processing conditions and properties of the sintered nano-Cu samples	19
Table 2.4	: Density and hardness of Al/SiC composites	20
Table 3.1	: Composition of zinc-aluminum alloy ( <a href="http://www.matweb.com">www.matweb.com</a> )	25
Table 3.2	: Parameters used in selection of mixing speed	27
Table 3.3	: Parameters used for mixing Zn-Al-Cu-Mg powders	27
Table 3.4	: The experimental condition for each experiment	29
Table 3.5	: Zinc alloy etchant	40
Table 4.1	: Dimensional changes of sintered ZA8, ZA12 and ZA27	52
Table 4.2	: CTE values of microwave sintered samples of ZA8, ZA12 and ZA27	58

## LIST OF SYMBOLS AND ABBREVIATIONS

P/M	Powder Metallurgy
HMS	Hybrid Microwave Sintering
Zn	Zinc
Al	Aluminum
Cu	Copper
Mg	Magnesium
SiC	Silicon Carbide
Al <sub>2</sub> O <sub>3</sub>	Alumina
$P$	Power absorbed
$D$	Depth of penetration
$E$	Magnitude of the internal field
$\sigma$	Total effective conductivity
$f$	Frequency
$\epsilon_0$	Permittivity of free space
$\epsilon_r$	Relative dielectric constant
$\tan \delta$	Loss tangent.
$\lambda_0$	Incident or free space wavelength.
$\mu\text{m}$	micron meter
nm	nano meter
Ds	Diameter after sintered
Dg	Diameter of green compact
A	Mass of specimen in air
B	Mass of specimen in water
$\rho$	Density of water at given temperature
Ws	Saturated weight of the specimen in air
Wd	Specimen in dry air
Wss	Saturated weight of the specimen when submerged in water
rpm	rotation per minute
HV	Hardness Vickers
ml	mililitre
HCl	Acid Hydrochloric

L	Length (mm)
N	Number of grains
n	Grain size
CTE	Coefficient of Thermal Expansion

# CHAPTER 1

## INTRODUCTION

### 1.1 Overview of the study

Powder Metallurgy (P/M) is a metalworking process used to fabricate net or near-net shape components for various applications and can be used for both metal and nonmetal-based composite. The P/M process is more competitive than other fabrication methods like casting, stamping or machining. It is chosen when requirements for strength, wear resistance or high operating temperatures exceed the capabilities of die casting alloys.

There are a few basic steps in P/M approach and one of the steps is sintering. In this process, the compacted powders are heated in a control-atmosphere furnace to a certain temperature which is below the melting point of major constituent to allow the bonding of the powder particles.

Conventional sintering involves the heating of the powder compacts from ‘outside-in’ with the usual mechanisms of heating such as conduction, radiation and convection (Saitou, 2006 and Moriguchi et al, 2006). However, this mechanism creates a temperature gradient within the powder metallurgical component being sintered as its outer part would be at a higher temperature than its inner part. This unequal heating rate means that the diffusion of the powders does not occur simultaneously and thus creates the possibility of non-uniform sintering.

On the other hand, the principle mechanism of microwave heating is a volumetric heating involving conversion of electromagnetic energy into thermal energy, which is instantaneous, rapid and highly efficient (Gan, 2005). This uniform heating would ensure

that the heating is evenly done on the whole part. In the past, microwave heating had been successfully used in areas such as tempering of meat, preheating rubber slugs, vulcanizing rubber, precooking bacon, drying pasta and other low temperature industrial activities.

However, beginning in the late 1980s, there was growing interest in high temperature microwave for processing of materials (Sethi et al, 2003). It has started with microwave application to polymer, followed by ceramic and recently it is used to heat metallic materials. Figure 1.1 shows the research history of microwave heating.

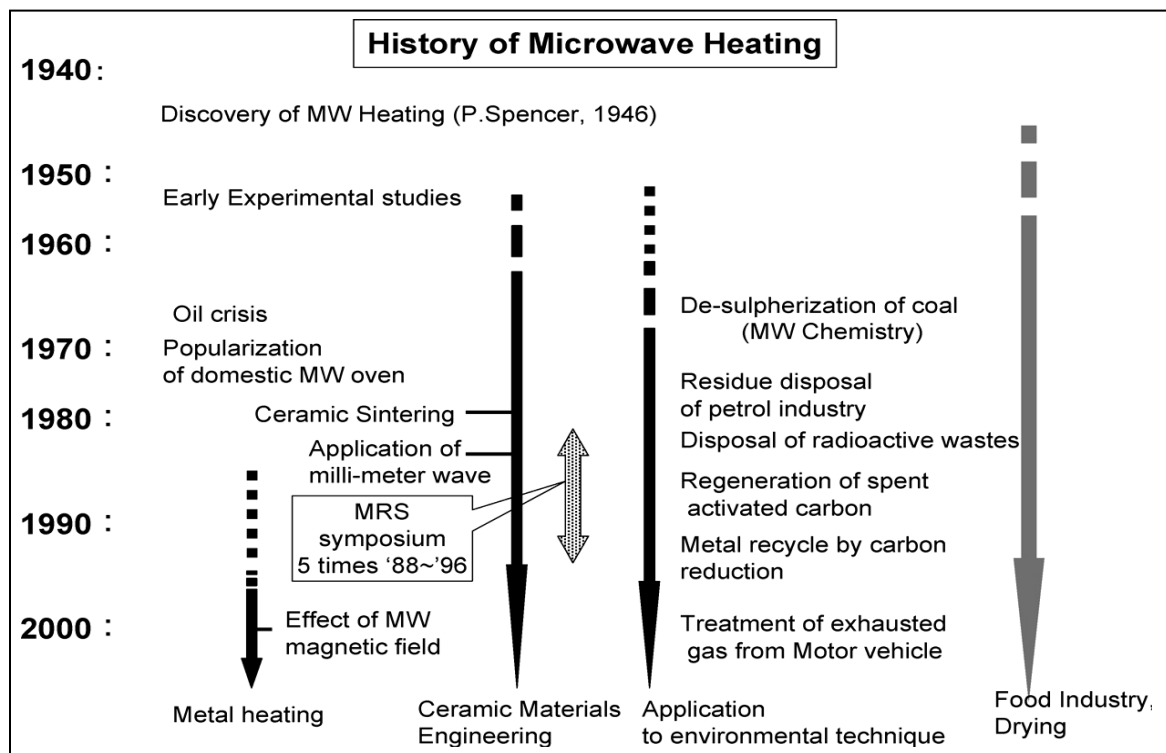


Figure 1.1: History of microwave heating (Yoshikaw et. al, 2007).

The advantages of microwave processing over conventional heating method includes rapid and uniform heating which reduces thermal stress and avoids cracking during processing. It also offers improvements in product quality with the production of unique microstructures and properties. In addition, it will efficiently remove volatile



constituents deep within materials and reduces manufacturing costs and processing time (Randall, 1994 and Hsieh et. al, 2006).

However, there is a limitation of using conventional sintering and normal microwave sintering system. Conventional heating uses the radiation, conduction and convection to transfer the heat which results in the poor microstructural characteristics in the core of the powder compact. Meanwhile, the microwave heating generates heat by using the energy conversion, results in the poor microstructural characteristic on the surface (Gupta et. al, 2004). A way to eliminate this limitation is by using hybrid microwave sintering (HMS) technique.

In HMS, it was direct heating of the compact from microwave forms one component and the radiative heating from the susceptor forms second component of the total heat imparted into the compacts (Gupta et. al, 2004). Susceptor are useful for initial heating due to its ability to absorb electromagnetic energy and convert it to heat.

The Zinc-aluminum alloys have been used for many years in the production of small components and to certain extent for plain bearings because they offered several advantages such as inexpensive high strength alloys, high resistance to wear and abrasion, good corrosion resistance, low melting point materials and have ability to withstand high bearing loads. This Zinc-base alloys has been widely studied in order to obtain the characteristic parameters of different processes such as casting, rolling, extrusion and forging (Martinez-Flores et. al, 2003).

From the literature survey, no literature is available in the area of hybrid microwave sintering of low temperature alloys such as Zn-Al-Cu-Mg alloy. In this research, hybrid microwave sintering of three alloys based on Zn-Al-Cu-Mg mixture are optimized and compared with the conventional sintering. Mechanical properties such as microhardness,

density, porosity, microstructure, grain size and coefficient of thermal expansion (CTE) are investigated and the results confirm each other.

## **1.2 Importance of the study**

The aim of this investigation is to develop a hybrid microwave sintering (HMS) technique and employ this approach to study sintering behaviors of Zinc-base alloy. These Zinc alloy containing different amounts of Aluminum powder would be synthesized using powder metallurgy technique. Theoretical explanations of the heating mechanism of powder metallurgical powders by microwaves would be formulated and supported with experimental confirmations. The results of hybrid microwave sintering would be compared to those of conventional sintering. The feasibility and efficiency of the process would be evaluated based on the successful sintering of powder metallurgical compacts. The sintered specimens would be characterized in terms of physical, microstructural and mechanical properties.

## **1.3 Objectives of the study**

- 1.3.1 To develop Hybrid Microwave Sintering (HMS) technique for Zinc-Aluminum alloys prepared by powder metallurgy processing.
- 1.3.2 To compare HMS of Zinc-Aluminum alloys with conventional sintering.
- 1.3.3 To determine the effect of compaction load on mechanical properties and microstructure of Zinc-Aluminum alloys by HMS.
- 1.3.4 To investigate the influence of three different masses of zinc, aluminum, copper and magnesium elements on mechanical properties of ZA8, ZA12 and ZA27 sintered alloys.

## **1.4 Scope of the study**

Within the limited period of this study, the scope of the research is limited to the evaluation of cylindrical P/M compacted samples of Zinc-Aluminum (Zn-Al) alloys. The P/M processes are started from powder composition, mixing process, powder compaction and sintering. In this study, three compositions of Zn-Al alloys are used; Zn-8Al-1Cu-0.02Mg (ZA8), Zn-11Al-1Cu-0.025Mg (ZA12) and Zn-27Al-2Cu-0.015Mg (ZA27). Meanwhile, in the mixing process, two different mixing speeds are used to determine the best mixing speed of Zn-Al alloys; 100 and 200 rotations per minute (rpm). 6, 8 and 10 tons are chosen as the compaction load for green compact samples. In the sintering process, two different heating mechanism of sintering are used which is conventional and hybrid microwave sintering.

A modification of 2.45 GHz domestic microwave oven is implemented into hybrid system by adding insulation box, susceptor and crucible. Silicon Carbide (SiC) powder is used as susceptor in the Alumina ( $\text{Al}_2\text{O}_3$ ) crucible to allow a controlled two-directional sintering process for low sintering temperature. The mechanical and physical properties such as density, porosity, micro hardness and microstructural characterization for both sintered samples are evaluated.

## **1.5 Report structure**

This thesis is divided into six chapters. Chapter 1 presented an introduction to the project such as the historical development of HMS, the importance of the study, objectives, scopes of the study and report structure.

The literature review presented in Chapter 2 covers introduction of P/M technique, microwave–materials interaction, the differences between conventional and microwave sintering techniques and mechanism of HMS. Some of the related research work in previous years are quoted in this chapter to further support and reinforce the author’s ideas in terms of the application of microwave energy as an alternative method of sintering process.

Chapter 3 describes the research methodology such as powder metallurgy samples preparation, the process of conventional and hybrid microwave sintering, the measurement of density, porosity and micro hardness, X-Ray Diffraction (XRD), Field Emission Scanning Electron Microscope (FESEM), Electron Dispersive X-Ray Spectrometer (EDX) analysis and Thermo Mechanical Analyzer (TMA).

Chapter 4 compiles all the results obtained from the experiment during mixing process, compaction and after sintering process using conventional and hybrid microwave sintering such as temperature profile of both sintering methods, micrographs, XRD patterns, tables and graphs of density, porosity, microhardness and grain size.

Chapter 5 discusses all the data in chapter 4 in term of effect of mixing speeds during mixing process, the comparison of conventional and hybrid microwave sintering methods, effect of compaction loads on sintered samples and the influence of Zn, Al, Cu and Mg element in Zn-Al alloys.

The research is concluded in Chapter 6 which outlines the most appropriate conditions for the application of microwave sintering for the manufacturing of Zn-Al products. Additionally, this chapter includes ideas for possible future work and recommendations in this field of research.

## CHAPTER 2

### LITERATURE REVIEW

#### 2.1 Powder Metallurgy

Powder metallurgy (P/M) is a process technology which parts are produced by compacting and sintering metallic and/or nonmetallic powders. P/M parts can be mass produced to net shape or near net shape. P/M parts are formed by a sequence of process as shown in Figure 2.1. The first steps are the selection of powders, followed by weighing and mixing process. The mixed powder is compacted by placing in the die under pressure. The green sample is placed in an oven and sintered in a controlled atmosphere at certain temperature to form metallurgical bonds between the powder particles. A secondary operation is carried out to improve the properties of sintered products.

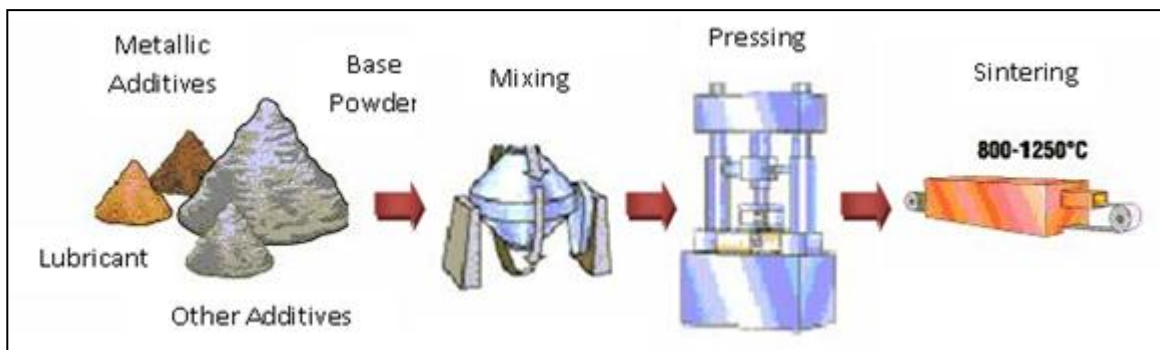


Figure 2.1: The steps involved in powder metallurgy process.

The P/M process is more competitive than other fabrication methods like casting, stamping or machining. It offers a number of advantages over other metalworking process such as:

- Eliminates or minimizes finish machining operation
- Eliminates or minimizes scrap losses
- Maintains close dimensional tolerances
- Avoid casting defects such as blow holes, shrinkage and inclusions
- Produces good surface finishes
- Provides predictable and consistent porosity
- Facilitates the manufacture of complex or unique shapes which would be difficult to produce with other metalworking processes
- Offers long term performance reliability in critical applications
- Energy saving

The biggest consumers of P/M parts are automotive industries. P/M components are used in auto engines and transmission parts such as gears, sprockets, pressure plates, cams and various structural components. However, powdered metals are not only utilized in components for automotive industries only, but also used for home appliances, business machines, military products and sporting goods.

## **2.2 Sintering**

Sintering is a processing technique used to produce density-controlled materials and components from metal or/and ceramic powders by applying thermal energy. Most metals are sintered at temperature 70 to 90% of their melting point. When compact mixture is composed more than one material, the sintering temperature may be above the melting temperature of one or more components (Tan, 2008).

The aim of sintering is to produce sintered parts with producible and if possible designed microstructure through control of sintering variables. Microstructural control means the control of grain size, sintered density and size and distribution of other phase include pores. Mostly, the final goal of microstructural control is to prepare a fully dense body with a fine grain structure.

Basically there are a few stages of sintering. Firstly, particle bonding is initiated at contact points. Then, contact points grow into necks and followed by the size reduction of pores between particles. Finally, grain boundaries developed between particles in place of the necked regions. Figure 2.2 shows stages of sintering on microscopic scale.

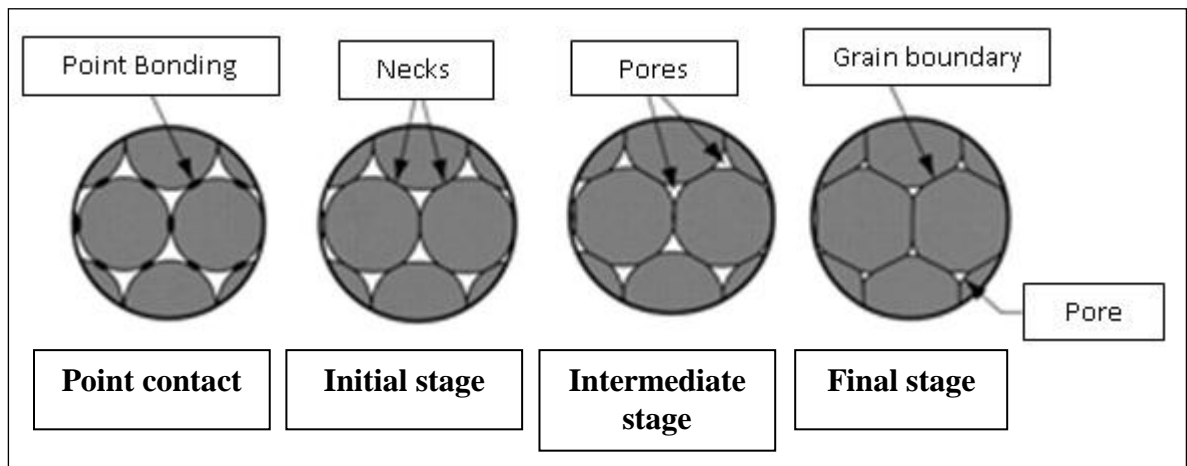


Figure 2.2: Stage of sintering on microscopic scale.

## 2.3 Electromagnetic radiation of microwave

Electromagnetic wave or also known as electromagnetic radiation produced by the motion of electrically charged particle. It is transport energy through empty space and stored in the propagating electric and magnetic field. Electric and magnetic fields oscillate together but perpendicular to each other and the electromagnetic wave moves in a direction perpendicular to both of the fields. Figure 2.3 shows the electromagnetic wave.

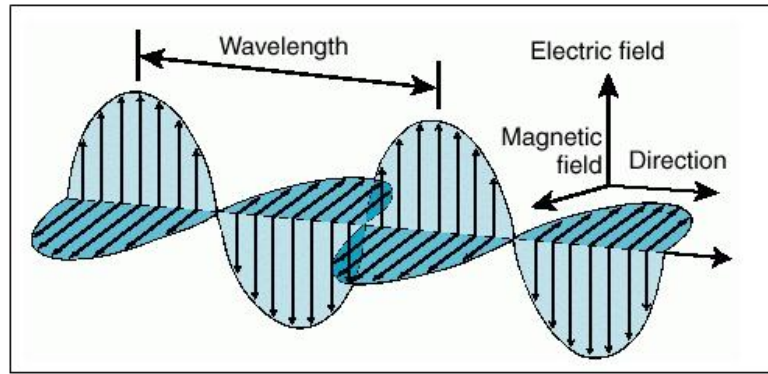


Figure 2.3: Electromagnetic wave.

Generally, electromagnetic radiation is classified by wavelength into radio, microwave, infrared, light, ultraviolet, X-rays and gamma rays. The range of all possible frequencies in electromagnetic wave is called electromagnetic spectrum as shown in Figure 2.4. Microwave is a part of electromagnetic spectrum with frequency between 300GHz and 300MHz and wavelengths ranging from 1mm to 1m in free space. There are two reasons of frequencies chosen for microwave heating. Firstly, they are in one of the industrial, scientific and medical (ISM) radio bands set aside for non-communication purposes and secondly, the penetration depth of microwaves is greater for these lower frequencies (Das et. al, 2008).

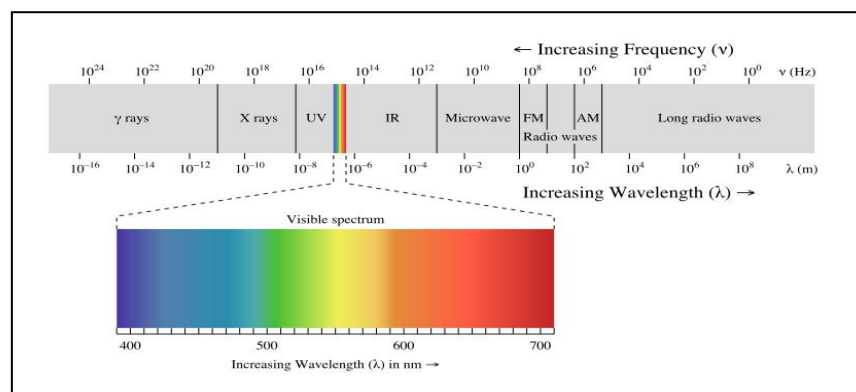


Figure 2.4: Electromagnetic spectrum.



## 2.4 Microwave-Materials Interaction

The capability of materials to absorb microwave energy is different. Based on the microwave-materials interaction, most materials can be divided into three categories as follows (David et. al, 2000):

- 1) **Transparent (low dielectric loss materials)** – microwave pass through with little
- 2) **Opaque (conductors)** – microwave are reflected and do not penetrate
- 3) **Absorbing (high dielectric loss materials)** – absorb microwave energy to a certain degree based on the value of the dielectric loss factor.

The proportion of energy that is transmitted, reflected or absorbed depends upon composition and physical properties of medium, wavelength or frequency of incident radiation and angle at which incident radiation strikes a surface. Figure 2.5 shows the microwave-materials interaction.

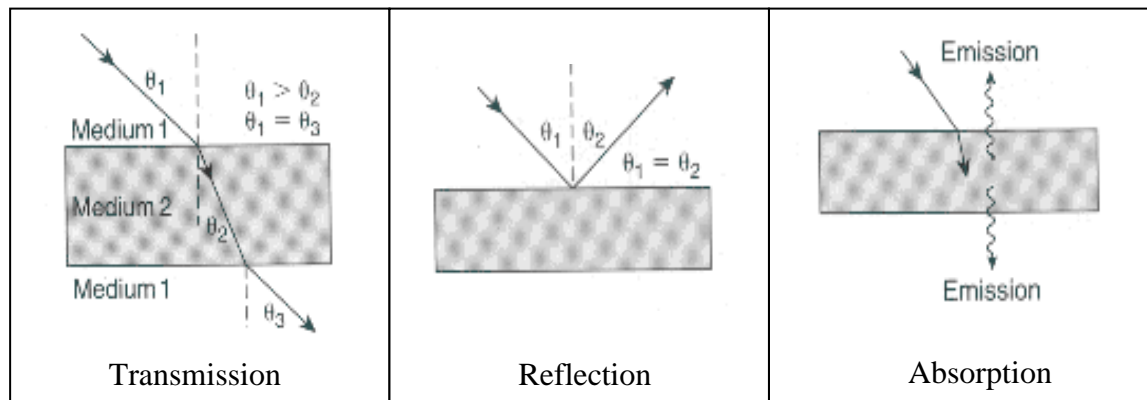


Figure 2.5: Categories of microwave-materials interaction.

Microwave energy is transferred to the materials by interaction of the electromagnetic field at the molecular level (Das et. al, 2008). The coupling of microwave energy in the medium depends on the dielectric properties of the materials to be heated

(Nuchter et. al, 2004). Two important parameters for microwave processing are power absorbed (P) and depth of penetration (D) (David et. al, 2000):

The power absorbed per unit volume, P (W/m<sup>3</sup>) is expressed as (Sutton, 1989):

$$P = \sigma |E|^2 = 2\pi f \epsilon_0 \epsilon_r \tan \delta |E|^2 \quad (\text{Equation 2.1})$$

where E (V/m) is the magnitude of the internal field,  $\sigma$  the total effective conductivity (S/m), f the frequency (GHz),  $\epsilon_0$  the permittivity of free space ( $\epsilon_0 = 8.86 \times 10^{-12}$  F/m),  $\epsilon_r$  the relative dielectric constant and  $\tan \delta$  is the loss tangent.

The penetration depth of microwaves (D) at which the incident power is reduced by one half is expressed as (Sutton, 1989):

$$D = 3\lambda_0 / 8.686\pi \tan \delta (\epsilon_r / \epsilon_0)^{1/2} \quad (\text{Equation 2.2})$$

where  $\lambda_0$  is the incident or free space wavelength.

The relative dielectric constant and the loss tangent are the parameters that describe the behavior of a dielectric material under the influence of the microwave field (Sutton, 1989).

## 2.5 Hybrid Microwave Sintering (HMS)

Pure microwave metal sintering required a long warming-up before the compact starts to couple with the microwave, which increase the risk of plasma formation in the cavity and lead to damage of microwave generator-magnetron (Tan, 2008). This problem was overcome by using hybrid microwave sintering which involves the combination of conventional and microwave energy source.

In hybrid microwave sintering, it was direct heating/sintering of the compact from microwaves forms one component and the radiative heating/sintering from the susceptor form the second component of the total heat imparted into the compacts (Gupta and Wong, 2005). It was two directional microwave assisted heating in sintering as microwave heat the sample from inside-outside direction while susceptor provides radiant heat from outside-inside direction. Figure 2.6 shows the concept of microwave hybrid sintering (Gupta and Wong, 2005).

Susceptor are useful for initial heating due to its ability to absorb electromagnetic energy and convert it to heat. In an earlier study, investigators indicated that similar heating occurs without using susceptors but the only difference is that with susceptors the overall heating is faster and fine microstructure was produced (Roy et. al, 1999).

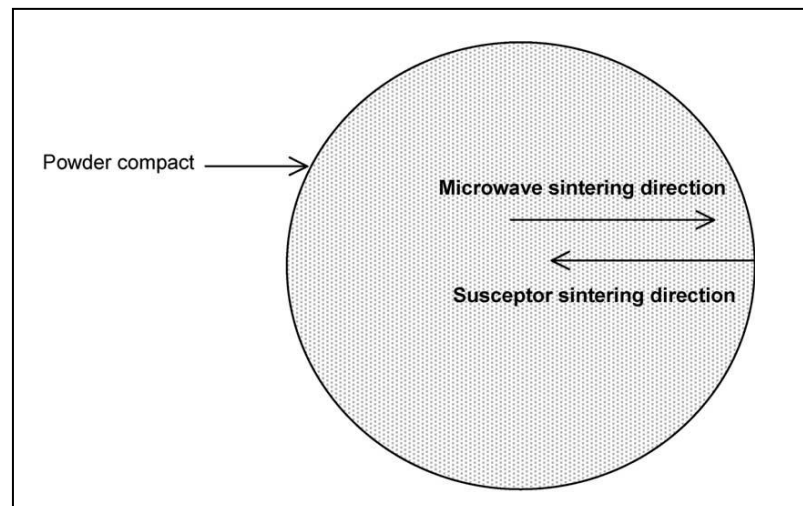


Figure 2.6: Schematic diagrams of two directional sintering concepts (Gupta and Wong, 2005).

## 2.6 Microwave Sintering of Metals

The application of microwave for the sintering of metals is a relatively new idea and limited work has been carried out. From the literature, only certain materials have been applied to microwave sintering such as ferrous alloys, copper alloys, aluminium alloys, magnesium alloy and composite alloy. The following section demonstrated the advantages of microwave sintering for some metals and metal matrix composites.

### *Ferrous alloys*

Ferrous alloys are the most commonly used metallic materials in various applications such as automobile, ships' hull and structural components for buildings.

The invention of sintered ferrous alloys using microwave was invented by a group of researchers from Penn State University (Roy et. al, 1999, Yang and German, 1999). In their studies, it was reported that microwave sintered specimen's posse's finer microstructure, higher densification, hardness, transverse rupture strength (TRS) and modulus rupture compared to conventional sintered sample. Table 2.1 shows the improvement in physical and mechanical properties of microwave sintered Fe-2Cu-0.8C and Fe-2Ni-0.8C iron steel samples.

It was also reported that non-uniform distribution of porosity was produced when sintered sample in a pure microwave system. This is due to the inverse temperature gradient found in the microwave heating (Yang and German, 1999 and Anklekar et. al, 2001). Meanwhile, by using hybrid heating, susceptors provided a faster heating rate and more uniform temperature profile, lead to uniform microstructure and improved mechanical properties (Gedevanishvili et. al, 1999 and Anklekar et. al, 2001).

Table 2.1: Physical and mechanical properties of microwave sintered FC-0208 (Fe-2Cu-0.8C) and FN-0208 (Fe-2Ni-0.8C) iron steel samples (Yang and German, 1999).

<b>Sample</b>	<b>Compaction pressure (MPa)</b>	<b>Sintering temperature (°C)</b>	<b>Density (g/cm<sup>3</sup>)</b>	<b>Hardness (HRB)</b>	<b>TRS (MPa)</b>
FC-0208-MS1	552	1170	7.01 ± 0.03	76.8 ± 1.6	963 ± 30
FC-0208-PM1	552	1120	7.00 ± 0.04	61.2 ± 0.4	865 ± 10
FC-0208-MS2	690	1230	7.20 ± 0.03	84.7 ± 1.1	1220 ± 33
FC-0208-PM2	690	1120	7.19 ± 0.03	62.0 ± 0.8	970 ± 10
FN-0208-MS3	552	1250	7.29 ± 0.03	71.8 ± 2.3	900 ± 10
FN-0208-PM3	552	1250	7.21 ± 0.02	66.5 ± 2.0	884 ± 4
FC-0208-PM4	552	1250	6.99 ± 0.01	72.9 ± 3.6	923 ± 14
FC-0208-PM5	690	1250	7.17 ± 0.02	74.3 ± 2.8	1070 ± 3

Studies by other researchers (Upadhyaya, 2002, Gupta and Wong, 2005) also revealed that microwave sintered metal powders can produce higher densification with a reduction of processing time. Veronesi et. al. (2003) reported that neck formation in the steel powder compacts started after 2 minutes in the microwave sintering and the temperature of samples reaches 1000°C within 4 minutes.

In another investigation on ferrous alloys (Petzoldt et. al, 2006), compacted MSP 1.5 Mo and Distaloy AE steel powder samples achieved higher density and hardness at lower sintering temperature in a microwave compared to conventional sintering as shown in Figure 2.7.

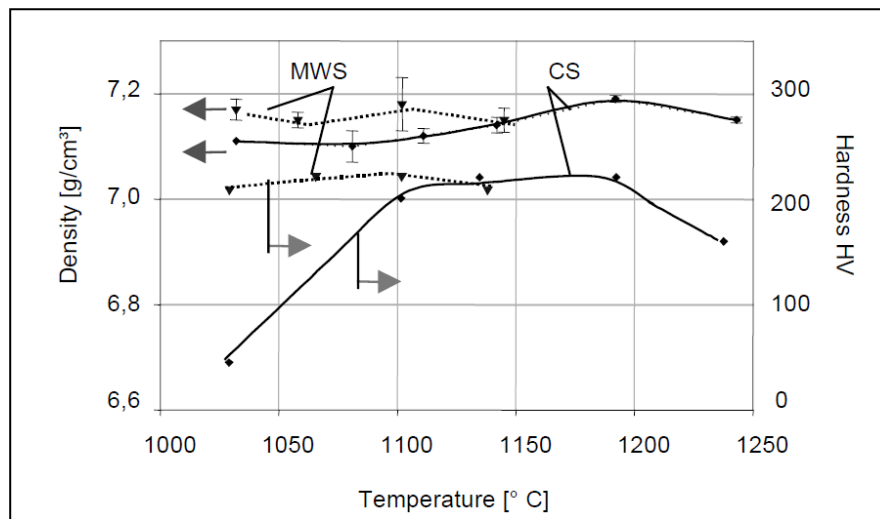


Figure 2.7: Densification and hardness of MSP 1.5 Mo tensile bars (Petzoldt et. al, 2006)

Panda et al. (2006) in their study on the effects of microwave and conventional sintering of ferritic (434L) and austenitic (316L) stainless steel reported that heating rate of microwave sintering is affected by the composition of the stainless steel powder. They revealed that ferritic stainless steel samples shown faster heating rate compared to austenitic stainless steel samples due to its coupling differences with microwave. The microwave sintered density of austenitic stainless steel compacts was lower than conventional sintered samples but the opposite trend to ferritic stainless steel, as shown in Table 2.2.

In 2006, the researcher further investigated by adding different weight percentage of yttria alumina garnet (YAG) on the densification and properties of 316L and 434L stainless steel using conventional and microwave sintering (Panda et. al, 2006 and Padmavathi et. al, 2006). As the results, the bulk hardness of microwave-sintered monolithic and YAG-reinforced 316L and 434L stainless steel were higher than the conventionally sintered samples at 1200°C but opposite trends to sintering at higher temperature, 1400°C. However, no explanation reported for this strange phenomenon.

Table 2.2: Effect of heating mode on the densification and mechanical properties of 316L and 434L stainless steel sintered at 1400 °C (Panda et. al., 2006)

	<b>Austenitic SS (316L)</b>		<b>Ferritic SS (434L)</b>	
	<b>CS</b>	<b>MWS</b>	<b>CS</b>	<b>MWS</b>
Sintered density, g/cm <sup>3</sup>	7.06	6.82	7.24	7.26
Densification parameter	0.31	0.14	0.61	0.63
Bulk hardness, HV	136	114	132	109
Strength, MPa	398	156	378	229
Elongation, %	63	3	29	5

### ***Copper alloys***

Copper is an important engineering material since it is widely used in its pure state and also in alloys with other metals. In its pure state it is the most important material in the electrical industry. It has high electrical conductivity and corrosion resistance and is easy to fabricate. Alloyed copper in the form of brass, and bronze is used extensively throughout the mechanical engineering industry.

A method to microwave copper metal was patented in 1990 by Sheinberg et. al, (1990). Compacted copper samples were heated by microwaves to 650°C in 35 minutes, and the end product produced a fine grain structure and uniform distribution of particles.

In 1991, Bescher and Mackenzie (1991) studied the heating rate of loosely packed copper-alumina composites. It was reported that the heating rate in microwave heating increases with the increasing weight percentage of copper from 20-80% and decrease thereafter due to the shielding effect. Gerdes and Willert-Porada (2004) also observed the heating rate increased with decreasing particle size.

Fang et. al. (2003) were successfully sintered nano copper pellets in microwave at sintering temperature 868-920°C for 5-20 minutes using a temperature ramp rate of 25-50°C. As a result, microwave sintered samples possess higher densification and finer microstructure compared to conventional sintering method as shown in Table 2.3.

Table 2.3: Comparison of processing conditions and properties of the sintered nano-Cu samples (Fang et. al. 2003)

Sintering process	Temperature (°C)	Time (min)	Density (g/cm <sup>3</sup> )		Crystallite (nm)	Coarsening (%)
			Green	Sintered		
Conventional	600	120	6.39	7.15	275	429
Conventional	700	120	6.43	6.60	382	635
Conventional	800	120	6.39	6.82	296	469
Microwave	868	5	6.42	7.33	71	36
Microwave	910	10	-	7.33	83	60
Microwave	920	20	6.35	7.38	88	69

In another study on Cu-12Sn alloy (Upadhyaya et. al, 2002 and Sethi et. al, 2003), the authors investigated the effects of sintering temperature and compaction pressure of premixed and prealloyed bronze on microwave and conventional sintering. The authors found that the heating rate of prealloyed bronze sample was faster than premixed bronze sample as shown in Figure 2.8. The difference of heating rate is due to anisothermal heating caused by the different absorption factors of the constituents inside the powders (Sethi et. al, 2003).



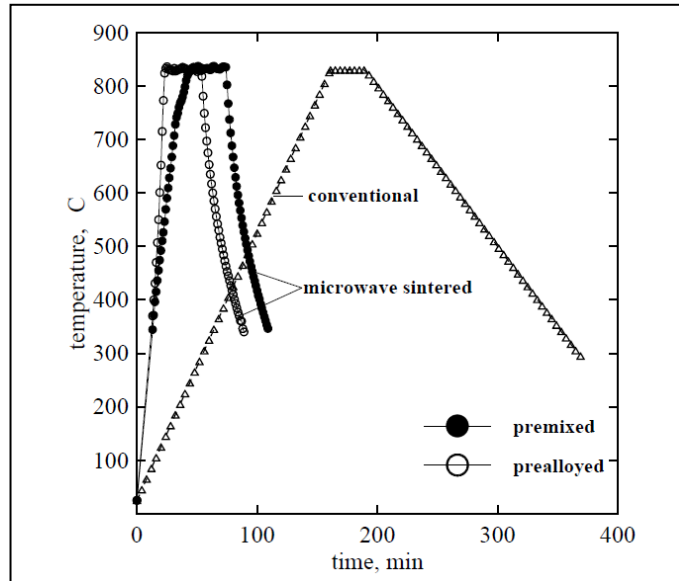


Figure 2.8: Thermal profile of conventional and microwave sintered Cu-12Sn alloy (Sethi et. al, 2003)

To study the effect of compaction pressure, the bronze was compacted in pressure between 150 - 600 MPa and sintered at temperature 775°C using microwave and conventional heating methods. It was reported that with increasing compaction pressure, slight densification in prealloyed bronze sample and swelling in premixed bronze sample for both sintering method as shown in Figure 2.9.

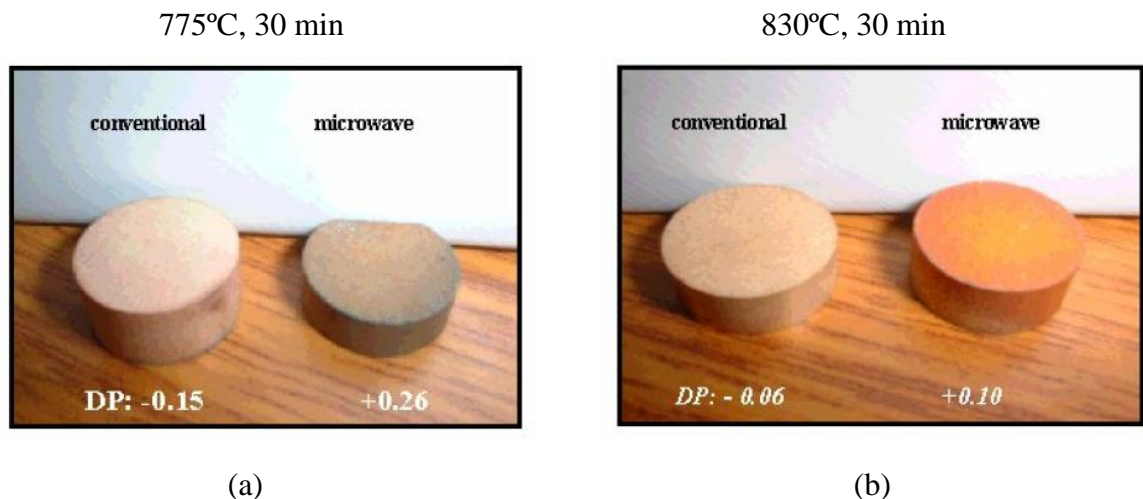


Figure 2.9: Photographs of the premixed Cu-12Sn compacts, conventionally and microwave sintered at (a) 775°C and (b) 830°C for 30 min compacted at 150 MPa. (Sethi et. al, 2003).

## ***Aluminum and Composites***

Aluminum is a lightweight metal with a range of properties such as has an excellent strength to weight ratio, resistance to oxidation and corrosion and usually used in the transportation, packaging and construction industries.

Bescher et. al. (1992) was carried out the microwave heating of pure aluminum (20  $\mu\text{m}$ ) with addition of 10-30 wt.% of SiC (1  $\mu\text{m}$ ) particles. The authors reported the addition of SiC particles enhanced the heating rate of composites and hardness obtained in microwave heating is similar with conventional sintered samples, as well as microstructure. Table 2.4 shows the results produced in this study.

Table 2.4: Density and hardness of Al/SiC composites

<b>Material</b>	<b>Density(% theoretical)</b>	<b>Hardness (VHN)</b>
90 % Al / 10 % SiC	98	$60 \pm 5$
80 % Al / 20 % SiC	96	$63 \pm 5$
70 % Al / 30 % SiC	93	$59 \pm 5$

Leparoux et. al (2002) investigate the influence of SiC particle size reinforced with pure aluminum on microwave sintering and it was found that heating rate of smaller SiC particle was significantly faster compared to larger particle size. The microstructure of the composite revealed that the degree of sintering is higher in microwave sintered sample compared to conventional sintered samples.

Comparison of pure aluminum properties sintered using microwave and conventional method was done by Gupta and Wong (2005). The result revealed that microwave sintered samples improved densification, lower porosity level, higher hardness, 0.2% yield strength and ultimate tensile strength compared to conventionally sintered aluminum.

Thakur et. al (2007) was proposed two directional microwave assisted sintering of Al/(Ti + SiC) hybrid composite. Addition of SiC nanoparticulate to Al-Ti formulations increasing micro and macro hardness, yield strength and ultimate tensile strength.

### ***Magnesium and Composites***

Magnesium is the lightest structural metal currently available in the world. It is approximately 34% lighter by volume than aluminum and 50% lighter than titanium. Besides light-weight construction, a few of the other advantages that magnesium offers are: excellent fatigue resistance, denting and buckling resistance, and the highest known damping capacity of any structural metal.

Microwave sintering of magnesium was first reported by Gupta and Wong (2005) which they used hybrid heating method in sintered magnesium billet. Microwave sintered samples improved hardness and tensile properties compared to conventionally sintered samples. The sintering time also reduced to 85% with the use of hybrid microwave heating. No oxides or other impurity phases were detected in the X-ray diffraction of magnesium compact after microwave sintering.

Further work was carried out by the research group to synthesis different types of reinforcements in magnesium based composite using hybrid microwave heating. Mechanical characterization in term of hardness and tensile strength of microwave sintered samples revealed superior properties compared to conventional sintered samples.

### ***Tungsten Alloys***

Tungsten has highest melting point and usually used for high temperature applications and wear resistant materials in the form of tungsten carbide. It requires high

sintering temperatures ( $T > 2773$  K) and relatively long soaking time to achieve densities above 90% of theoretical density.

Prabhu et al (2008) was carried out microwave sintering of tungsten powder with average particle size 5-7  $\mu\text{m}$  at maximum sintering temperature, 2073 K. The density of microwave sintered was improved to 93% of theoretical density, higher hardness and shorter processing time.

This chapter presents briefly summarizes the researches have been done in microwave sintering of metal and alloys. It is clear that microwave sintering offered great beneficial results in term of improved density, hardness, strength, finer grain size and uniform microstructure compared to conventional sintering method.

## CHAPTER 3

### EXPERIMENTAL PROCEDURE

Experimental works were carried out to achieve the objectives of the research. This research was divided into three main stages; P/M sample preparation, sintering process and data analysis. Figure 3.1 shows a flowchart summarizing the methodology of the experiment.

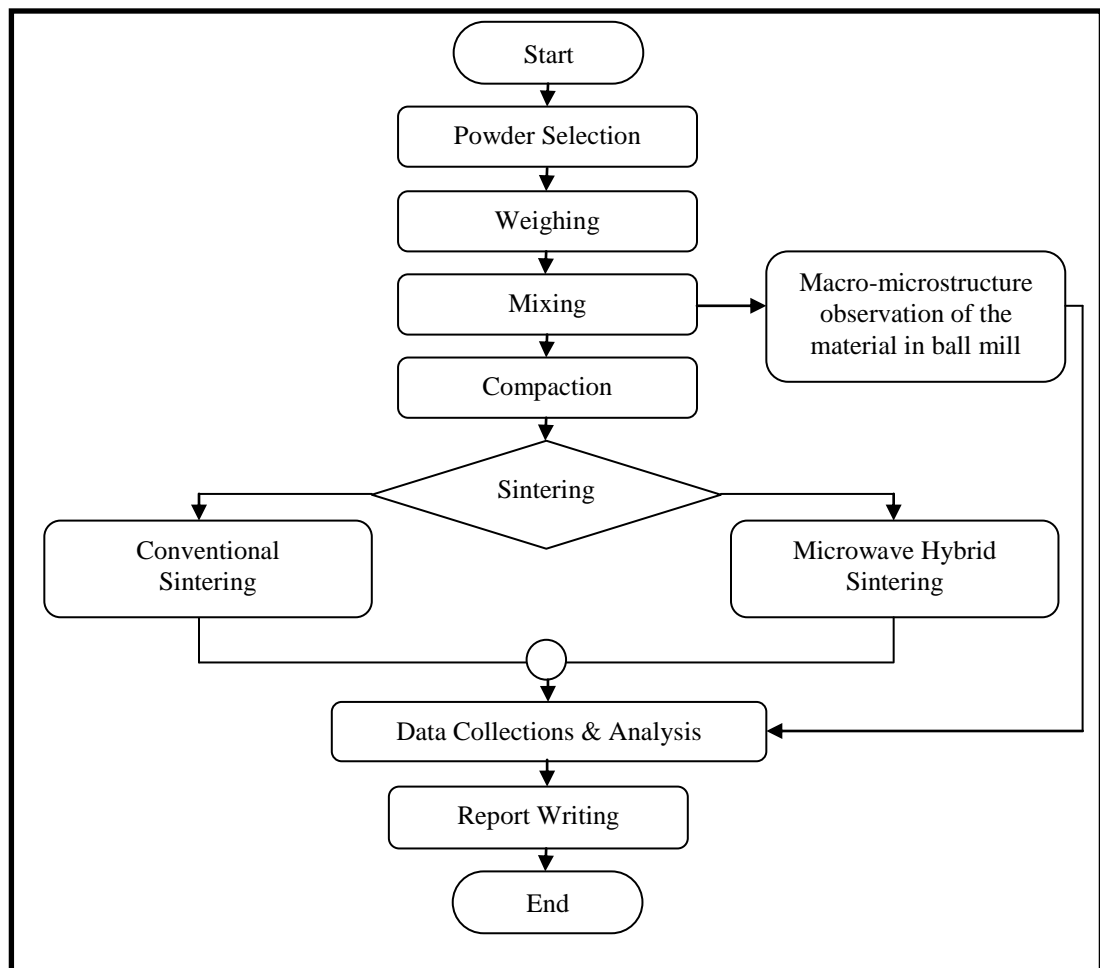


Figure 3.1: The flowchart of experiment.

## 3.1 Specimen Preparation

### 3.1.1 Powder Selection

Zinc-base alloy is selected for this project due to three main reasons. First, it was a low melting point temperature materials, ranging from 375 to 484°C. Second, this was a continuity study from a previous researcher in University of Malaya who was successfully sintered pure Zinc (Zn) via a hybrid microwave sintering (HMS) system. Lastly, Zinc-Aluminum (Zn-Al) alloys was the first time applied to be sinter using HMS system.

### 3.1.2 Powder Weighing

In this research, three compositions of Zn-Al alloys are used as shown in Table 3.1. These compositions are based on the standard composition of casting process. Figure 3.2 shows the pure powder elements used to make these alloys through P/M technique.

Table 3.1: Composition of zinc-aluminum alloy (www.matweb.com).

Name of Zinc Aluminum Alloy	Element composition (wt.%)			
	Zinc (Zn)	Aluminum (Al)	Copper (Cu)	Magnesium (Mg)
ZA-27	Balance	27	2	0.015
ZA-12	Balance	11	1	0.025
ZA-8	Balance	8	1	0.020

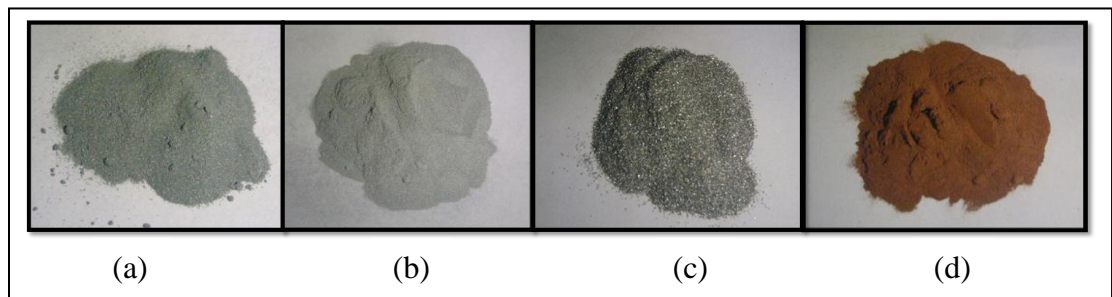


Figure 3.2: (a) Zn-150  $\mu\text{m}$ , (b) Al-60  $\mu\text{m}$ , (c) Mg-250  $\mu\text{m}$ , (d) Cu-10  $\mu\text{m}$ .

### 3.1.3 Powder Mixing

Mixing is a process of combination powders of different chemistries and its main purpose is to produce a uniform distribution of particles sizes and shapes. The variables involved in mixing powders include the materials, particle sizes, mixer type, relative powder volume in the mixer, speed of mixing, shear and time of mixing. In this research, planetary ball mill (Retsch PM400) is used as a mixer (Figure 3.3). It is chosen due to its mechanism where the difference speeds between the balls and grinding jars produces an interaction between frictional and impact forces, which releases high dynamic energies. The interplay between these forces produced the high effective mixing compared to other mixer.

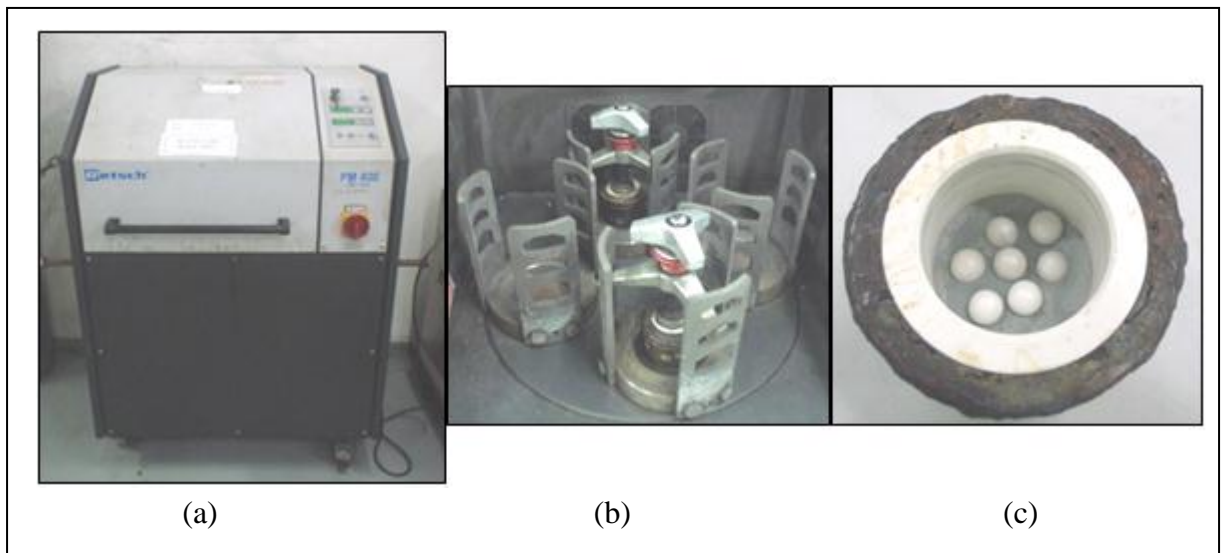


Figure 3.3: (a) Retsch Planetary ball mill (PM400), (b) Ball mill's jar were clamp inside the planetary ball mill, (c) Powders and zirconia balls inside the jar.

#### *Selection of mixing speed*

Mixing speed is one of main variables in the mixing process. In this research, two different speeds are used to select the best mixing speed of Zn-Al alloys as shown in Table 3.2. No lubricants used during the mixing process in a planetary ball mill. From the experimental results, 100 rpm is chosen as the suitable mixing speed of Zn-Al alloys. The

details of experimental results are discussed in Chapter 5. Then, all the compositions of Zn-Al alloys are mixed at lower rpm; 100 rpm as shown in Table 3.3.

Table 3.2: Parameters used in selection of mixing speed.

Specifications and Parameters	Alloy composition (wt.%)	Mixing speed (rpm)	Mixing time (hours)	Ball to powder ratio
Planetary ball mill (Retsch PM400)	Zn-27Al-2Cu-0.015Mg	<b>100</b>	4	7:1
	Zn-27Al-2Cu-0.015Mg	<b>200</b>	4	7:1

Table 3.3: Parameters used in mixing process of Zn-Al alloys.

Specifications and Parameters	Alloy composition (wt.%)	Mixing speed (rpm)	Mixing time (hours)	Ball to powder ratio
Planetary ball mill (Retsch PM400)	Zn-27Al-2Cu-0.015Mg	100	4	7:1
	Zn-11Al-1Cu-0.025Mg			
	Zn-8Al-1Cu-0.020Mg			

### 3.1.4 Powder Compaction

The main goal of compaction is to impart uniform density. In this study, the mixed powders are cold compacted to pellets,  $3 \pm 0.02$  mm height with  $14.8 \pm 0.002$  mm diameter in average by using cylindrical die as shown in Figure 3.4. The samples are pressed in three different loads; 6, 8 and 10 tons by using hydraulic press machine (Model Specac) with holding time; 5 minutes. The work part after compaction called a ‘green compact’, which green means not yet fully processed. The density of the compacted powder is directly proportional to the amount of loads applied. Increasing the compaction loads will increase the density of compact powder.



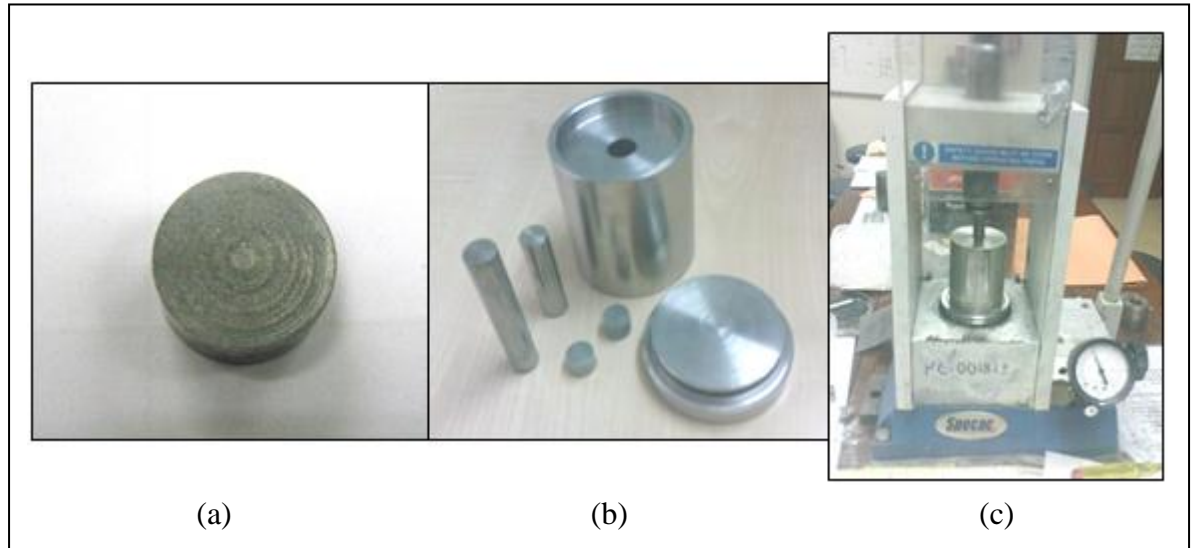


Figure 3.4: (a) Green compact (b) Die and punch (c) Hydraulic Press Machine

## 3.2 Sintering process

Sintering phenomenon is a process that a powder compact becomes a consolidated body due to thermal activation of powder particles and its driving force is a decrease of surface energy (Kim et. al, 2002). Out of the 18 samples are prepared from the die. Table 3.4 shows the design of experiment for Zn-Al alloys sintered in both sintering methods.

Table 3.4: The design of experiment for Zn-Al alloys.

<b>Alloy Composition</b>	<b>No. of sample</b>	<b>Compaction loads (tons)</b>	<b>Sintering method</b>	<b>Sintering temperature (°C)</b>
ZA 27	1	6	Conventional	360
	2		Microwave	
	3	8	Conventional	
	4		Microwave	
	5	10	Conventional	
	6		Microwave	
ZA 12	7	6	Conventional	360
	8		Microwave	
	9	8	Conventional	
	10		Microwave	
	11	10	Conventional	
	12		Microwave	
ZA 8	13	6	Conventional	360
	14		Microwave	
	15	8	Conventional	
	16		Microwave	
	17	10	Conventional	
	18		Microwave	

### 3.2.1 Conventional Sintering

Elite Chamber Furnace, model BSF 1216-2408CP (Figure 3.5) with maximum heating temperature up to 1100°C is employed for conventional sintering. The heating and cooling rate were set to 5°C/min and holding time; 30 minutes in order to avoid thermal shock to the equipment. No inert gas applied during conventional sintering as to be comparing with hybrid microwave sintering environment.



Figure 3.5: Elite Chamber Furnace.

### 3.2.2 Hybrid Microwave Sintering

In this research, a Sharp R989MS domestic microwave oven is modified into the hybrid system to sinter the sample. It had 900W output power and frequency of 2.45 GHz. A hybrid microwave sintering technique is attempted by employed Silicon Carbide (SiC) powder as susceptor and crucibles setup to separate between specimen and SiC powder. The schematic diagram of experimental set up is shown in Figure 3.6. This hybrid heating methods results in more uniform temperature gradient within the sample and circumvents the disadvantages of heating using either conventional or microwaves heating only (Kotecha et. al 2008).

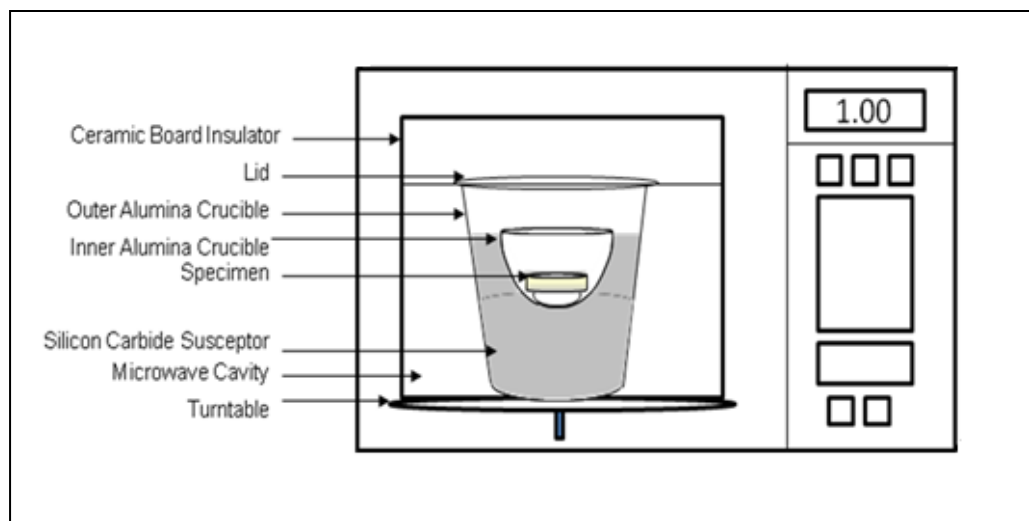


Figure 3.6: Schematic diagram of hybrid microwave sintering system.

### 3.2.2.1 Crucible

The functions of the crucibles are acted as susceptor and sample container and also as an additional heating element to absorb microwave energy. There were a few types of crucible materials in the market; Alumina ( $\text{Al}_2\text{O}_3$ ), Zirconia ( $\text{ZrO}_2$ ), Quarts ( $\text{SiO}_2$ ), porcelain etc. In this hybrid microwave sintering setup, two size of Alumina crucibles were used; 250 ml as outer crucible and 100 ml as inner crucible. Alumina material is chosen as crucibles due to its high resistance temperature up to  $1750^\circ\text{C}$ , highly resistant to chemicals, alkalines and other fluxes. Besides that, it has the ability to provide thermal insulation and good thermal shock during microwave sintering process (Azrina Arshad, 2010). Figure 3.7 shows the 100 ml and 250 ml of Alumina crucibles.

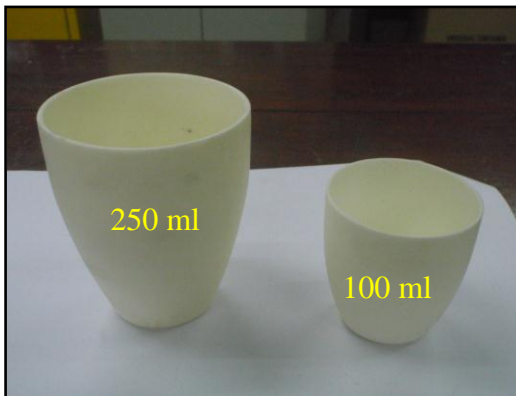


Figure 3.7: Alumina crucibles.

### 3.2.2.2 Susceptor

The main function of susceptor was to initiate raising the temperature of the compact and they usually couple very well with the microwaves (Mondal et. al, 2009). In hybrid microwave sintering, there were two ways of heating directions. First, microwave heat the sample from inside-outside and secondly, susceptor provides radiant heat from outside-inside direction. The parameter determining the coupling property is the dielectric loss factor where the high loss factor materials will couple well with the microwaves.

Dielectric loss factor is the product of dielectric constant and tangent for the dielectric loss angle. SiC powder was chosen as susceptor due to its high dielectric loss factor and refractory properties (Zhao et. al, 2000) compared to others ceramics materials such as alumina ( $\text{Al}_2\text{O}_3$ ), zirconia oxide ( $\text{ZrO}_2$ ) and silicon nitride ( $\text{Si}_3\text{N}_4$ ) which have a low loss factor.

In the early of this research, nano particle size of SiC powder is used as susceptor with the assumption, small particle size will lead to accelerate the heating rate and better microwave absorption (Zhao et. al, 2000). However, after using 50 nm particle size of SiC powder, within 5 minutes heating, the sample start molten and solidified. The experiment results were discussed in Chapter 4. Then, the particle size of SiC powder is changed to 75  $\mu\text{m}$  which provide more stable temperature profile. 100g amount of SiC is chosen due to previous researcher stated that higher susceptor amount will lead to higher sintering rate (Gupta and Wong, 2007). Figure 3.8 shows 100g of SiC powder inside the crucibles.

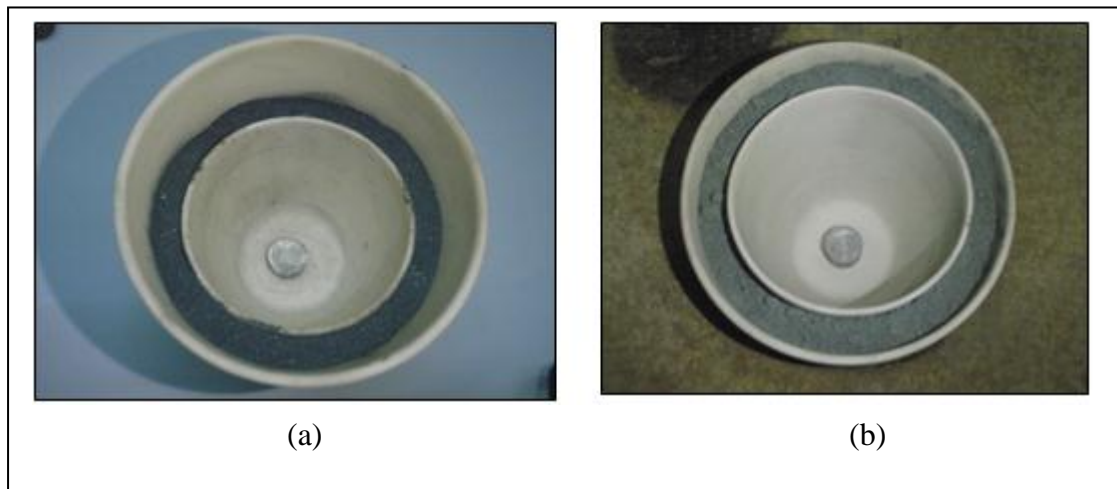


Figure 3.8: 100g of SiC powder with (a) 75  $\mu\text{m}$  (b) 50-60 nm.

### 3.2.2.3 Ceramic Insulation Box

An insulation box is another critical component for hybrid microwave sintering setup, besides susceptor. The function was to reduce the rate of heat transfer or prevent heat loss. Low density and very low dielectric loss are required for the box to make it microwave transparent (Fall et. al, 2002). In this study, ceramic fibre insulation box (Mackim Industries Sdn. Bhd) are used due to its low thermal conductivity, excellent shock resistance and superior corrosion resistance. Besides that, it has ability to be stable at high temperature for continuous use at temperature up to 1260°C. Figure 3.9 shows the steps of preparing the insulation box which used in the hybrid microwave sintering system.

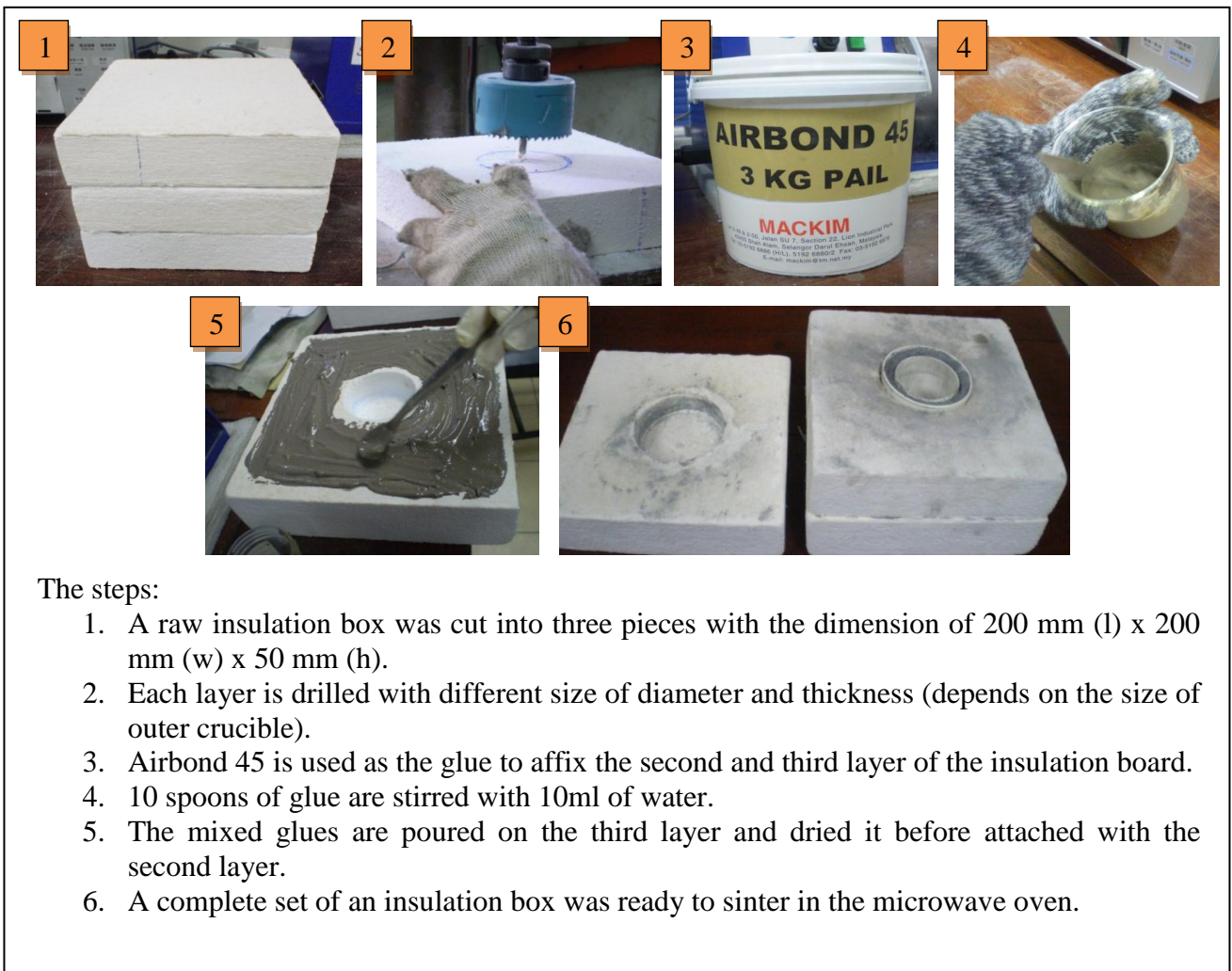


Figure 3.9: The steps of preparing a set of an insulation box.

### 3.3 Measurement Techniques and Calculation

#### 3.3.1 Temperature Measurement

Temperature calibration of the microwave sintering setup is performed using K-type thermocouple thermometer (Model: Testo 925) with accuracy of  $\pm (0.5^{\circ}\text{C} + 0.3\% \text{ of mv})$ . A surface probe is used for better stability at high temperature. Figure 3.10 shows the thermocouple and the surface probe.



Figure 3.10: Thermocouple Thermometer.

#### 3.3.2 Dimensional Changes

The dimensional change of sintered compacts is influenced by several factors, including particle size, density, composition, sintering time and temperature, cooling rate and microstructure. In this study, dimensional changes of diameter and thickness of microwave and conventional sintered samples are measured using an electronic digital vernier caliper (Model: Mitaka), as shown in Figure 3.11. The dimensional changes are calculated using Equation 3.1.

$$\% \text{ Dimensional changes} = \frac{D_s - D_g}{D_s} \times 100$$

Equation 3.1

where:

$D_s$  = Diameter after sintered

$D_g$  – Diameter of green compact



Figure 3.11: Electronic digital vernier caliper.

### 3.3.3 Density

The density of green sample is calculated from the sample mass and volume. Meanwhile, the density of the sintered samples is determined by using liquid displacement method, Archimedes' technique. Equation 3.2 shows the Archimedes formula. An electronic balance (Model: Shimadzu AY220) is used to determine the density of sintered sample as shown in Figure 3.12.



$$\text{Density} = \left[ \frac{A}{A - B} \right] \times \rho$$

Equation 3.2

where:

A = Mass of specimen in air

B = Mass of specimen in water

$\rho$  = Density of water at given temperature

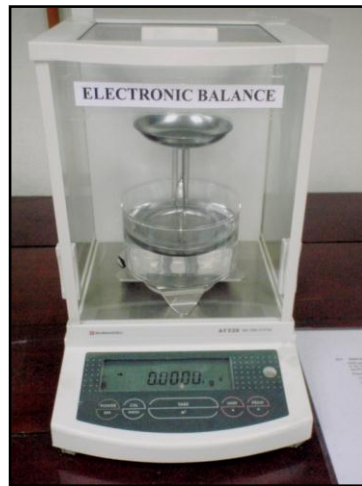


Figure 3.12: Electronic balance.

### 3.3.4 Porosity

The porosity is a controllable function of the raw material and processing techniques. The porosity of sintered sample is calculated using the water saturation method (Equation 3.3). After sintering, the sample is immersed in boiling water at temperature 100°C for 30 minutes and put in the vacuum jar for 12 hours. Figure 3.13 shows the magnetic hot plate used for porosity process.

$$\% \text{ Porosity} = \left[ \frac{W_s - W_d}{W_s - W_{ss}} \right] \times 100$$

Equation 3.3

where:

$W_s$  = Saturated weight of the specimen in air

$W_d$  = Specimen in dry air

$W_{ss}$  = Saturated weight of the specimen when submerged in water



Figure 3.13: Magnetic Hot Plate.

### 3.3.5 Microhardness

Microhardness is the hardness testing of materials with low applied loads. In this study, a microhardness tester (Model: Shimadzu HVM-2 series) is used to determine the Vickers hardness (HV) on sintered samples (Figure 3.14). In microhardness testing, a diamond indenter of specific geometry is impressed into the surface of the test specimen using a known applied force. The test load used to indent the Zn-Al alloys samples were 5 Newton with 20 seconds of dwell time.

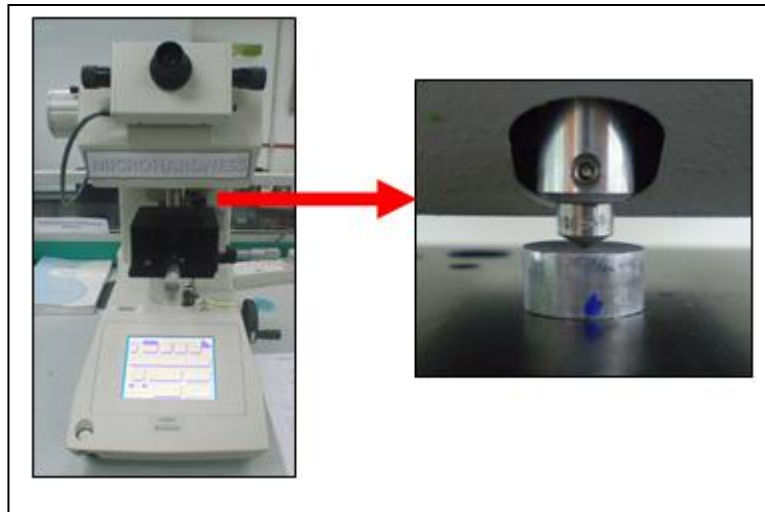


Figure 3.14: Microhardness tester.

### **3.4 Metallographic Examination**

Metallographic study is performed to determine the microstructure and content of zinc-based alloy. In sequence, the preparation steps of metallographic specimens including sectioning, mounting, grinding, polishing, etching and microscopic examination.

#### **3.4.1 Specimen Preparation**

##### ***Sectioning and Cutting***

Proper sectioning is required to minimize damage, which may alter the microstructure and produce false metallographic characterization. Specimens were cut using low diamond speed saw machine (Model: Buehler), as shown in Figure 3.15(a) meanwhile Figure 3.15 (b) shows the specimen sectioning before and after cutting.

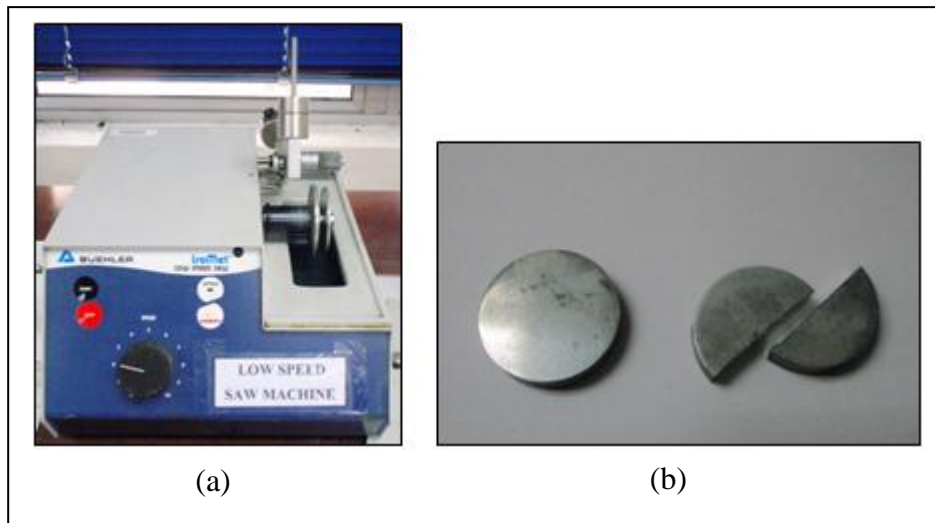


Figure 3.15: (a) Low diamond speed saw machine (b) Specimen sectioning.

### ***Mounting***

The functions of mounting were to improve handling of irregular shaped samples and fills voids in porous materials. There are two types of mounting, hot and cold mounting. In this study, specimens are mounted using cold mounting technique. These mounting compounds were consists of two main components, resin and hardener with ratio 8:2. After mixed, it will be pouring over a specimen that is positioned face down in a cold mounting ring. Figure 3.16 shows the steps of cold mounting process.



Figure 3.16: Basic steps of cold mounting process.

### ***Grinding and Polishing***

Grinding is required to planar the specimen and reduce the damage created by sectioning. This step is accomplished by decreasing the abrasive grit/particle size sequentially to obtain surface finishes that are ready for polishing. For ductile materials such as zinc alloy, the steps are started from 800, 1200, 2400 and 4000 grit Silicon Carbide (SiC) grinding paper to reduce scratches. Polishing stage with 5-micron suspended alumina oxide particles is carried out at a slower speed of 180 rpm using a napped cloth. Figure 3.17 shows a grinder and polisher machine (Model: Buehler).



Figure 3.17: Grinder and polisher machine.

### ***Etching***

The purpose of etching is to optically enhance microstructural features such as grain size and phase features. Table 3.5 shows the etchant used for zinc alloy.

Table 3.5: Zinc alloy etchant

Etchant	Concentration	Condition
Distilled water	100 ml	A few minutes
Acid Hydrochloric (HCl)	20 ml	

### 3.4.2 Microstructural examination

#### *Optical Microscope (OM)*

The microstructure of sintered samples are observed using Optical Microscope (Model: Olympus) starting at low magnification 50x to 100x.

#### *Field Emission Scanning Electron Microscope (FESEM)*

The Field Emission Scanning Electron Microscope (Model: Ziess) is used to observe microstructure of sintered samples at low and high magnification started from 100x to 1000x.

#### *Grain size measurement*

The grain sizes of sintered Zn-Al-Cu-Mg alloy are determined on thermally etched specimens from scanning electron micrographs using the Linear Intercept Method (ASTM E112 Standard). It is calculated from the mean intercept lengths between grain boundaries and the selected measurement line pattern.

The basic steps of the procedure are as below:

- i. Draw a line of length,  $L$  (mm) randomly on the micrographs.
- ii. Count the number of grains,  $N$ , intercepted by the line.
- iii. Obtain  $N_L$  by divide the number of grains,  $N$  with the test line length,  $L$  and multiple with micrograph magnification.
- iv. The ASTM grain size number is given as

$$n = -3.3 + 6.65 \log_{10} (N_L) \quad \text{Equation 3.4}$$

where  $N_L$  is given in  $\text{mm}^{-1}$ .

### ***Energy Dispersive X-ray Spectrometer (EDS)***

The FESEM used in this work also features a Ziess electron dispersive x-ray spectrometer (EDS) which can be used to ascertain the elemental composition of the portion of a sample being visualized.

### ***X-ray Diffraction (XRD)***

X-ray diffraction (XRD, Model: X'Pert PRO MRD) is used to characterize the composition of sintered samples and also to determine the phase constitution of samples after sintering (using  $\text{CuK}\alpha$  radiation).

## **3.5 Thermo Mechanical Analyzer (TMA)**

Thermo Mechanical Analyzer (Model: Shimadzu TMA-60H) is used to measure the coefficient of thermal expansion (CTE) of sintered sample (Figure 3.18). In this experiment, the load force used; 5 N and a constant heating rate;  $10^\circ\text{C}/\text{min}$ . Samples prepared for TMA test should have standard specifications (size, shape). Therefore, the samples of 5 mm diameter and 10 mm height are prepared for the investigation. Changes in the length of samples as a function of temperature in the  $50\text{--}400^\circ\text{C}$  interval are measured.



Figure 3.18: Thermo Mechanical Analyzer.

## **CHAPTER 4**

### **RESULTS**

The goal of this research is to make ZA8, ZA12 and ZA27 alloys from powder elements (P/M steps) and study its sintering behavior by using hybrid microwave sintering method and compared with the conventional sintering. Therefore, this chapter is divided into two sub-chapter; 4.1 and 4.2. Sub-chapter 4.1 will show the results of thermo-mechanical interaction between the powders in the process of selecting the best mixing speed of the Zn-Al alloy. Meanwhile, sub-chapter 4.2 will compile the results of hybrid microwave sintered samples as well as conventional sintered samples.

#### **4.1 Thermal mechanical during mixing process.**

##### **4.1.1 Introduction**

In this experiment, ZA27 alloy is used to determine the suitable mixing speed of Zn-Al-Cu-Mg powders. The powders are mixed at different speeds; 100 and 200 rotations per minute (rpm). However, after run 200 rpm of mixing speed, a thin layer and thorn shape feature are observed on the zirconia balls which shown very unique phenomena. Optical microscope (OM), field emission scanning electron microscope (FESEM), Electron Dispersive X-Ray Spectroscopy (EDX) and X-Ray Diffraction (XRD) are used to analyze the mechanism of this thermo-mechanical interaction.



### 4.1.2 Macroscopic features

Figure 4.1 shows the condition of powders and zirconia balls before and after mixing with speeds 100 and 200 rpm. Figure 4.1(c) shows that the zirconia balls have reacted with the elements and produced a thorn shape feature covered the entire surface of the balls. The rest of the powders were joined and made big particles in different shapes and sizes.

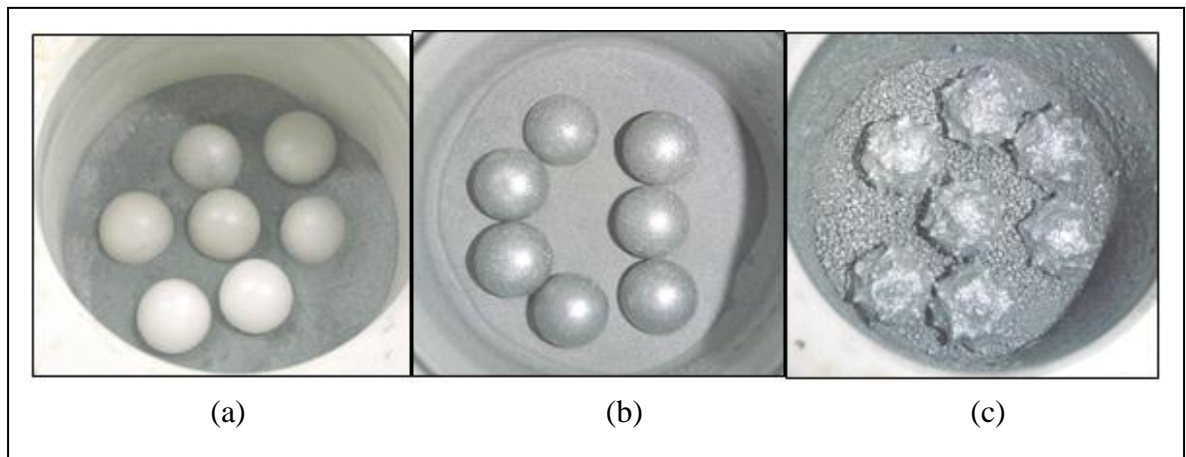


Figure 4.1: Zn-Al-Cu-Mg powders (a) before milling, (b) after milling 100 rpm and (c) after milling 200 rpm

### 4.1.3 Microstructure analysis

#### *XRD Pattern*

The composition of the thorn and powders are studied by XRD. In this step, some of the thorns are scratched and collected from the surface of the balls for XRD characterization. The result is shown in Figure 4.2. The figure shows the presence of two elements of Zn and Al that have highest fractions in the initial mixture.

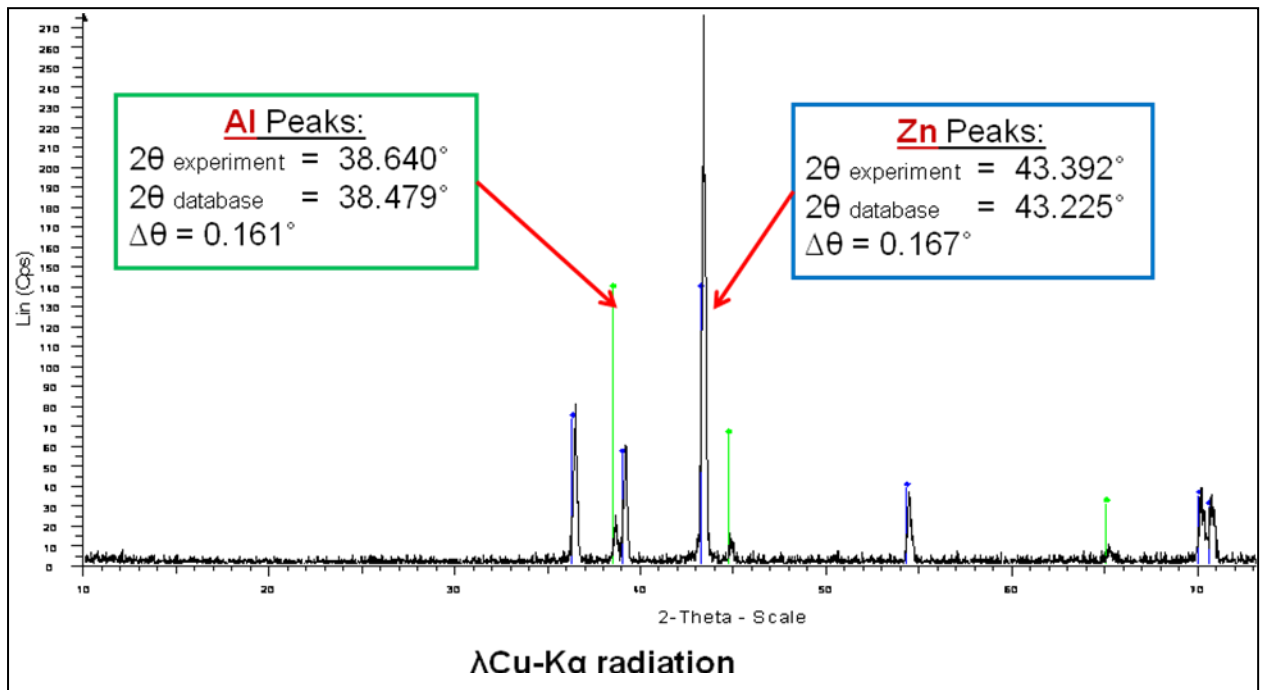


Figure 4.2: XRD pattern of scratched thorns grown on the zirconia balls.

### *Optical Microscope*

Distribution of elements in the interface between ball and grown layers are investigated after etching the cross section of a cut zirconia ball by optical microscope. Diluted Hydrochloric acid (HCl) in distilled water used as an etchant. A typical result is shown in Figure 4.3. Four different phases (red, brown, green and yellow) can be distinguished easily in the figure.

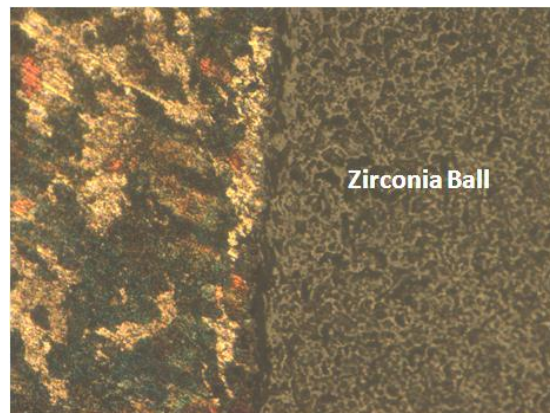


Figure 4.3: Distribution of Zn, Al, Cu, and Mg in the interface between zirconia ball and grown layer after etching.

### ***Element mapping by FESEM***

Distribution and diffusion of elements in the region near to the interface is studied by elemental Scanning Electron Microscope (SEM) mapping in more details. Figure 4.4 shows distribution of Zn, Al, Cu and Zirconia (Zr) in yellow, red, blue and green colors, respectively.

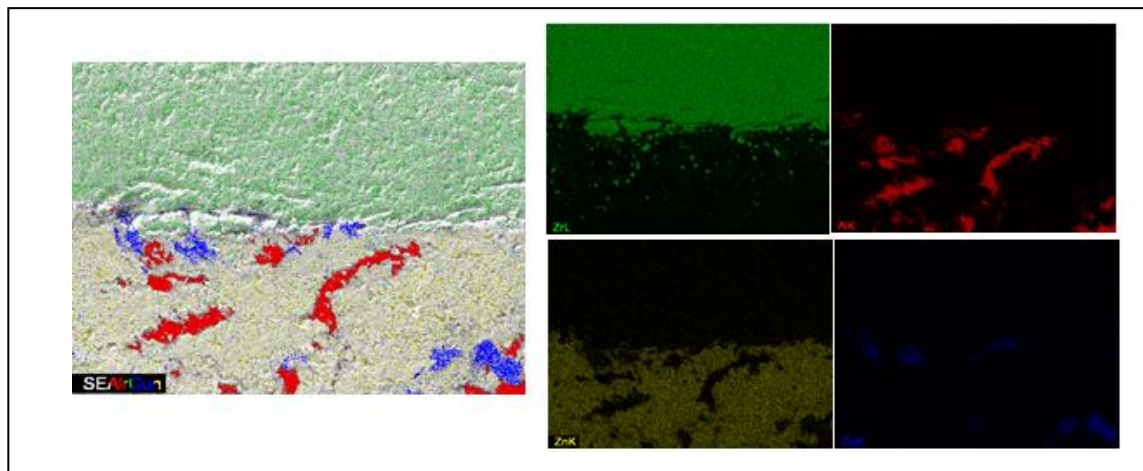


Figure 4.4: Elemental SEM mapping has detected Zn, Al, Cu and Zr in the region.

### ***EDX Characterization***

The EDX characterization of elements in the regions shows the presence of Zn, Cu, Zr, O, Al, and C elements (Figure 4.5). The layer grown on the surface of the zirconia balls majorly is covered by Zn and Al (Figure 4.6). The Mg and Cu were not significantly detected on the grown layer.

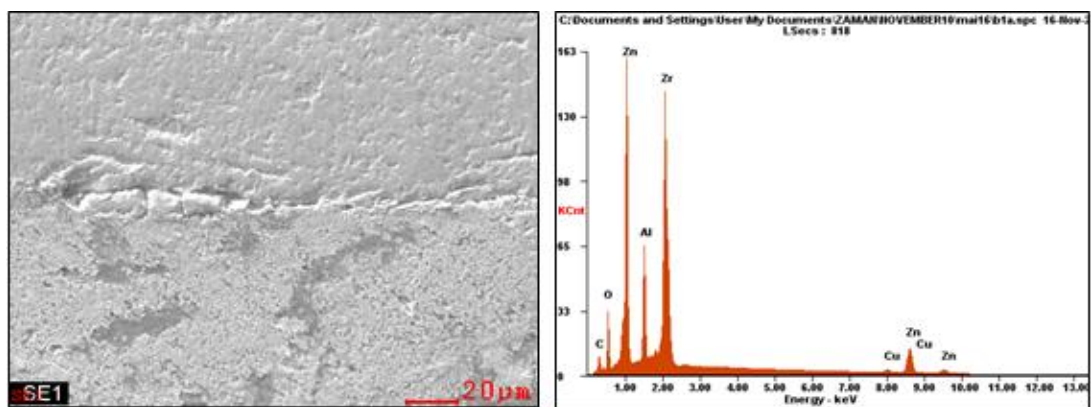


Figure 4.5: EDX characterization of elements in the region.

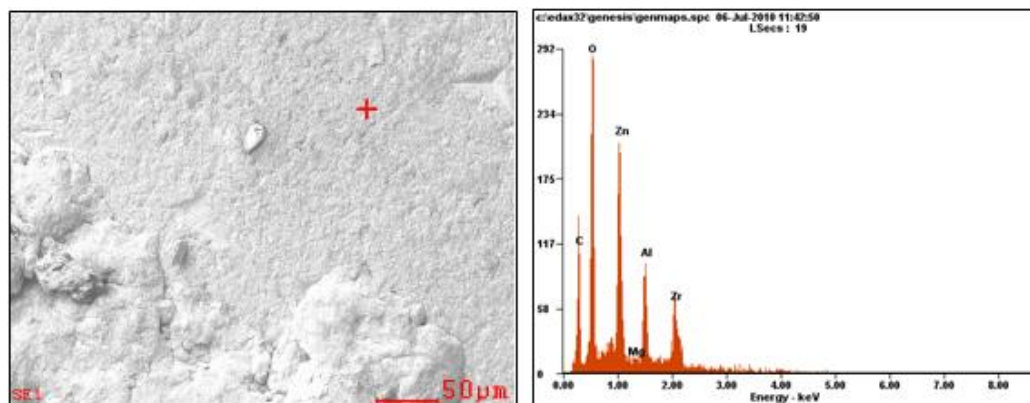


Figure 4.6: EDX on the thin layer covered the surface of the ball.

#### 4.1.4 Morphology of the thorn surface

Figure 4.7 (a) shows the formation of thorn growth on the ball surface. It was a multistage process which is formed layer by layer. The shapeless of powder inside the jar which is not stick on the ball surface was shown in Figure 4.7(b).

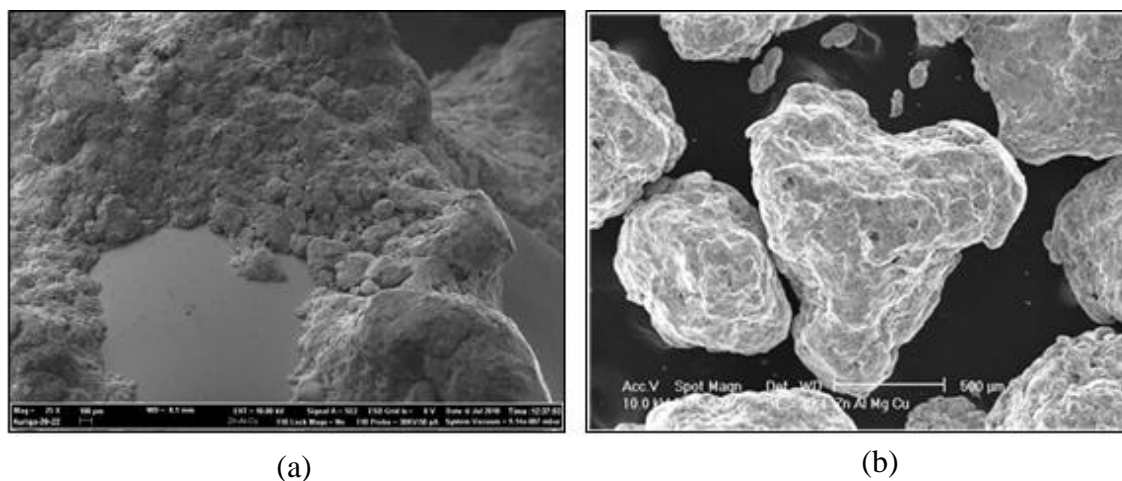


Figure 4.7: (a) Multistage process of thorn growth, (b) Shapeless of powder.

## **4.2 Evaluation of hybrid microwave sintering of Zn-Al alloy**

### **4.2.1 Introduction**

This sub-chapter aims to identify the optimum processing parameters for sintering Zinc-Aluminum (Zn-Al) alloys with varying compositions (Zn-8Al-1Cu-0.02Mg (ZA8), Zn-11Al-1Cu-0.025Mg (ZA12) and Zn-27Al-2Cu-0.015Mg (ZA27)). The compositions are compacted at different compaction load (6, 8 and 10 tons) and sintered at temperature 360°C for conventional and hybrid microwave sintering methods. The effect of processing parameter is analyzed by mechanical, thermal and microstructural analysis. Mechanical analysis comprised density measurement and microhardness testing. Meanwhile thermal analysis comprised coefficient of thermal expansion measurement. Microstructural analysis is carried out by using FESEM (micrographs), SEM (grain size measurement), EDX and XRD. The performance of the process is evaluated by comparing the sintered samples using hybrid microwave sintering and conventional sintering.

### **4.2.2 Temperature Profile and Performance**

In chamber furnace sintering, there are three stages requires, 1<sup>st</sup> purge stage, 2<sup>nd</sup> solid state diffusion stage and 3<sup>rd</sup> the cooling down step. Figure 4.8 shows the typical temperature profile of conventional heating during the sintering of Zn-Al alloy compacts. In this research, the setup for 1st and 3rd stage was 5°C per minute and the holding time was 30 minutes. It was seen that the temperature setting for conventional sintering was 360°C and it took about 160 minutes to complete the sintering process in chamber furnace.

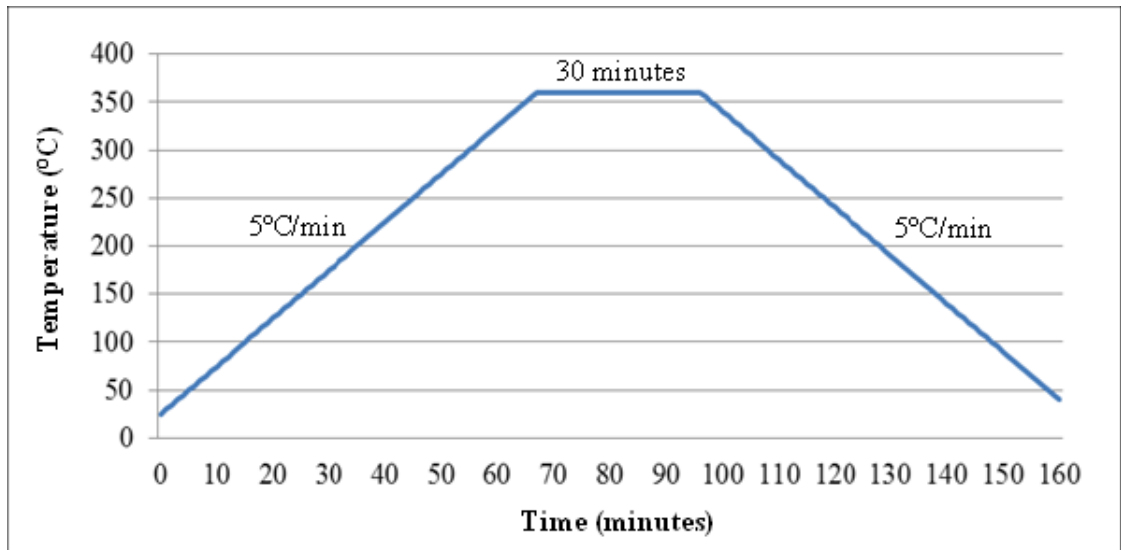


Figure 4.8: Temperature profile of conventional sintering

In hybrid microwave sintering technique was attempt by employing SiC as susceptor and crucible setup to separate between specimens and SiC powder. Figure 4.9 shows the temperature profile of hybrid microwave sintering of Zn-Al compact by using 75  $\mu\text{m}$  and 50 nm particle size of SiC powder as susceptors. It shown that 50 nm SiC powder particle size took about 32 minutes to complete the sintering process compared to 75  $\mu\text{m}$  particle size; 50 minutes. However, the temperature gradient of 75  $\mu\text{m}$  particle size was more stable compared 50 nm particle size.

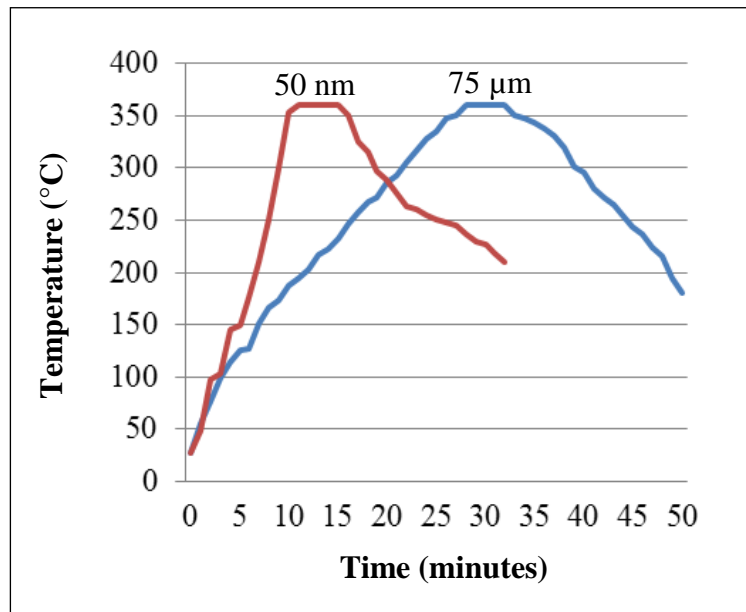


Figure 4.9: Temperature profile of hybrid microwave sintering with different particle size of SiC powder.

Figure 4.10 shows a microwave sintered samples which are compacted at 10 tons after 10 minutes sintered using 50 nm SiC particle size. It can be seen that wire spots are formed on the sample surface and a selected spots started molten and solidified. It is assumed that thermal shock had occurred due to the short amount of heating time and it is related to the usage of nano size of SiC powder in this experiment.



Figure 4.10: Zinc alloy sample started melt after 10 minutes sintered in microwave with 50 nm SiC particle size as susceptor.

Furthermore, thermal shock also has affected the crucible inside the insulation box which had been cracked after 5 times used with 50 nm particle size of SiC powder as



shown in Figure 4.11. Thermal shock occurred due to rapid temperature change and its cause cracked.

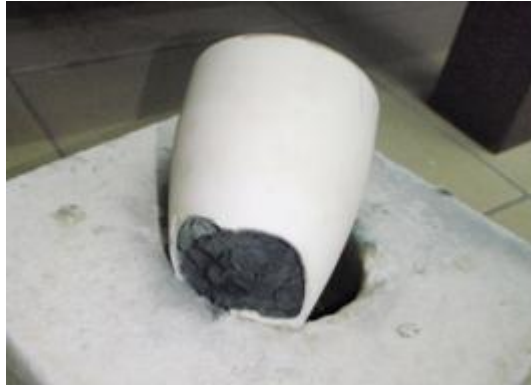


Figure 4.11: Alumina crucible cracked due to the thermal shock.

### 4.2.3 Dimensional changes

Dimensional changes of sintered ZA8, ZA12 and ZA27 for three various compaction loads for 6 tons, 8 tons and 10 tons are presented in Table 4.1.

For ZA8 alloy conventional sintered samples, there are no changes in diameter at compaction load 6 tons but swelled at 8 and 10 compaction loads. This is different with microwave sintered samples where at 6 compaction load; the sample was shrinking but swelled at 8 and 10 compaction loads.

For ZA12 alloy conventional sintered samples, at 6 tons compaction load, the sample shrank no changes in diameter at 8 compaction loads and swelling happened at 10 tons compaction load. This phenomenon is contradicted with microwave sintered samples where all the samples swelled at all compaction loads.

Meanwhile for ZA27 alloy both conventional and microwave sintered samples are swelling in range of 0.1 to 0.4 percent for conventional sintered samples and 0.2 percent for microwave sintered samples.



Among ZA8, ZA12 and ZA27 alloys, all sintered samples of ZA27 alloy tends to swell compared to the others alloys. Microwave sintered samples were more swelled than conventional sintered samples.

Table 4.1: Dimensional changes of sintered ZA8, ZA12 and ZA27

Alloy	Sintering method	Compaction load (ton)	Change in diameter $\Delta\phi / \phi$ (%)	Change in height $\Delta h / h$ (%)
ZA8	Conventional sintering	6	0.0	0.0
		8	+0.2	-1.0
		10	+0.2	1.4
	Microwave sintering	6	-0.1	-2.4
		8	+0.1	-2.3
		10	+0.1	1.3
ZA12	Conventional sintering	6	-0.1	0.6
		8	0.0	-1.3
		10	+0.1	-1.6
	Microwave sintering	6	+0.1	2.0
		8	+0.1	0.7
		10	+0.2	0.0
ZA27	Conventional sintering	6	+0.3	2.1
		8	+0.1	4.0
		10	+0.4	5.7
	Microwave sintering	6	+0.2	0.6
		8	+0.2	1.9
		10	+0.2	-2.1

#### 4.2.4 Density

Theoretical densities for zinc-aluminum alloys in this research are 6.8031 g/cm<sup>3</sup> (ZA8), 6.6700 g/cm<sup>3</sup> (ZA12) and 5.9947 g/cm<sup>3</sup> (ZA27) which is calculated based on rule of mixture principle as stated in chapter 3. Figure 4.12 shown the density of the conventional and microwave sintered samples of ZA8, ZA12 and ZA27 for three various compaction loads; 6 tons, 8 tons and 10 tons. Both conventional and hybrid microwave sintered samples of ZA8 alloy are denser compared to ZA12 and ZA27 alloys.

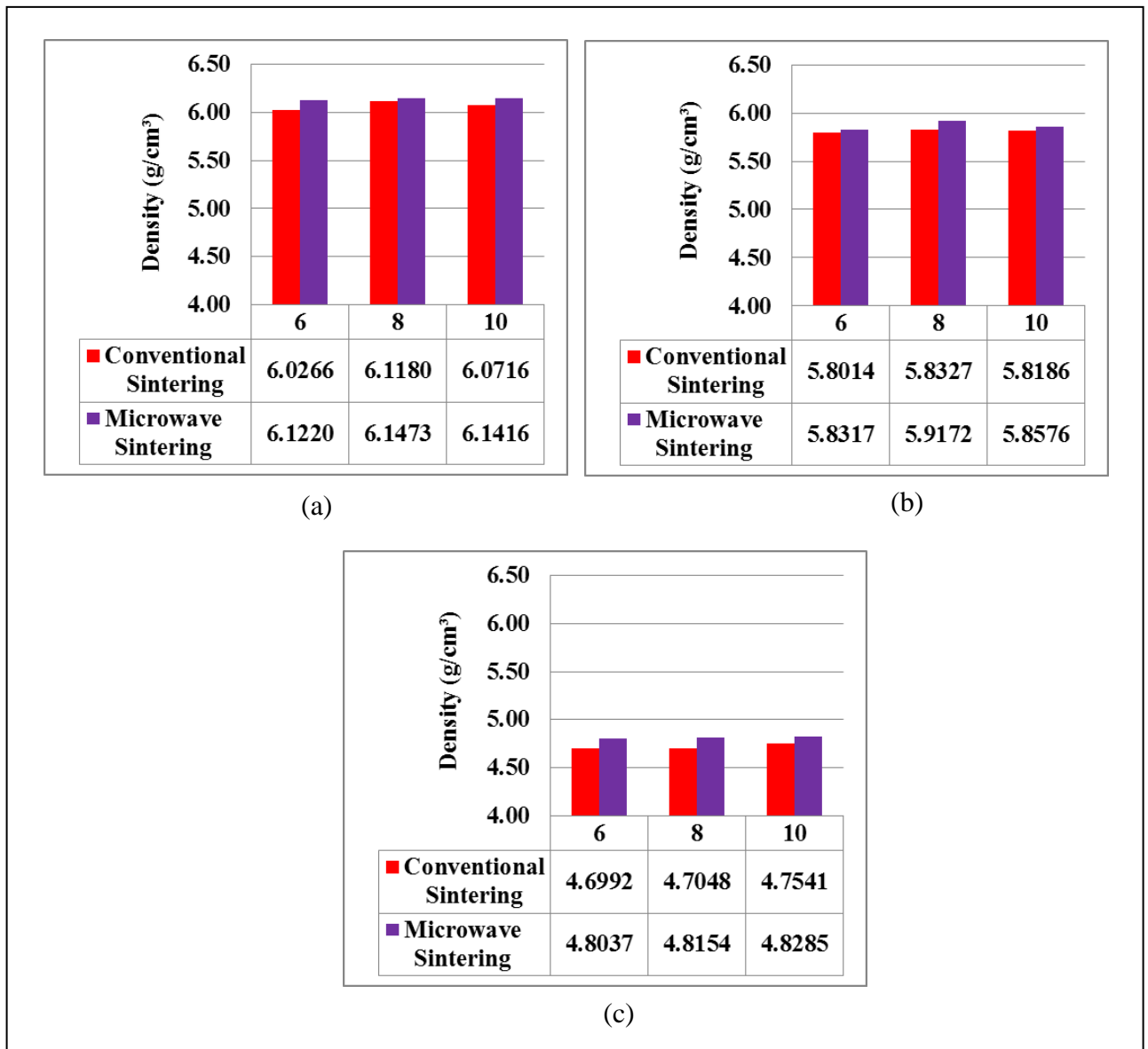


Figure 4.12: The density of sintered (a) ZA8, (b) ZA12 and (c) ZA27 alloys.

#### ***Density of sintered Zn-8Al-1Cu-0.02Mg (ZA8) alloy***

For ZA8 alloy (Figure 4.12(a)), it is observed that hybrid microwave sintered samples possessed higher density compared to conventional sintering samples. The highest density is obtained from sample compacted and sintered at 8 ton compaction load, followed by 10 tons and 6 tons.

#### ***Density of sintered Zn-11Al-1Cu-0.025Mg (ZA12) alloy***

Generally, hybrid microwave sintering samples' densities are more superior compared to conventional sintered samples. Similar trend are observed for ZA12 alloy samples (Figure 4.12(b)) where at 8 tons compaction load, the sintered samples are denser than the others two compaction loads.

#### ***Density of sintered Zn-27Al-2Cu-0.015Mg (ZA27) alloy***

The overall densities results followed the general prediction; higher compaction load leads to higher density (Figure 4.12(c)). All hybrid microwave sintered samples are denser than conventional sintered samples.

### **4.2.5 Porosity**

In general prediction; porosity was inversely proportional to density. Figure 4.13 shows the porosity of sintered Zn-Al alloys at three various compaction load; 6, 8 and 10 tons. These findings were similar to the density results. Both conventional and hybrid microwave sintered samples of ZA8 alloy were less porous compared to ZA12 and ZA27 alloys.

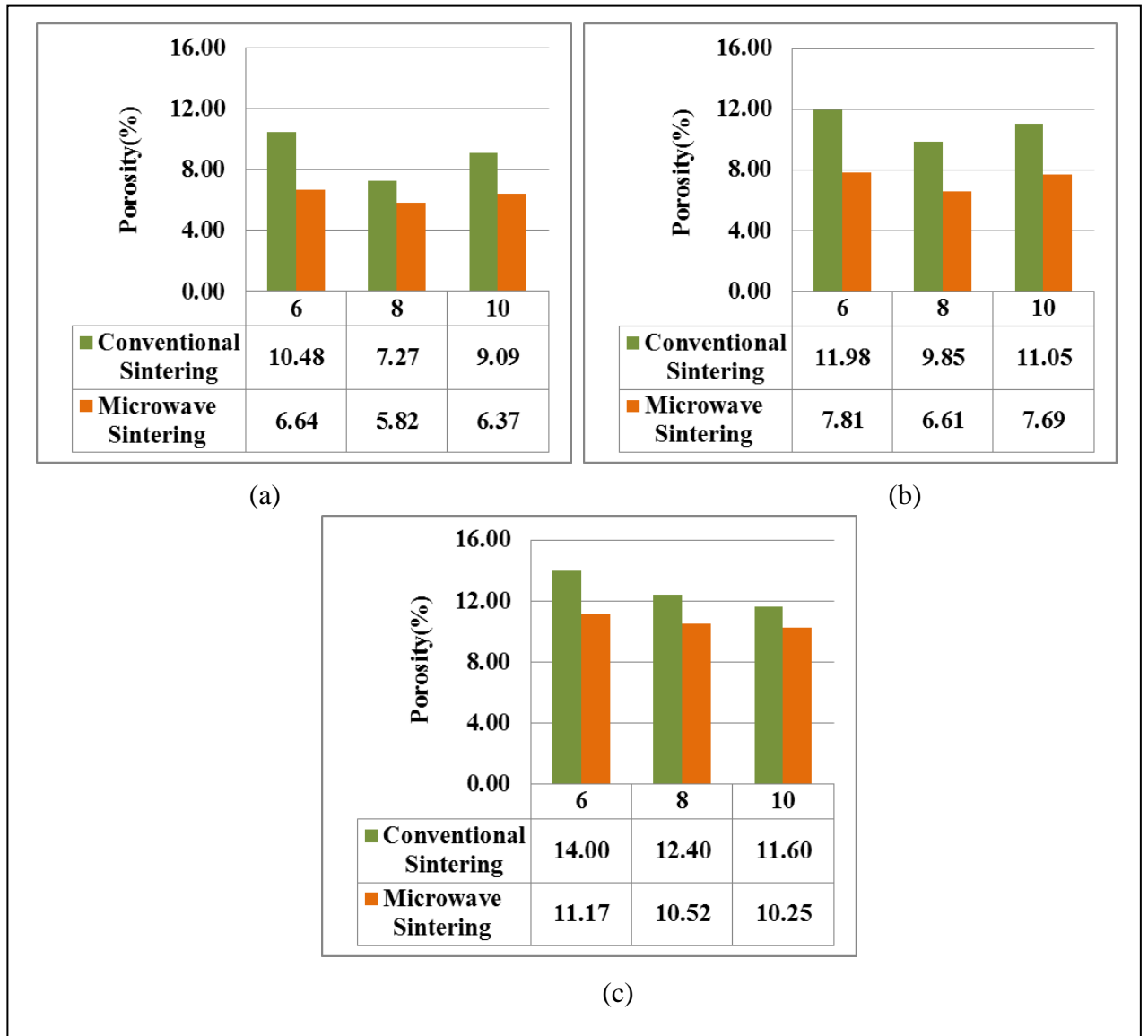


Figure 4.13: The porosity of sintered (a) ZA8, (b) ZA12 and (c) ZA27 alloys.

#### ***Porosity of sintered Zn-8Al-1Cu-0.02Mg (ZA8) alloy***

For ZA8 alloy (Figure 4.13(a)), hybrid microwave sintering samples managed to produce samples with lower porosity compared to conventional sintering samples. Among these three compaction loads, samples compacted and sintered with 8 tons compaction loads possessed the lowest porosity followed by 10 tons and 6 tons.

#### ***Porosity of sintered Zn-11Al-1Cu-0.025Mg (ZA12) alloy***

Hybrid microwave sintered samples were generally less porous than conventional sintered samples. There were a similarity trend of ZA12 alloy samples' results with ZA8 alloy (Figure 4.13 (b)) where at 8 ton compaction loads exhibits the lowest porosity among the others.

#### ***Porosity of sintered Zn-27Al-2Cu-0.015Mg (ZA27) alloy***

For ZA27 alloy (Figure 4.13(c)), it is observed that hybrid microwave sintered samples possessed lower porosity compared to conventional sintered samples. The lowest percentage of porosity is obtained at 10 tons compaction load. This followed the common prediction; lowest porosity was proportional to the highest compaction loads.

### **4.2.6 Microhardness**

Figure 4.14 shown the microhardness values of sintered ZA8, ZA12 and ZA27 alloys for three various compaction loads; 6 tons, 8 tons and 10 tons. Hybrid microwave sintered samples were generally harder than conventional sintered samples. When comparing performance between three composition alloys, the hardness values are remain in the same range although the density of ZA8 alloy were higher than ZA12 and ZA27 alloys.

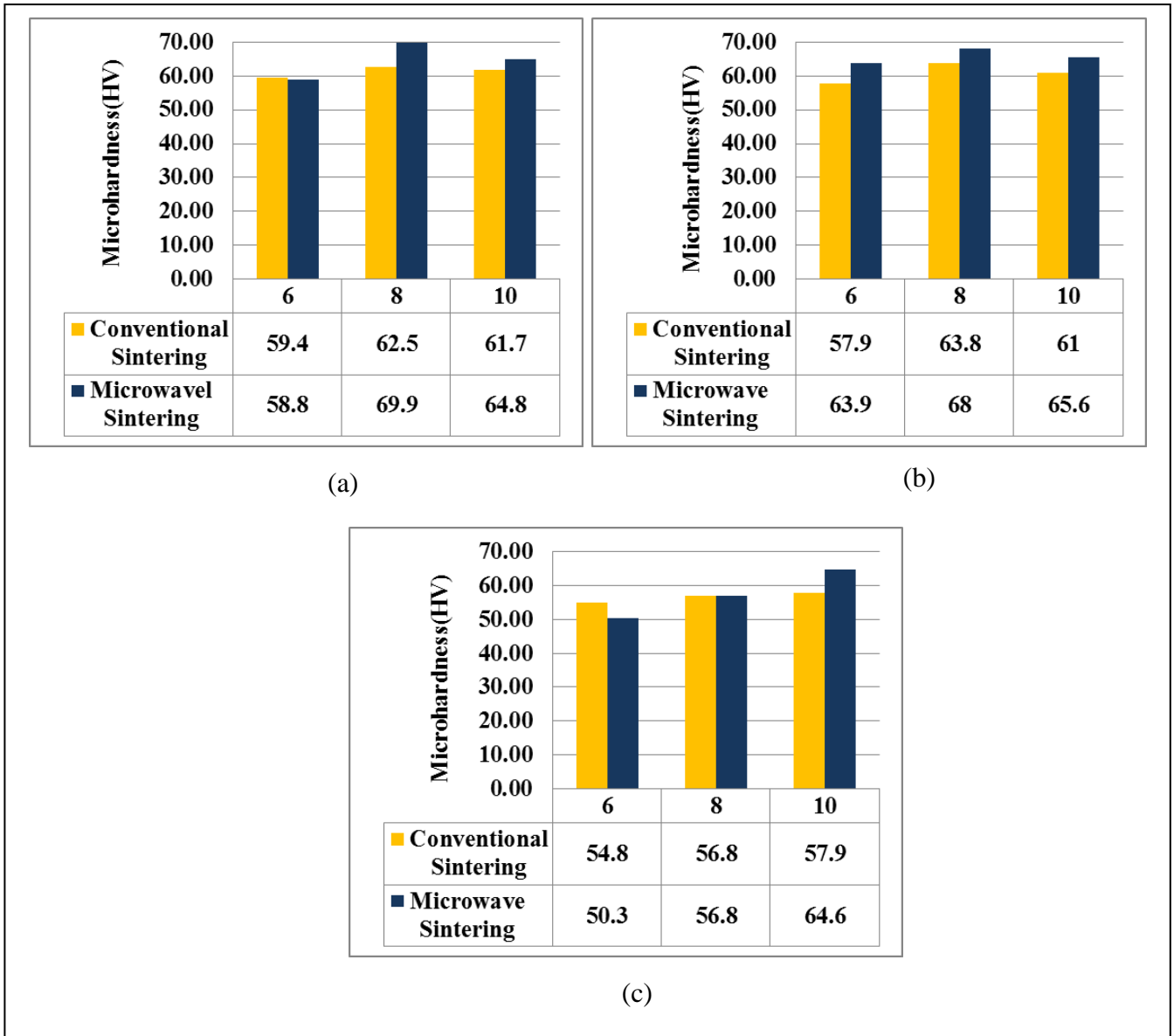


Figure 4.14: The micro hardness (HV) of sintered (a) ZA8, (b) ZA12 and (c) ZA27 alloys.

#### ***Microhardness of sintered Zn-8Al-1Cu-0.02Mg (ZA8) alloy***

For ZA8 alloy samples (Figure 4.14(a)), all hybrid microwave sintering samples demonstrated higher hardness compared to conventional sintering samples. Samples prepared under 8 tons compaction loads gave the highest hardness values compared to 10 tons and 6 tons.

#### ***Microhardness of sintered Zn-11Al-1Cu-0.025Mg (ZA12) alloy***

For ZA12 alloy samples (Figure 4.14 (b)), it is observed that hybrid microwave sintered samples exhibit higher hardness compared to conventional sintered samples. The highest hardness values are obtained from samples prepared under 8 tons compaction load.

#### ***Microhardness of sintered Zn-27Al-2Cu-0.015Mg (ZA27) alloy***

For ZA27 alloy samples (Figure 4.14 (c)), hybrid microwave sintered samples were harder than conventional sintered samples. As the compaction loads increased, the hardness values also increased.

### **4.2.7 Thermo Mechanical Analysis**

#### ***Coefficient of thermal expansion (CTE)***

Coefficients of thermal expansion (CTE) of the microwave sintered alloys are investigated in order to find out more details about their thermo-mechanical behavior. The average value of CTE for each alloy sintered is given in Table 4.2. The results show that CTE of MZA8 and MZA12 were about 28  $\mu\text{m/m. }^{\circ}\text{C}$ , while CTE of MZA27 was about 21  $\mu\text{m/m. }^{\circ}\text{C}$ .

Table 4.2: CTE values of microwave sintered samples of ZA8, ZA12 and ZA27.

<b>Composition</b>	<b>CTE (<math>\mu\text{m/m.}^{\circ}\text{C}</math>)</b>
ZA8	$28.25 \pm 3.33$
ZA12	$28.10 \pm 2.43$
ZA27	$21.23 \pm 2.06$

#### **4.2.8 Microstructure Analysis**

##### ***Field Emission Scanning Electron Microscopy (FESEM)***

The shape, size and distribution of Zn and Al phases can be observed using FESEM at lower magnification, x100. The diffusion of one element in another boundaries of grains can be seen clearly at higher magnification, x500. The dark phase belongs to Al and the white phase represents Zn. It is clearly observed that the total area cover by Al is increased from ZA8 to ZA27 in both conventional and hybrid microwave sintered alloy. Two types of features are found in the microstructures; either Al grain is surrounded by Zn phase, or Zn is surrounded by Al phase.

##### ***FESEM analysis of Zn-8Al-1Cu-0.02Mg (ZA8)***

Figure 4.15, 4.16 and 4.17 show micrographs of conventional and hybrid microwave sintered samples of ZA8 alloys prepared under compaction load; 6, 8 and 10 tons respectively. It is clearly observed at lower magnification (x100), the total area covered by Zn phase in ZA8 alloy in both conventional and hybrid microwave sintered samples. In this alloy, the Al grain is surrounded by Zn phase in both conventional and hybrid microwave sintered samples.

Meanwhile, at higher magnification (x500), the boundaries between Al particles in hybrid microwave sintered samples cannot be detected while there is clear boundary between Al grains in conventional sintered samples. It is also observed that the distributions of Al particles were more uniform in conventional sintering samples prepared under 8 tons compaction loads. However, hybrid microwave sintered samples produced uniform pores compared to conventional sintered samples at 8 tons compaction loads.



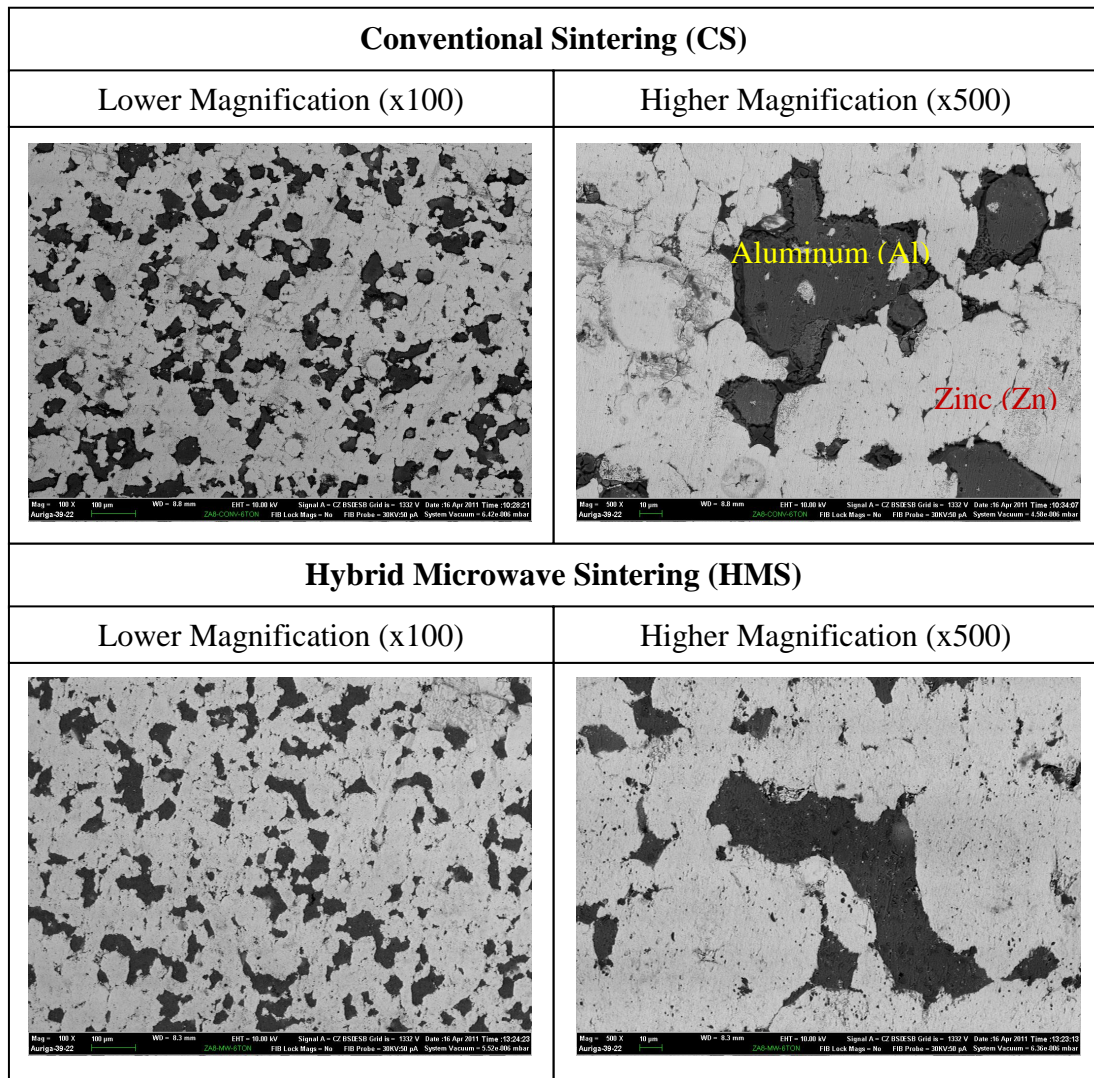


Figure 4.15: Micrographs of CS and HMS samples of ZA8 alloy (6 tons).

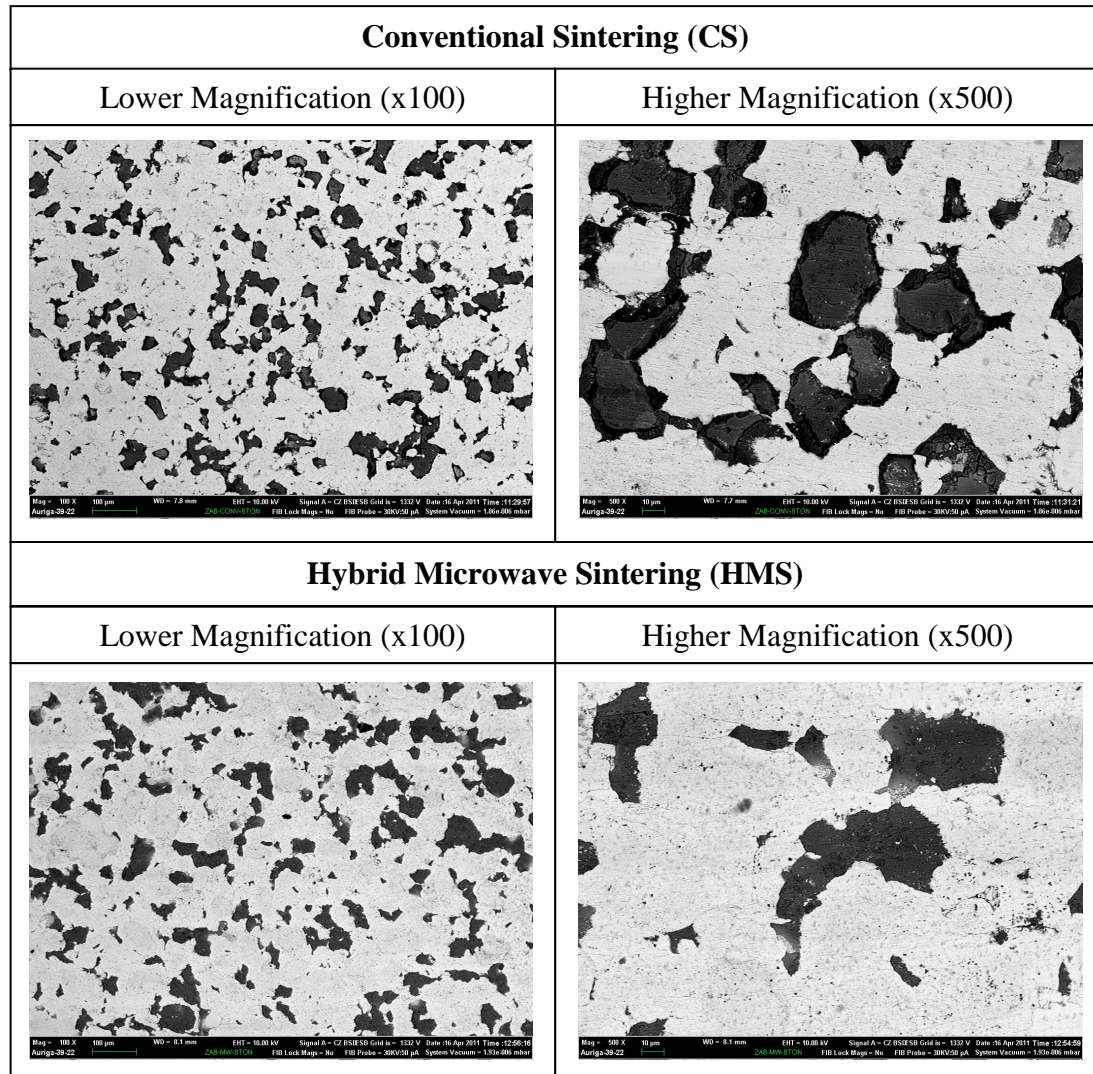


Figure 4.16: Micrographs of CS and HMS samples of ZA8 alloy (8 tons).

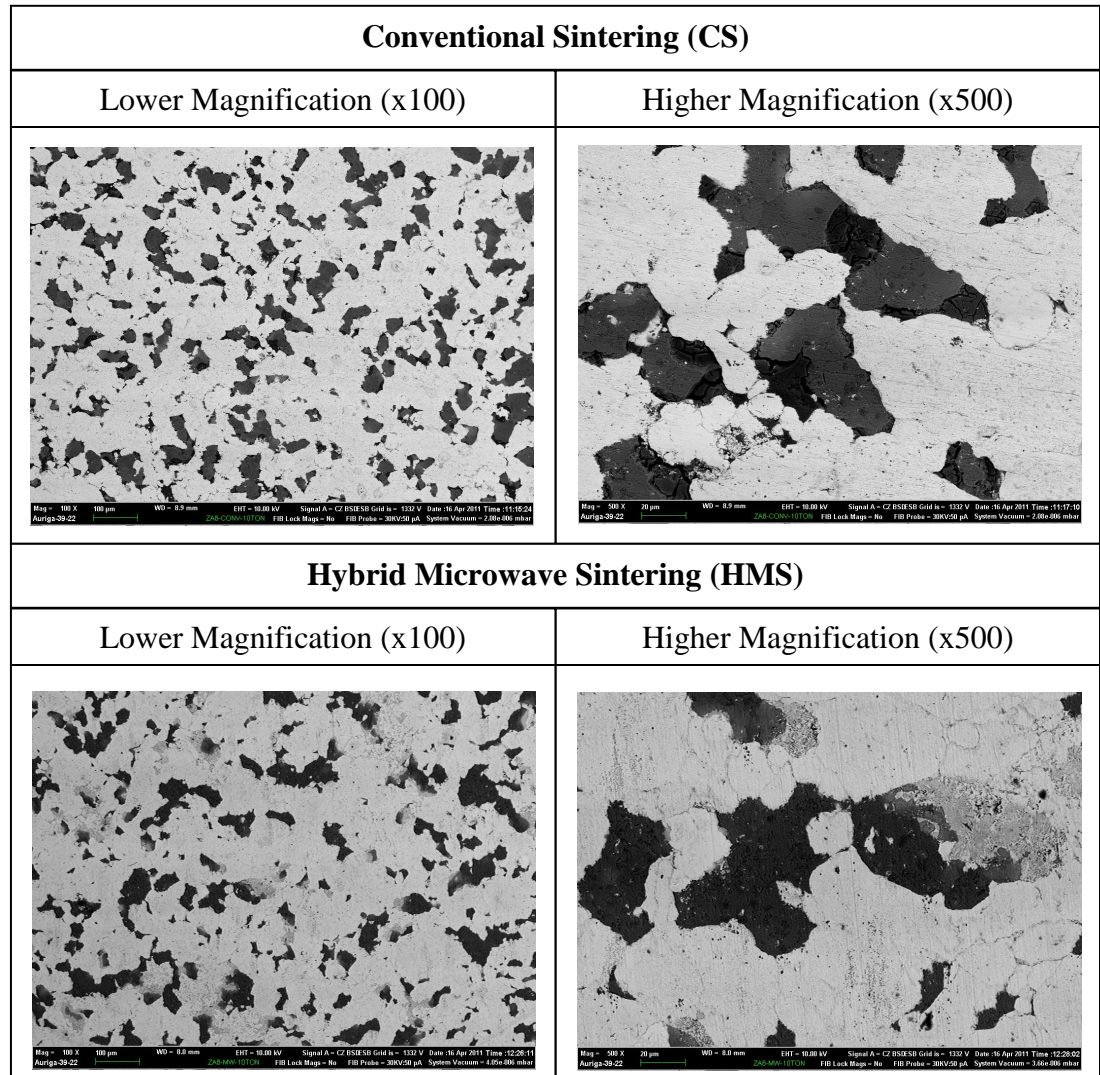


Figure 4.17: Micrographs of CS and HMS samples of ZA8 alloy (10 tons).

### *FESEM analysis of Zn-11Al-1Cu-0.025Mg (ZA12)*

Figure 4.18, 4.19 and 4.20 show micrographs of conventional and hybrid microwave sintered samples of ZA12 alloys prepared under compaction loads 6, 8 and 10 tons respectively. From the micrographs, it can be seen at lower magnification (x100), the total area covered by Zn phase in both conventional and hybrid microwave sintered samples but there is an increasing Al phase compared to ZA8 alloy. In this alloy, although



the amount of Al increased, it is can be seen also that Al grain is surrounded by Zn phase in both conventional and hybrid microwave sintered alloy.

At higher magnification (x500), the boundaries between Al particles in conventional sintered samples are observed clearly for all three compaction loads. However, it is only observed in hybrid microwave sintered sample prepared under 6 tons compaction loads. Meanwhile, for samples compacted and sintered at 8 and 10 tons, the boundaries are cannot be detected. Moreover, the Al particles are integrated perfectly in hybrid microwave sintered samples at 8 and 10 tons compaction loads.

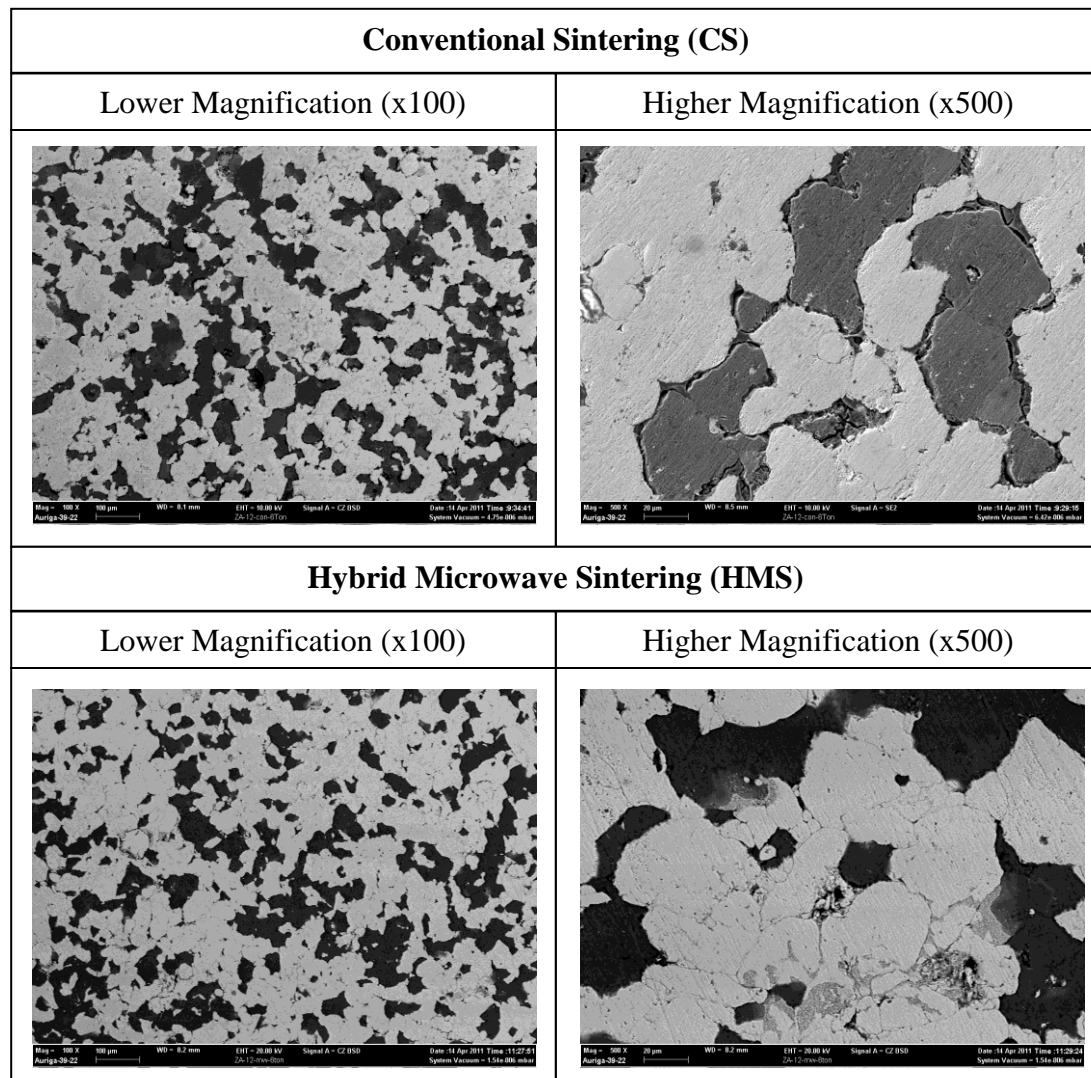


Figure 4.18: Micrographs of CS and HMS samples of ZA12 alloy (6 tons).

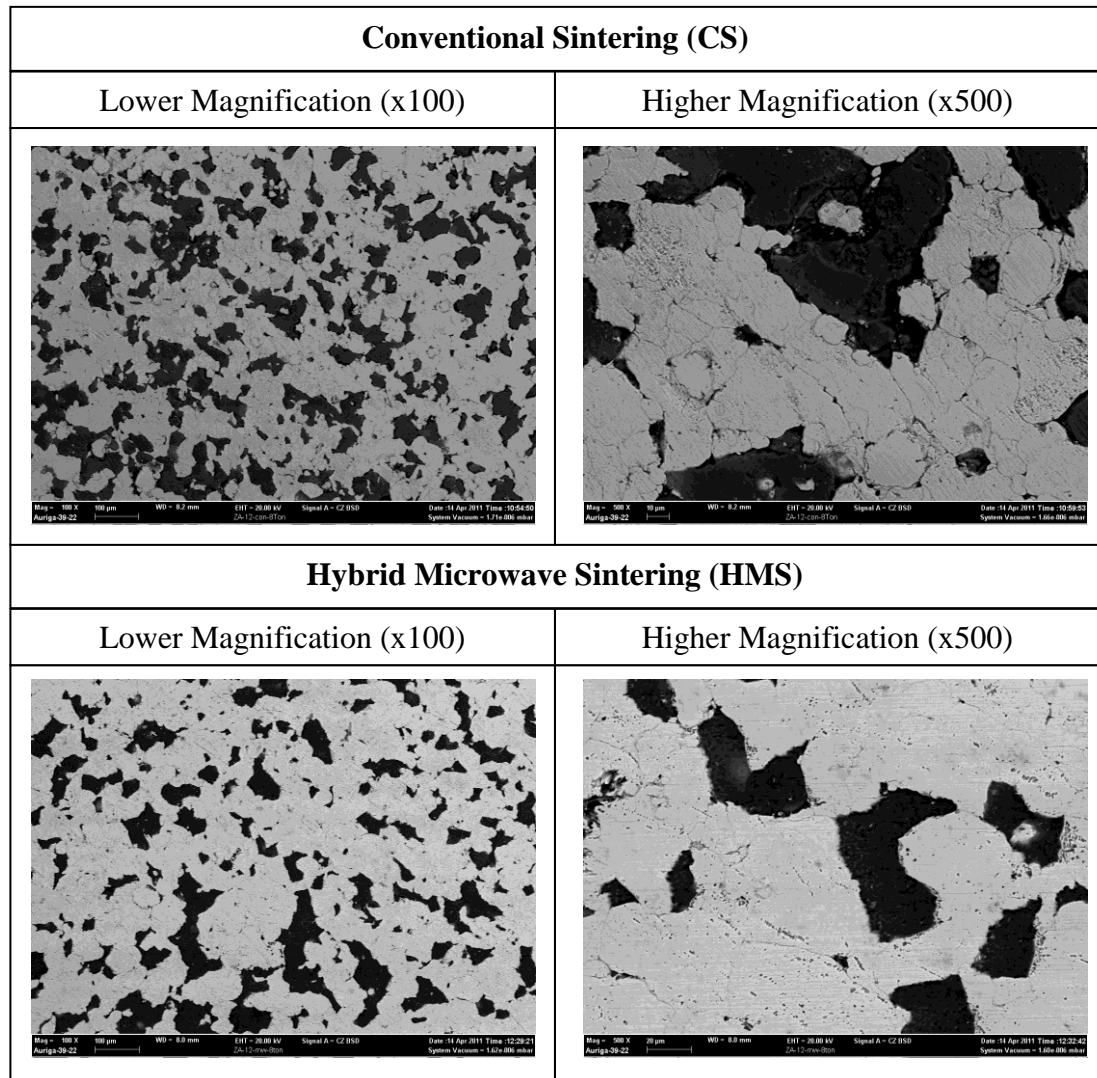


Figure 4.19: Micrographs of CS and HMS samples of ZA12 alloy (8 tons).

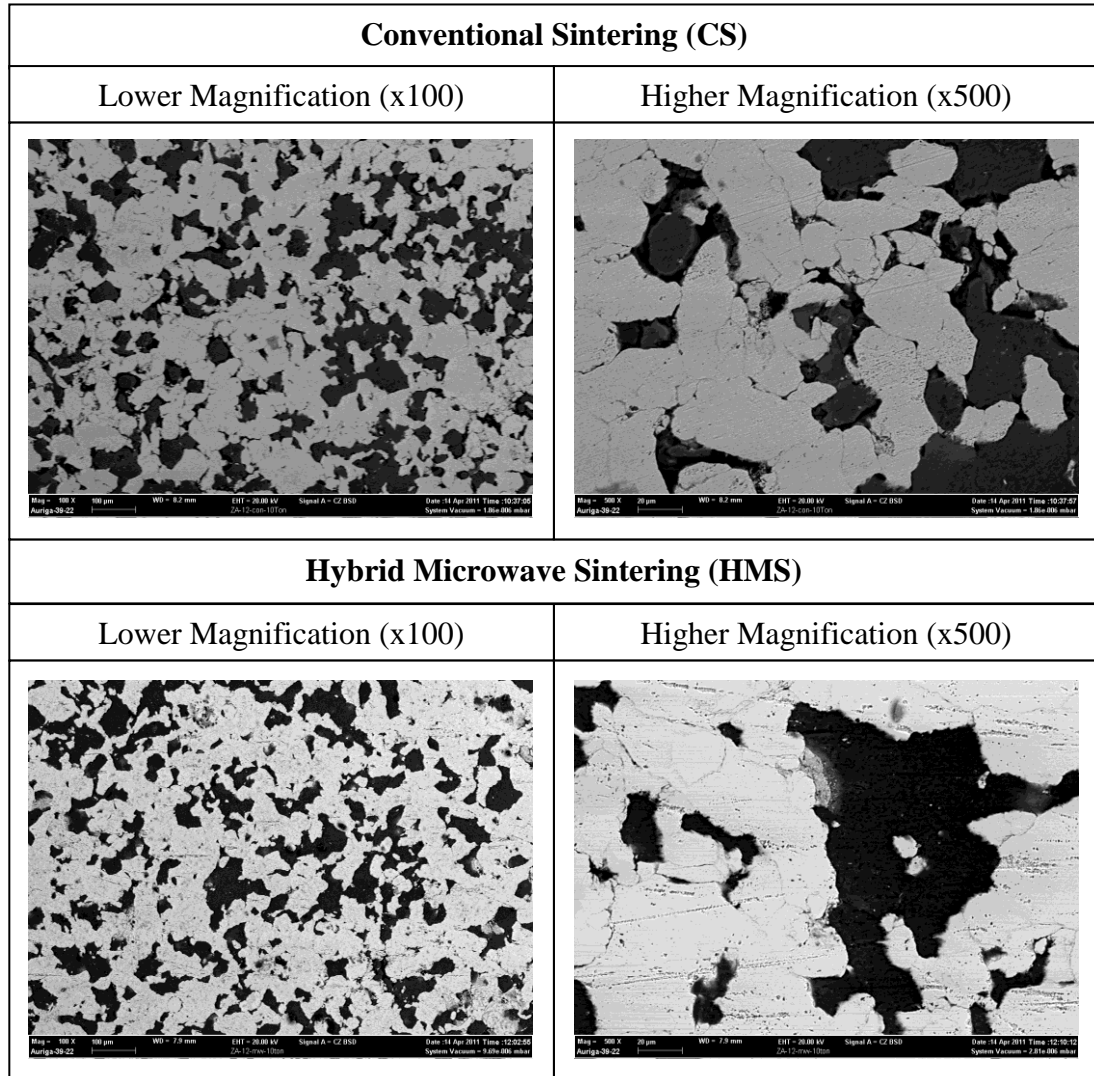


Figure 4.20: Micrographs of CS and HMS samples of ZA12 alloy (10 tons).

#### ***FESEM analysis of Zn-27Al-2Cu-0.015Mg (ZA27)***

Figure 4.21, 4.22 and 4.23 show micrographs of conventional and hybrid microwave sintered samples of ZA27 alloys prepared under compaction loads 6, 8 and 10 tons respectively. From the figure, it is observed at lower magnification (x100), the total area covered by Al phase in both conventional and hybrid microwave sintered samples. Increasing the fraction of Al resulted in more Zn is surrounded by Al phase in both conventional and hybrid microwave sintered alloy.

At higher magnification (x500), the Al particles are integrated perfectly in hybrid microwave sintered samples at all compaction loads and 8 and 10 tons compaction loads in conventional sintered samples.

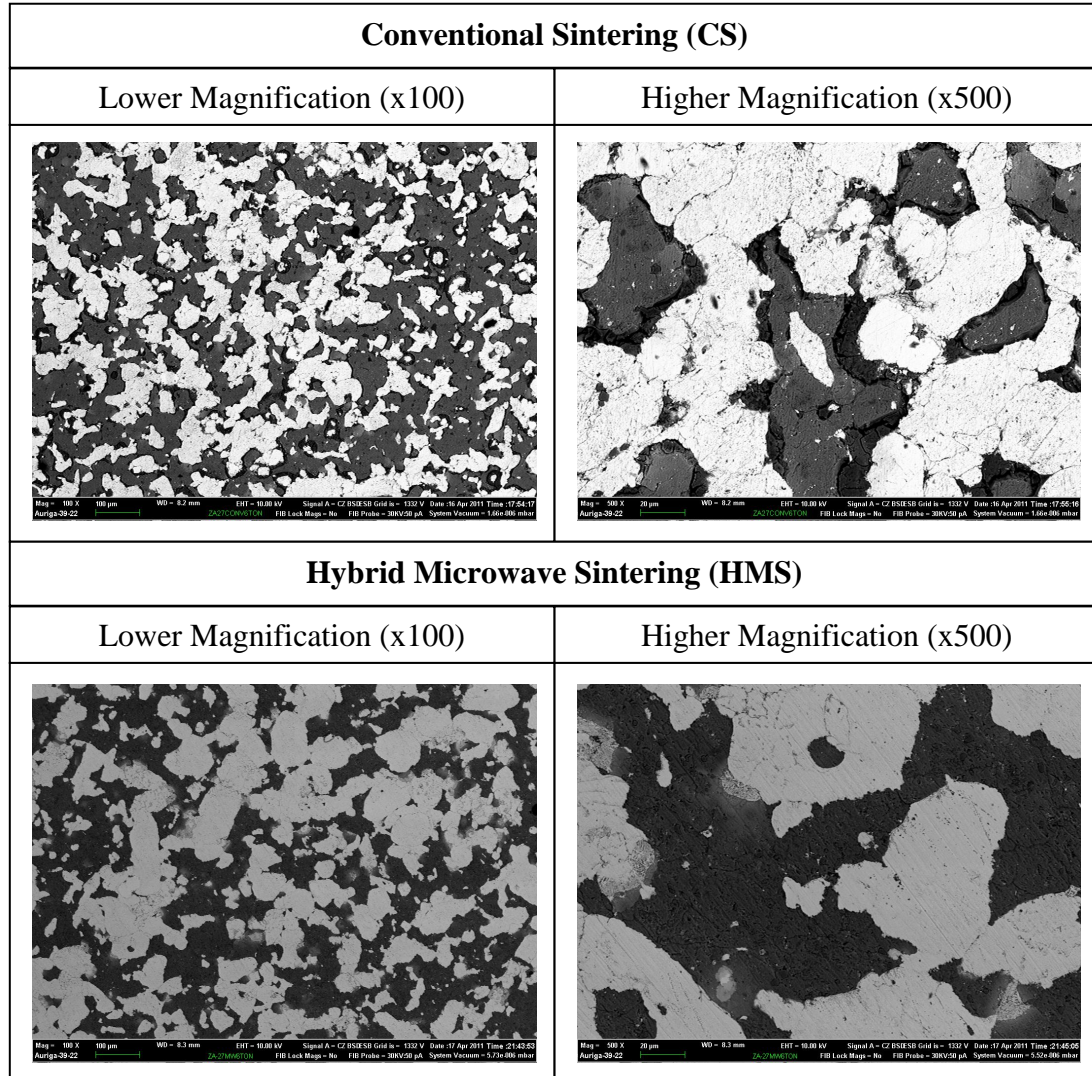


Figure 4.21: Micrographs of CS and HMS samples of ZA27 alloy (6 tons).



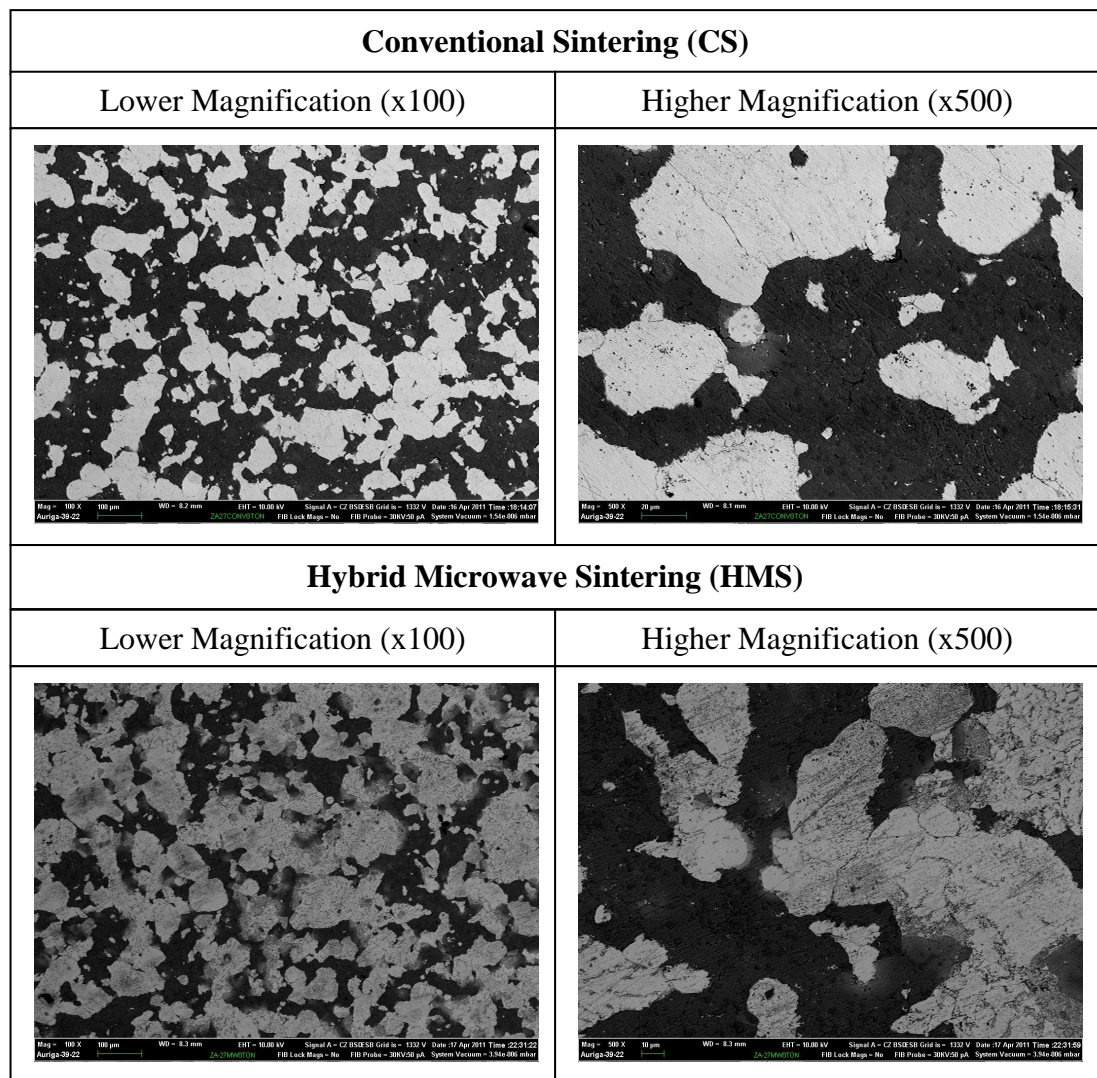


Figure 4.22: Micrographs of CS and HMS samples of ZA27 alloy (8 tons).



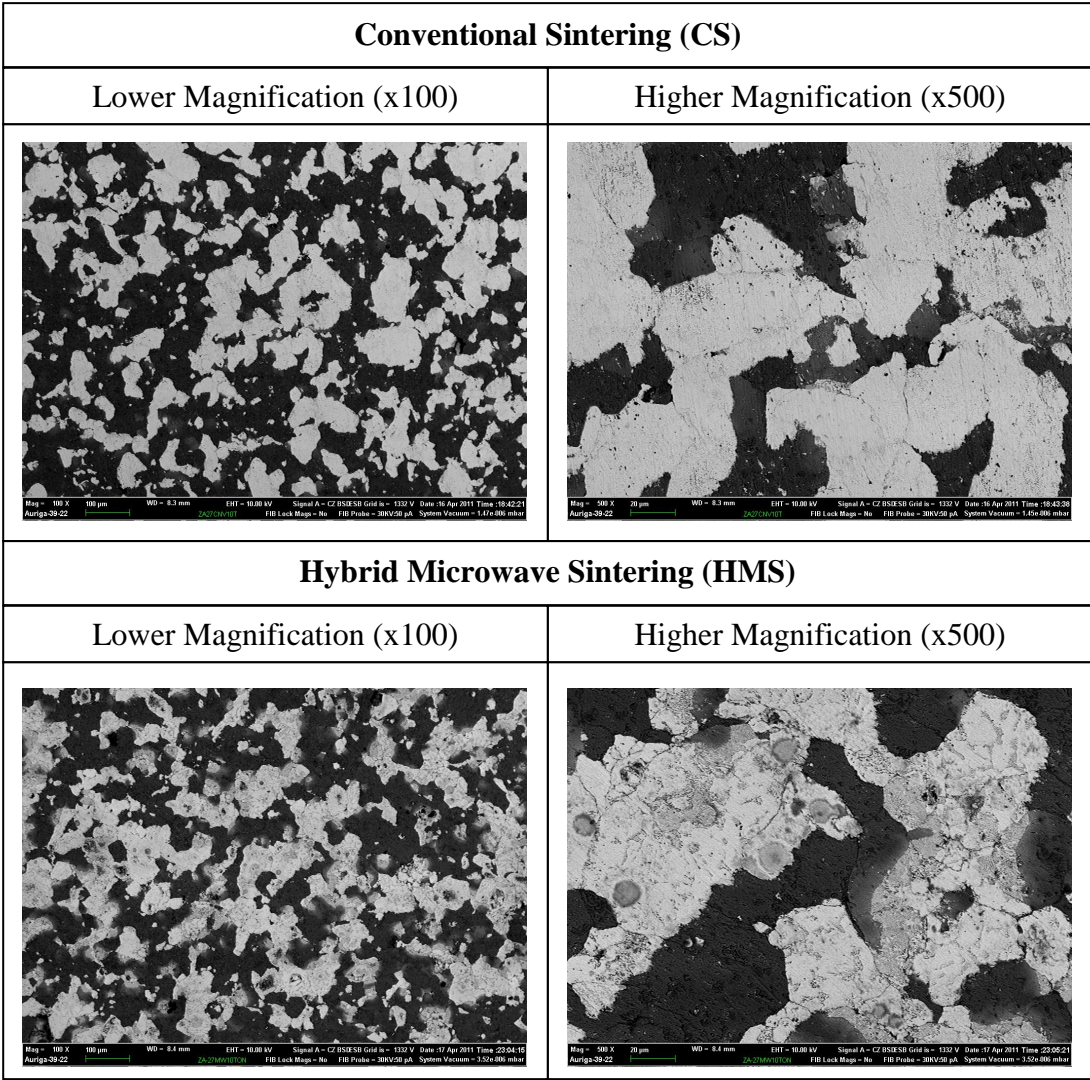


Figure 4.23: Micrographs of CS and HMS samples of ZA27 alloy (10 tons).

### *Electron Dispersive X-ray (EDX)*

EDX element analysis is carried out to get better picture of the composition distribution and related microstructure. For each alloy, only conventional and hybrid microwave sintered samples which possessed the best combination of properties in term of density, porosity and micro hardness are sent for EDX analysis. Figures 4.24, 4.25 and 4.26 show the element analysis of ZA8, ZA12 and ZA27 alloys respectively. It can be seen that the elemental composition analyzed consisted of Zinc (Zn), Aluminum (Al), Copper (Cu), Oxygen (O) and Silicon (Si).

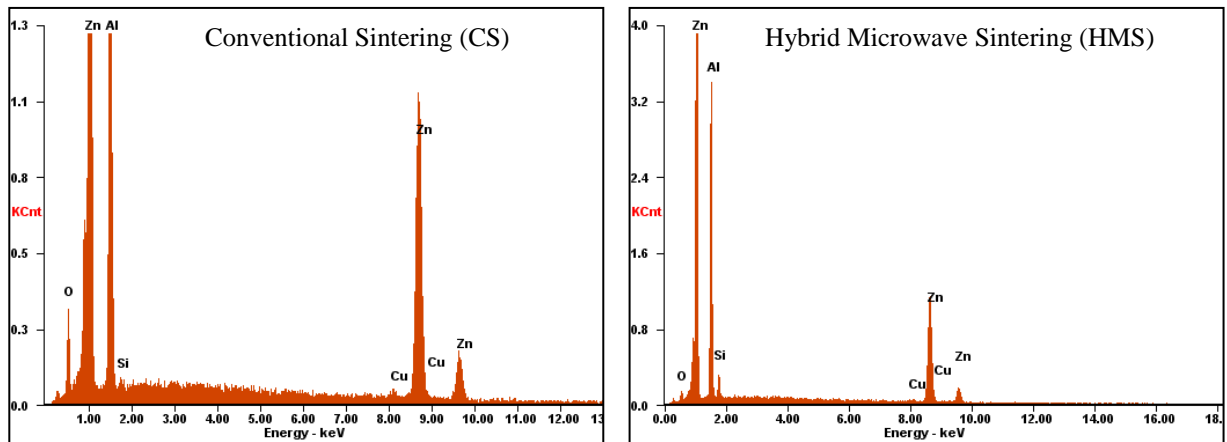


Figure 4.24: EDX of ZA8 sintered alloy (8 tons).

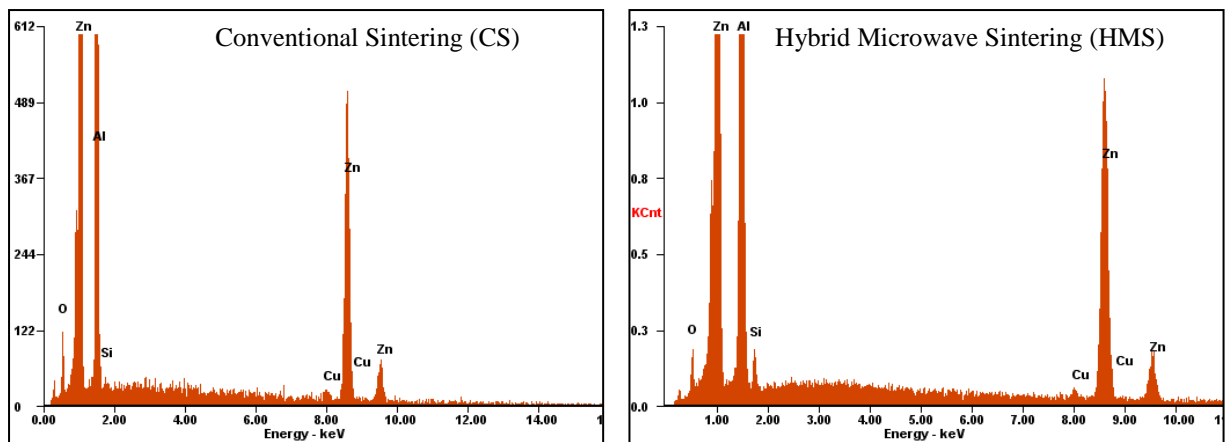


Figure 4.25: EDX of ZA12 sintered alloy (8 tons).

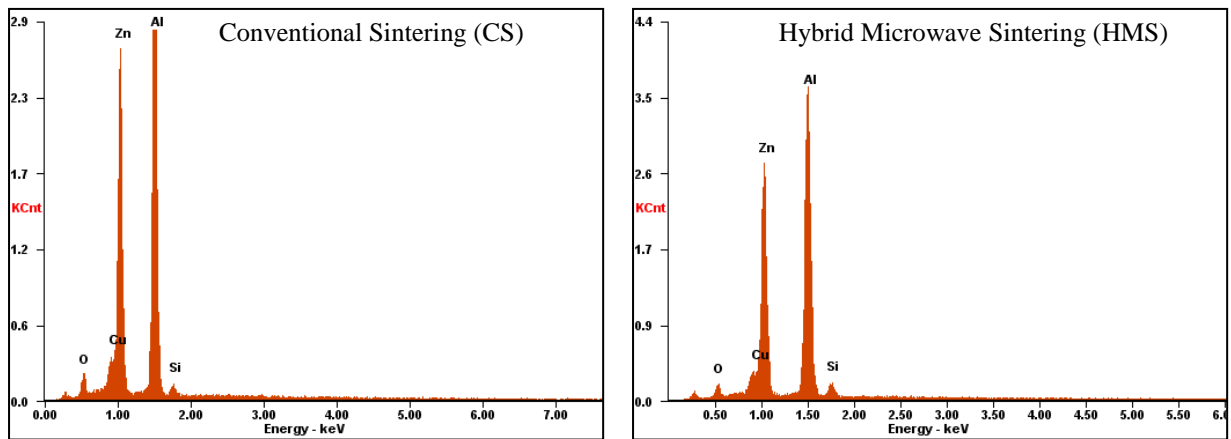


Figure 4.26: EDX of ZA27 sintered alloy (10 tons).

### *X-ray Diffraction (XRD)*

The XRD patterns of ZA8, ZA12 and ZA27 after hybrid microwave sintering are shown in Figure 4.27. It can be seen that only two components of Zn and Al are detected in all cases and the highest intensity belongs to Zn. The concentration of Al is increasing according to its increasing fraction in ZA8, ZA12 and ZA27, respectively. But the rate of increasing in concentration of Al in product is not exactly the same as the fraction of Al in the green mixture. There were no chemical reactions, oxides or impurity phases in the sintered alloys.

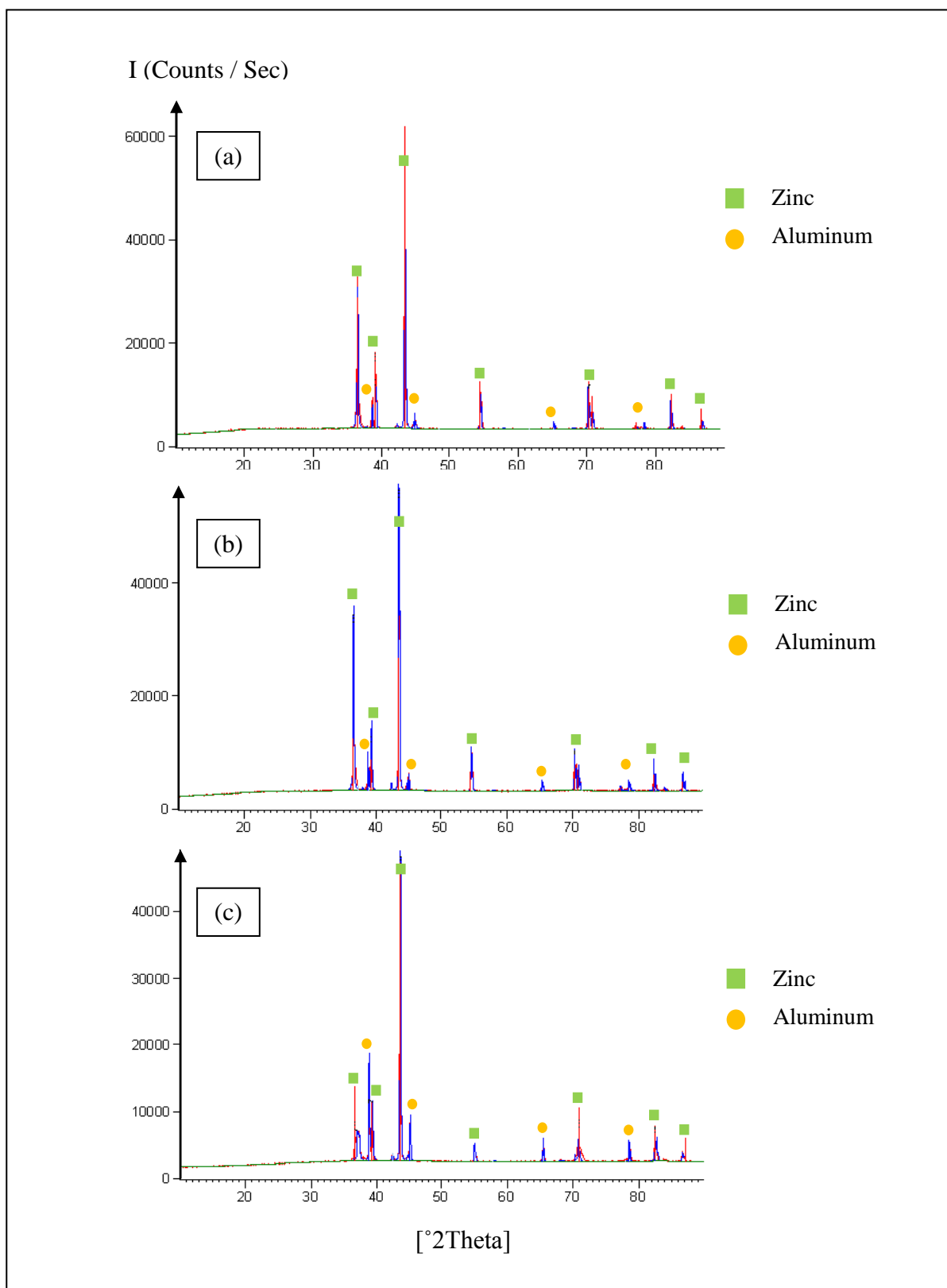


Figure 4.27: XRD results of (a) ZA8, (b) ZA12 and (c) ZA27 after hybrid microwave sintering.

## Grain size

Figure 4.28 shows the grain size of sintered ZA8, ZA12 and ZA27 alloys for three various compaction loads; 6, 8 and 10 tons. Hybrid microwave sintered samples are demonstrated smaller grain size compared to conventional sintered samples in all compaction loads.

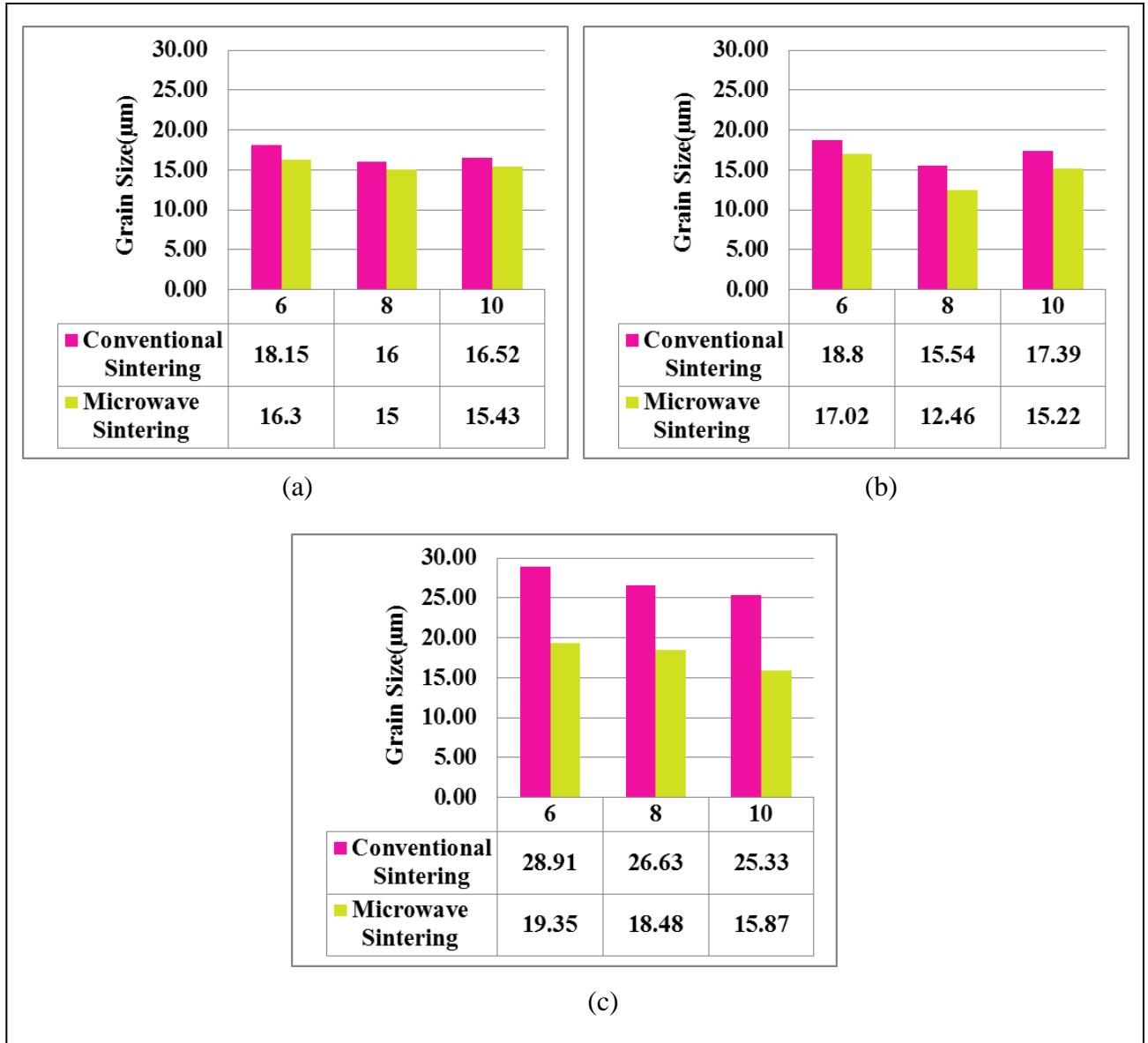


Figure 4.28: The grain size of sintered (a) ZA8, (b) ZA12 and (c) ZA27 alloys.

***Grain size of sintered Zn-8Al-1Cu-0.02Mg (ZA8) alloy***

For ZA8 alloy (Figure 4.28 (a)), it is observed that hybrid microwave sintered samples possessed small grain size compared to conventional sintering samples. The smallest grain size is obtained from sample compacted and sintered at 8 ton compaction loads, followed by 10 tons and 6 tons.

***Grain size of sintered Zn-11Al-1Cu-0.025Mg (ZA12) alloy***

Generally, hybrid microwave sintering samples' grain sizes are smaller than conventional sintered samples. Similar trend are observed for ZA12 alloy samples (Figure 4.28 (b)) where at 8 tons compaction loads, the sintered samples were denser than the others two compaction loads.

***Grain size of sintered Zn-27Al-2Cu-0.015Mg (ZA27) alloy***

The overall grain size results followed the general prediction; higher compaction load leads to smaller grain size (Figure 4.28 (c)). All hybrid microwave sintered samples were denser than conventional sintered samples.

## **CHAPTER 5**

### **DISCUSSIONS AND ANALYSIS**

#### **5.1 Effect of mixing speed during mixing process in a planetary ball mill**

Zinc-aluminum (Zn-Al) alloys have been used for many years as foundry alloys for various applications particularly in automobile industry (Bozic et. al, 2011). It is known that zinc based commercial alloys such as ZA8, ZA12 and ZA27 have good physical, mechanical and tribological properties such as high strength, high resistance to wear and abrasion, good corrosion resistance and low melting point materials (Mojaver and Shahverdi, 2010). These commercial Zn-Al alloys commonly manufactured through the traditional process of melting and casting. However, the problems with the casting process in producing mass production parts are associated with segregation, machining and maintaining final tolerance. Therefore, powder metallurgy technique was one of the alternative processes to manufacture these commercial Zn-Al alloys.

In this study, ZA8, ZA12 and ZA27 alloys were successfully produced through powder metallurgy approach; weighing, mixing, compaction and sintering. Mixing was the necessary step to prepare particle size distribution before compaction. There were various variables in the powder mixing process and one of them was rotational speed of a mixer (Upadhaya, 1997). Thus, the effect of mixing speed on the powders' element during mixing process in a planetary ball mill is studied in this research.

The experiment is started by mixing ZA27 composition alloy with speed 200 rpm and mixing time of 4 hours. Based on the literature, certain metal tended to form metal

composites during mixing in the absence of a lubricant (Benjamin, 1976). It is observed in the Figure 4.1(c) that the Zn-Al-Cu-Mg particles are interacted with Zirconia (Zr) balls during mixing and thorn growth has occurred in particular points on the balls surface, symmetrically. However, the Zr balls are covered by a thin layer of elements and the thorns grown on this layer. This is consistent as reported by the previous researchers that milling process is involved plastic deformation, particle size reduction, cold welding, and fracture (Islam S.Humail et. al., 2006).

The XRD results of the scratched thorns grown on the zirconia ball revealed that only Zn and Al element presence in the initial mixture (Figure 4.2). The absence of Cu and Mg elements is due to the small fraction of these elements in the initial mixture, namely 2.2wt% and 0.015wt%. They are penetrated in the Zn-Al matrix and since they occupied the crystal lattice positions of the matrix, XRD cannot detect them at all. Obviously, the according peaks have very low intensities compared to the intensities of Zn and Al peaks.

The all peaks of Zn and Al were shifted about  $\Delta\theta=0.161^\circ$  to the lower angles. Local high temperatures at collision zones resulted deformations in the powder particles (Pouriamanesh et. al., 2009) of Zn and Al. This means a uniform deformation / macrostress has been occurred in Zn and Al powders due to thermal and mechanical processes on the curvature, spherical, surface of the balls.

The distributions of Zn, Al, Cu and Zr in the elemental FESEM mapping are shown in Figure 4.3. However, Mg element was not detected in this region, but the diffusion of Zr from the ball into the grown layers is well detected. Some micro cracks like free surface are formed by cold welding between different powder particles (Lu and Lai, 1995).

EDX characterization detected oxygen in the region near to the interface that means the zirconia molecules from the ball are diffused into the grown layers (Figure 4.5). The



result shows the presence of Zn, Cu, Zr, O, Al, and C in the region. The fraction of the elements is different from the initial proportion. This means the small region does not reflect the whole picture of the mixture. The small amount of C observed probably related to some contamination during the process.

In Figure 4.6, Mg and Cu elements were not detected on the grown layer and clearly that small amount of Mg and Cu cannot cover entire the ball surface. Although the amount of Mg is less than Cu in the mixture, Cu was not detected on the covered layer. It means Cu distribution is much localized than Mg. this fact can be seen from optical microscope mapping of etched samples in Figure 4.3 as well.

The experimental data from optical microscopy, FESEM, EDX and XRD results confirm that multi-stage processes of symmetrical grown thorns are occurred on the Zirconia ball surface (Figure 4.7). In the jar during mixing process the crystal growth (sintering) is happened. The locations of elements growth crystals are depended on it weight percentage (wt. %). The elements distributed based on their thermo-physical properties in their preferred location on the balls. However, that was not the goal in this research to grow the alloy on the Zirconia balls surface. Therefore, lower of mixing speed (100 rpm) is chosen as suitable mixing speed for Zn-Al alloys as no reaction occurred between Zn, Al, Cu and Mg powders with Zirconia ball surface (Figure 4.1 (b)).

## **5.2 Conventional sintering versus hybrid microwave sintering**

The experimental work on the sintering of Zn-Al alloys has shown that the rapid heating during hybrid microwave sintering reduces processing time compared to conventional sintering (Figures 5.1 and 5.2). Conventional sintering took about 160 minutes to complete the sintering process but in hybrid microwave sintering, it took only 50 minutes, almost 30% reduction of sintering time. This is similar to the behavior reported by Azrina, 2010 that pure zinc sintered samples in a microwave system reduces the sintering time to more than 50%. Another researcher also reported that the use of microwave processing reduces the typical sintering time by a factor of 10 or more in many cases (Agrawal, 2006). This phenomenon is related to the mechanism of a hybrid microwave heating process. In hybrid microwave system, microwave heat the sample from inside to outside while susceptor provided radiant heat from outside to inside, thus reducing the thermal gradient. Besides that, microwaves interact with individual particulates within the press compacts directly and thereby provide rapid volumetric heating (Upadhyaya et. al, 2007).

It is also interesting to note that the hybrid microwave sintered samples showed higher sintered density compared to conventional sintered samples for all Zn-Al alloys (Figure 5.5). Most of the previous researcher found that microwave heating improved densification compared to conventional heating (Sethi et. al, 2003, Panda et. al, 2006 and Gupta and Wong, 2005). This is due to the slow heating process and long dwelling time in a conventional sintering process. During conventional sintering, the heating rate is limited to achieve fast heating rate due to slow heating of heating elements and heat transfer via thermal radiation to the materials and also to prevent large thermal variation within the compacts to avoid cracking or warpage (Wong and Gupta, 2010).

Good sintering condition could be indicating through a uniform distribution of pores. It is clear from the FESEM micrographs of the porosity distribution (Figures 5.8 - 5.16) that the conventional sintered samples show non-uniformly distributed pores and vice versa to microwave sintered samples. This proved the point that uniform microstructure can be achieved via hybrid microwave sintering. Anklekar et. al, (2001) also reported that microwave sintered samples of compacted copper steel attributed to be small, rounded and uniformly distributed pores as against large, angular and non-uniformly distributed pores in case of conventional sintered samples. Microwave managed to produce lower porosity compared to conventional sintering as shown in Figure 5.6. Takayama (2006) reported that when inside of the sample is allowed to achieve high density before the surface layer density, the internal porosity is minimized since fewer pores are trapped inside the sample.

Apart from that, Vickers hardness values of all microwave sintered samples exhibited higher than conventionally sintered samples (Figure 5.7). It is shown although the differences did not appear to be very large, but it may enough to improve the mechanical properties. Hybrid microwave sintering also provide an improvement in microhardness for others metals such as WC tools (Varadarajan et. al, 2006), Cu-12Sn alloy (Upadhyaya et. al, 2002), Al/SiC composite (Leparoux et. al, 2003), etc. One of the possible reasons was primarily as a result of the reduced extent of high temperature thermal exposure as cooling time was eliminated (Gupta and Wong, 2005). Zhijian Huang et al, 2009 reported that the reason microwave sintered samples produced higher microhardness values due to the fine-grained microstructure attained by microwave sintering.

### **5.3 Effect of compaction load on hybrid microwave sintering**

The aim of compaction was to obtain an adequate green strength for subsequent handling before and during the sintering process. Swelling is one the problem faced after sintering process. In present research revealed that in all Zn-Al alloys; ZA8, ZA12 and ZA27, swelling increased as compaction load increased (Table 5.1). Swelling occurs because the melt penetrates the grain boundaries in the solid phase and the solid phase disintegrates into smaller particles and separates (Rajiv Asthana et al, 2006). Takayama et. al, (2004) reported that deformation in shape of sintered compacts is a consequence of high compaction applied during the compaction process. Sethi et. al, 2003 found that increasing compaction load, slight densification in prealloyed bronze samples and swelling in premixed bronze samples for conventional and microwave sintering. Swelling can be controlled by selecting fine particles, low compaction load and slow heating rate.

In a study of microwave sintering of Al/Al<sub>2</sub>O<sub>3</sub> composites (Gerdes and Willert-Porada, 1994) researchers found that heating rate is inversely related to the compaction pressure used in consolidating the powders for pure aluminium. This is due to increasing connectivity between the metal phase and distortion of the oxide layer with increasing compaction pressure. This is consistent with results reported by Takayama et. al, (2004), with higher compaction loads and temperatures; the temperature inside the sample was lower than at the surface, due to shielding caused by the increasing contact between metal particles. However, in this study revealed that hybrid microwave sintering heating rate is independence of compaction pressure due to low sintering temperature (360°C) and small size of samples used in present research.

Theoretically, increasing compaction load provide better density and lead to decrease porosity by formation of new particle contacts. However, in this present research

found that only ZA27 sintered samples followed the general prediction; highest density obtained at 10 tons compaction loads (Figure 5.5). Another two alloys; ZA8 and ZA12 revealed that highest density obtained at 8 ton compaction loads. The porosity results are inversely proportional to the density results (Figure 5.6). These density and porosity results suggested that low compaction loads; 8 tons is favoured during hybrid microwave sintering of zinc-aluminum alloys. Gerdes and Willert-Porada, 1994 found that when compaction loads are too high, overall densification of microwave sintered samples is reduced due to metal particles are in very close contact, microwave shielded from penetrating into samples and volumetric heating cannot be realized.

Besides provide better density, by increasing compaction load also resulted in reducing grain size in all three alloys. Hybrid microwave sintered samples shown smaller grain size compared to conventional sintered samples (Figure 5.21). This proved the advantages of hybrid microwave sintering that provided volumetric heating; fine grained microstructure and increased densification of sintered samples. Geng-fu Xu et al (2001) reported that grain size drastically decreased with increased heating rates.

## **5.4 Influence of different masses of Zn, Al, Cu and Mg element on mechanical properties of hybrid microwave sintering**

The density of Zn-Al alloys decreased with increasing aluminum weight percentage; 8, 11 and 27 (Figure 5.5). The densities of the alloys are influenced by the weight percent of zinc not aluminum. The density of pure zinc was 7.14 g/cm<sup>3</sup> which higher than density of pure aluminum; 2.7 g/cm<sup>3</sup>. Therefore, ZA8 alloy (Zn-8Al-1Cu-0.02Mg) shown higher density than ZA12 (Zn-11Al-1Cu-0.025Mg) and ZA27 (Zn-27Al-2Cu-0.015Mg) alloys for both sintering methods.

Although there was a different of density among three of alloys, the hardness values shown a similar range (Figure 5.7). The highest density for ZA8, ZA12 and ZA27 were 69.9±1.9 HV, 68±2.5 HV and 64.6±2.1 HV respectively. This is maybe due to the uniform distribution and particle integration among of zinc, aluminum, copper and magnesium after sintering process. Another possibility which contributed to this result was the diffusion of one element in another and boundary of grains as can be seen clearly in the Figures 5.8 – 5.16 at higher magnification x500. Mehdi et al (2009) stated that diffusion bonding plays major roles in the formation and growth of interparticle bonding which effect on microstructure and mechanical properties.

Moreover, it can be observed that increasing Al content, Al particles are more integrated especially in hybrid microwave sintered samples. Besides that, hybrid microwave sintered samples produced uniformly distributed pores compared to conventional sintered samples. This is consistent with reported by Agrawal 2000, that pores in microwave sintered samples had round edge while sharp edge porosity in conventional sintered samples. This proved the advantages of hybrid microwave sintering of materials including metal alloys compared to the conventional sintering.

Consistently, FESEM microstructure result and XRD analysis revealed that increasing the fraction of Al resulted in more Zn surrounded by Al phase and concentration of Al also increased in the XRD result (Figure 5.20). Although in the alloys composition contained of Cu and Mg, but the peaks of them were not appeared in the XRD result probably due to their low concentration compared to Zn and Al elements.

From the EDX results (Figure 5.17-5.19), the element analysis of the three alloys showed similar results. It can be seen that Silicon (Si) and Oxygen (O) are detected in the investigated region. The source of Si in the product was the polish paper used to clean the sample surface after sintering. Since the microwave sintering and conventional sintering are carried out in the air ambient, the sintering is progressed in the presence of oxygen. Moreover, some air is trapped inside the closed pores during compaction. Obviously, oxygen must be in the form of an oxide phase which is most probably aluminum oxide. The oxide phase was not detected in XRD result possibly due to its very small fraction that makes it to be localized in some areas. Although the oxide is polished from the surface, but still the oxide phase formed inside the sample existed and could be detected by EDX.

The Coefficients of thermal expansion (CTE) of the microwave sintered alloys showed that increasing Al fraction in the alloy resulted in reduction of CTE (Table 5.2). This fact can be related to the significant difference between microstructure of ZA27 hybrid microwave sintered alloy (Figure 5.16) compared to ZA8 (Figure 5.9) and ZA12 (Figure 5.12). Clearly in ZA27 sintered samples, the boundary between different phases is much larger than that of ZA8 and ZA12 sintered samples. So, mismatch in CTE of adjacent grains in the alloy prevented free expansion of the grains. In addition, it may be related to amount of possible more oxide phases in ZA27 sintered alloy.

## CHAPTER 6

### CONCLUSIONS AND FURTHER WORKS

#### 6.1 Conclusions

Hybrid microwave sintering is a promising method to for processing metallic materials due to its advantages rapid and uniform heating which reduces thermal stress, improving microstructure and mechanical properties, reduces manufacturing cost and processing time and much less expensive equipment. The following conclusions can be made from the present study:

- a) Metallic Zinc-Aluminum alloys; ZA8, ZA12 and ZA27 were successfully produced via Hybrid Microwave sintering from the elemental components.
- b) 100 rpm was the best mixing speed of Zinc-Aluminum alloys; ZA8, ZA12 and ZA27.
- c) Hybrid microwave sintering of metallic alloys based Zinc-Aluminum alloys takes considerably shorter processing time compared with conventional sintering.
- d) The best compaction loads for processing ZA8 and ZA12 alloys were 8 tons meanwhile for ZA27 was 10 tons according to microstructure analysis.
- e) The hybrid microwave heating mechanisms caused less micro-crack and enhanced better integration among the grains.
- f) Coefficient of thermal expansion (CTE) was decreased by increasing Al fraction in the all ZA8, ZA12 and ZA27 alloys.



- g) ZA8 obtained the highest density compared to ZA12 and ZA27 because of weight percentage of zinc in the compositions. However, the ranges of micro hardness values were similar in all three alloys.

## **6.2 Further Works**

It is evident from these and other studies that hybrid microwave sintering is associated with specific characteristics which can prove advantageous in materials processing especially in metallic alloys. However, there are a few limitations and difficulties faced in scaling up the hybrid microwave system and operation for commercialization. Therefore, there are several recommendations to improve and strengthen the current hybrid microwave system in the laboratory such as:

- a) The existing domestic microwave oven requires to be modified to be able to read real time temperature of the sample during heating.
- b) Other mechanical properties such as compressive, tensile and wear resistance test should be investigated after sintering process to strengthen the results.
- c) The effect of susceptor particle size (nano and micron size) should be investigated to compare the effect of susceptor particle size on the temperature profile in hybrid microwave sintering.

## LIST OF PUBLICATIONS

1. **Maisarah Lutfi**, Rahbari R. G., M. Hamdi, M. Fadzil, Farazila Yusof, Characteristics of Hybrid Microwave Sintering of Zn-Al-Cu-Mg Alloys.  
(Submitted to the journal of Materials and Design for review)
2. **L.Maisarah**, Rahbari R.G., M.Hamdi, Microscopic and Microscopic Aspects of Zn-Al-Cu-Mg Alloying, International Conference on Advancement of Materials and Nanotechnology II (ICAMN 11-2010), November 29 –December 1, 2010, Prince Hotel, Kuala Lumpur, Malaysia
3. A.Azrina, M.Hamdi, A.R.Bushroa, M.Fadzil, **L.Maisarah**, Microwave Hybrid Sintering: Improving of Zinc Compaction Metal Powder, International Conference on Materials Processing Technology 2010 (MAPT 2010), January 5-6, 2010, Bangkok, Thailand
4. **L.Maisarah**, N.A.Mardi, M.Fadzil, Development of Animation-Based Learning Aid for the Teaching of Engineering Drawing in Secondary Schools in Malaysia, In Proc. Of the 3<sup>rd</sup> Regional Conference on ICT Applications for Industries and SMALL Companies in ASEAN Countries (RCICT 2011), March 10-11, 2011, Donchan Palace, Vientiane, Lao PDR

## REFERENCES

- Agrawal, D. (2000). Microwave sintering of metallic materials. Proceedings of 2000 powder metallurgy world congress.
- Agrawal, D. (2006). Microwave Sintering, Brazing and Melting of Metallic Materials. Sohn International Symposium Advanced Processing of Metals and Materials.
- Anklekar, R.M., Agrawal, D.K. and Roy, R. (2001). Microwave Sintering and mechanical properties of PM copper steel. Powder Metallurgy. 44, 355-362.
- Azrina Arshad (2010). Sintering of Compacted Zinc powder via a modified microwave oven. University of Malaya.
- Benjamin, J.S., (1976), Scientific American, 234, 40.
- Bescher, E.P. and Mackenzie, J.D. (1991). Microwave heating of cermets in Microwaves: Theory and Applications in Materials Processing, Ceramic Transaction, 21, The American Ceramic Society, Westerville, Ohio, 557-563.
- Bescher, E.P., Sarkar, U. and Mackenzie, J.D. (1992). Microwave processing of aluminium-silicon carbide cermets, in Proc. Microwave Processing of Materials III, MRS Symposium Proceedings, 269, MRS, Pittsburg, Pennsylvania, 1992, 371-378.
- Bozic, D., Stasic, J. and Rajkovi, V. (2011). Microstructures and Mechanical Properties of ZA27-Al<sub>2</sub>O<sub>3</sub> Composites Obtained by Powder Metallurgy Process. Science of Sintering 43, 63-70.
- Das, S., Mukhopadhyay, A. K., Datta, S. and Basu, D. (2008). Prospects of microwave processing: An overview. Bulletin of Materials Science. 31(7), 943-956.

David, E.C., Diane, C.F., and Jon, K.W. (2000). Processing materials with microwave energy. *Materials Science and Engineering A287*, 153-158.

Fall, M.L., Shulman, H.S., Walker, W.J., Wolfe, L. (2002). Sintering Wear Parts with Microwave Heating. *Ceramics Transaction, USA*.

Fang, Y., Agrawal, D.K. and Roy, R. (2003). Microwave sintering of nano-phase MgO, TiO<sub>2</sub> and Cu metal powders, in *Proc. Sintering 2003*, Penn State University, Pennsylvania, USA.

Gan, B.K. (2005). Microwave sintering of Tin Base Alloys and composites, University of Malaya.

Gedevanishvili, S., Agrawal, D. and Roy, R. (1999). Microwave combustion synthesis and sintering of intermetallics and alloys. *Journal of Materials Science Letter*. 18, 665-668.

Geng-fu Xu, Isabel K. Lloyd, Yuval Carmel, Tayo Olorunyolemi and Otto C. Wilson, Jr. (2001). Microwave sintering of ZnO at ultra-high heating rates. *Journal of materials research*. 16(10), 2850-2858.

Gerdes, T. and Willet-Porada, M. (2004). Microwave sintering of metal-ceramic and ceramic-ceramic composite in *Proc. Microwaves Processing of Materials IV*, Materials Research Society Symposium Proceedings, 347, 531-537.

Gupta, M., Wong, W.L.E, (2004). Enhancing overall mechanical performance of metallic materials using two directional microwave assisted rapid sintering. *Scripta Materialia*. 52, 479-483.

Gupta, M. and Wong, W.L.E, (2005). Enhancing overall mechanical performance of metallic materials using two directional microwave assisted rapid sintering. *Scripta Materialia*. 52, 479-483.

Gupta, M. and Wong W.L.E. (2007). Microwave and Metals. John Wiley & Sons (Asia) Pte. Ltd. Singapore.

Hsieh, C.Y., Lin, C.N., Chung, S.L., Cheng, J. and Agrawal, D.K (2006). Microwave Sintering of AlN powder synthesized by a SHS method. Journal of the European Ceramic Society, 27, 343-350.

Islam S.Humail, Xuanhui Qu, Chengchang Jia, MingliQin and Xinbo He (2006), Morphology and Microstructure Characterization of 95W-3.5Ni-1.5Fe Powder Prepared by mechanical alloying. Journal of University of Science and Technology Beijing. 13(5), 442.

Kotecha, R.D., Nai, S.M.L., Gupta, M. (2008). Development of Al and Al/Cu (composite/alloy) formulations with enhanced properties through microwave power variation during hybrid sintering. Journal of Physics D: Applied Physics 41.

Leparoux, S., Vaucher, S. and Beffort, O. (2002). Influence of SiC particle size on microwave sintering of metal matrix composites, Werkstofftechnischnishes Kolloquium, 24-25, 13-19.

Leparoux, S., Vaucher, s. and Beffort, O. (2003). Assessment of microwave heating for sintering of Al/SiC and for insitu synthesis of TiC. Advanced engineering materials. 5, 449-453.

Lu, L. and Lai, M.O. (1995). Formation of new materials in the solid state by mechanical alloying. Materials Design 16(1), 33-39.

Martinez-Flores, E., Negrete, J., and Torres Villasenor, G. (2003). Structure and properties of Zn-Al-Cu alloy reinforced with alumina particles. Journal of Materials and Design, 24, 281-286.

Mehdi Rahimian, Naser Ehsani, Naser Parvin, Hamid Reza Bharvandi (2009). The effect of particle size, sintering temperature and sintering time on the properties of Al-Al<sub>2</sub>O<sub>3</sub>

composites, made by powder metallurgy. *Journal of Materials Processing Technology*. 209, 5387 – 5393.

Mojaver R., Shahverdi H.R. (2010). The Relationship Between The Wear Behavior And Microstructure Features In End-Chill Cast Zn–27%Al Alloy. *Wear* 268(3-4), 605-611.

Mondal A., Agrawal D., Upadhyaya A. (2009). Microwave heating of pure copper powder with varying particle size and porosity. *Journal of Microwave Power & Electromagnetic Energy*. 43, 1-5.

Moriguchi, H., Tsuduki, K., Ikegaya, A., Miyamoto, Y., Morisada, Y. (2006). Sintering behavior and properties of diamond/cemented carbides. *Journal of Refractory Metals and Hard Materials*. 25, 237-243.

Nuchter, M., Ondruschka, B., Bonrath, W., and Gum, A. (2004). Microwave assisted synthesis – a critical technology overview. *The Royal Society of Chemistry*, 6, 128-141.

Padmavathi, C., Panda, S.S., Agrawal, D. (2006). Effect of microstructural characteristics on corrosion behavior of microwave sintered stainless steel composites. In *Proc. Materials Science and Technology 2006: Processing*, October 15-19, Ohio, USA, 517-528.

Panda, S.S., Singh, V., Upadhyaya, A. and Agrawal, D. (2006). Sintering response of austenitic (316L) and ferritic (434L) stainless steel consolidated in conventional and microwave furnaces. *Scripta Materialia*. 54, 2179-2183.

Petzoldt, F., Scholz, B., Park, H.S. and Willert-Porada M. (2006). Microwave sintering of PM steels, report from the 8th International Conference on Microwave and High Frequency Heating, 598-608.

Pouriamanesh. R., Vahdati-Khaki, J. and Mohammadi, Q. (2009). Coating of Al substrate by metallic Ni through mechanical alloying. *Journal of Alloys and Compounds* 488, 430-436.

Prabhu, G., Chakraborty, A., Sarma, B. (2008). Microwave Sintering of Tungsten. International Journal of Refractory Metals and Hard Materials, 27, 545-548.

Rajiv Asthana, Ashok Kumar, Narendra B. Dahotre (2006). Materials processing and manufacturing science.

Randall, M.G.(1994). Powder Metallurgy Science, 2<sup>nd</sup> edition, New Jersey, Metal Powder Industry Federation.

Roy, R., Agrawal, D., Cheng, J., and Gedevanishvili, S. (1999). Full sintering of powdered-metal bodies in a microwave field. Nature. 399, 668-670.

Saitou, K. (2006). Microwave sintering of iron, cobalt, nickel, copper and stainless steel powder. Scripta Materialia. 54, 875-879.

Sethi, G., Upadhyaya, A. and Agrawal, D. (2003). Microwave and conventional sintering of premixed and prealloyed Cu-12Sn Bronze. Journal of Science of Sintering. 35, 49-65.

Sheinberg, H., Meek, T.T. and Blake, R.D. (1990). Microwaving of normally opaque and semiopaque substances. US Patent 4942278.

Sung-Ki Kim, Hwan-Tae Kim, Ji-Soon Kim, and Young-Soon Kwon (2000). Production of metal powder compact with controlled porosity by spark plasma sintering process. The 4th Korea-Russia International Symposium.

Sutton, W.H. (1989). Microwave processing of ceramic materials. American Ceramic Society Bulletin, 68, 376–386.

Tan, M.M. (2008). Microwave Hybrid Sintering for Tin-Base Alloy. University of Malaya.

Takayama, S., Link, G., Sato, M. and Thumm, M. (2004) Microwave sintering of metal powder compacts. Proceedings of the fourth world congress on microwave and radio frequency applications. 311-318.

Takayama, S. (2006). Sintering behavior of metal powder involving microwave-enhanced chemical reaction. Journal of Apply Physics. 45.

Thakur, S.K., Kong, T.S., Gupta, M. (2007). Microwave synthesis and characterization of metastable (Al/Ti) and hybrid (Al/Ti + SiC) composites. Materials Science and Engineering A. 452-453, 61-69.

Upadhyaya, G.S. (1997). Powder Metallurgy Technology. Cambridge International Science Publishing.

Upadhyaya, A., Sethi, G., Kim, H., Agrawal, D.K. and Roy, R. (2002). Densification of pre-mixed and prealloyed Cu-12Sn bronze during microwave and conventional sintering. Proceedings of the 2002 World Congress on Powder Metallurgy & Particulate Materials. 364-375.

Upadhyaya, A., Tiwari, S.K., and Mishra, P. (2007). Microwave sintering of W-Ni-Fe alloy. Scripta Materialia. 56, 5-8.

Varadarajan, Y. S., Vijayaraghavan, L., Krishnamurthy, R. and Bhanuprasad, V. V. (2006). Performance enhancement through microwave irradiation of K20 carbide tool machining Al/SiC metal matrix composite. Journal of Materials Processing Technology. 173, 185-193.

Veronesi, P., Leonelli, C., Bassoli, E., Gatto, A. and Iuliano, L. (2003). Microwave assisted sintering of SLS green metal parts, in Proc. Sintering 2003, Penn State University, Pennsylvania, USA.



Wong, W.L.E. and Gupta, M. (2010) Characteristics of Aluminum and Magnesium Based Nanocomposites Processed Using Hybrid Microwave Sintering. *Journal of Microwave Power and Electromagnetic Energy*. 44 (1), 14-27.

Yang, M.J. and German, R.M. (1999). Comparison of conventional sintering and microwave sintering. *Proceedings of the 1999 International Conference on Powder Metallurgy & Particulate Materials*, Vancouver, Canada, 207-219.

Yoshikaw, N., Ishizuka, E., Mashiko, K., Che, Y. and Taniguch, S. (2007). Brief Review on Microwave (MW) Heating, Its Application to Iron & Steel Industry and to the Relevant Environmental Techniques. *ISIJ International*. 47(4), 523–527.

Zhao, C., Vleugels, J., Groffils, C., Luypaert, P.J., And Van Der Biest, O. (2000). Hybrid Sintering With A Tubular Susceptor In ACylindrical Single Mode Microwave Furnace. *Acta Materialia*. 48, 3795–3801.

Zhijian Huang, Masahide Gotoh, Yukio Hirose (2009). Improving sinterability of ceramics using hybrid microwave heating. *Journal of materials processing technology*. 209, 2446-2452.